UNIVERSITY OF CAPE TOWN
IYUNIVESITHI YASEKAPA • UNIVERSITEIT VAN KAAPSTAD

BEHAVIOUR OF NON-PRISMATIC STEEL MEMBERS

Prepared by

DAVID OCHAN

Supervised by

Dr. ALVIN MASARIRA

This thesis is submitted in partial fulfilment for the requirements for the degree of Master of Science in Engineering at the University of Cape Town, August, 2008.

Declaration

I, Ochan David Okello, declare that this thesis is totally my own work and any other works included from outside has been clearly referenced. This work has never been submitted for any form of evaluation or any other purposes in any Institution or University.

Signed……. date……

Dedication

I must say, I am highly indebted to the Almighty God who has always protected me in any circumstances and I would like to dedicate this work to Him**.**

Acknowledgement

Considering the difficult time we had in the second year of the thesis preparation, Dr. Alvin Masarira kept on with his constant and tireless effort on supervision and quality advice. This is highly appreciated by the author.

The author is truly indebted to the Department of Civil Engineering because of the financial assistance rendered to him when it was most needed.

Not forgetting to thank my parents for all the assistance provided during the course of my studies in the University of Cape Town.

Finally, I would like to extend my sincere gratitude to all the Post Graduate students in the Department of Civil Engineering for their moral supports.

Abstract

Material savings, cost effectiveness, weight reduction, Strength and aesthetics of steel structures are some of the key factors to be considered in structural design. In the last decade, non-prismatic steel members have proved to be more effective in structural design than the prismatic members, i.e. they have higher load carrying capacity when their geometry closely resemble the bending moment envelope as compared to prismatic members with the same material properties, loading and boundary conditions. However, there is a unique point (degree of non-uniformity) for which every non-prismatic member loses its load carrying capacity due to a change in its failure position and mechanism. Therefore, in order to investigate the effect of geometrical non-uniformity on steel members, non-prismatic steel members with different steel sections were simulated using ADINA/M 8.4.2 version whose function is based on finite element method. Furthermore, the non-prismatic steel members were modeled under different geometrical arrangements, degree of non-uniformity, boundary and loading conditions. Deflections, stress distributions, torsional effect and critical buckling load were recorded. The numerical results obtained in this study combine effectively an optimized check for different geometrical arrangements and degree of non-uniformity leading to a relatively improved economic and safe design.

Table of Contents

Lists of figures

Lists of tables

Chapter 1

Introduction

1.1 Background

At the beginning of the 19th century, steel was used for construction of simple roof structures and bridges. However, in the middle of the 19th century, new methods of steel production such as the Martin process were introduced. This increased the possibilities of using steel on a greater scale for complex bridges, roof trusses, columns, civil and industrial buildings, reservoirs and even pipes. This was followed by the introduction of welding at the end of the 19th century.

The introduction of welding enhanced the design and construction of light weight and thin-walled structures such as domes, pipes and building skeletons. During this period of introduction, different theories for analysis were developed. As a result, codes and standards were published for design and production of steel structures.

Since the beginning of the 20th century, the demand for steel increased. This led to the discovery of high standard equipments like automatic welding machine, thus Fig 1.1. This machine makes the production of steel structures faster, easier and relatively cheaper [54].

Figure 1.1 Automatic welding machines [29].

Steel is preferred to other construction materials like timber, wattle, concrete and bricks because of its durability, ductility, stability, safety, strength and malleability. It is the only metallic item that can be conveniently and economically produced in tonnage quantity. In addition, steel possesses a unique advantage such as the high strength to weight ratio i.e. 25 times greater than wood and it continues to replace timber in most of the construction activities [27].

1.1.1 *Structural Behaviour of Steel members.*

Steel as construction material has three major failure criteria, namely; instability, strength and serviceability. Instability of steel member is a situation in which the load carrying capacity of the member is reduced to an acceptable degree. Therefore, the member can no longer carry the design load but it can still support load of lower value. On the other hand, yielding of a cross-section of the steel member is a change in its property from elastic to plastic behaviour but it can still support applied load as well though the displacement resulting from the applied load will be permanent. In most design procedures of steel structures, strength failure is not considered to be crucial compared to instability failure because of the slenderness of steel members. The instability failure is a snap-through failure without warning in most cases and makes it difficult to predict by most designers. However, serviceability failure affects mainly the occupants. In this case the design is based on the deflection limitation. Structure deflecting beyond the approved limits in the codes of practice is considered to have failed under serviceability limit state design [40].

1.1.2 Non-prismatic Steel members

Non-prismatic members can be defined as steel members with varying cross-sectional dimensions along or across longitudinal axis. For economic purposes, their contours should follow the bending moment envelope. Therefore, this provides a number of advantages such as; enhanced load bearing capacity of the cross-section of the members, provides effective usage of materials that directly leads to cost and weight reduction. Weight reduction of up to 15% of structures can be obtained; and the members still support the same loading which would have been supported by bigger prismatic steel members [42].

As one of the greatest effects of World War II, steel as a construction material became so scarce that the Germans came up with the practical application of cold formed non-uniform (non-prismatic) steel members which were mainly welded and/or riveted members for beams and beam-columns in buildings, bridges, roof trusses, lamp poles in order to optimize the use of available material.

Fig. 1.2 shows some examples for the application of non-prismatic steel members in building structures.

Figure 1.2. Steel frames with non-prismatic members [28].

In spite of the numerous advantages demonstrated by non-prismatic steel members, there still exist some challenges in the analysis and design procedures for such members since there is very little guidance in the available design codes at present. Therefore, there is the need to develop a simplified design procedure for use by practicing engineers as opposed to algorithmic procedure proposed by Muller [41], which seems tedious in computation and unfeasible for practical application on a larger scale.

1.2 Research problem

Non-prismatic steel members are becoming common in the construction industries due to the invention of automatic welding machine which increased their production and made them less expensive to fabricate since most of them are welded members. Apart from providing an effective usage of material (as most of their shapes closely resemble the bending moment envelop), they also improve the aesthetic features of the structures.

The few guidelines mentioned for the design of non-prismatic steel members are considered to be inadequate and limited for practical application. For example, Euro-code 3 mentions the design of such members in compression according to equation (1.0), but the procedure is conservative since it depends only on the geometrical and mechanical characteristic of the smallest cross-section. Based on the fact that the larger section of the member does not yield at the same time as the smaller section under a constant applied load, therefore, there is the need to develop a design guideline which optimizes the cross-sectional properties. More so equation (1.0) is limited to the design of linearly tapered member only where a correction factor, K, is determined from the plots of K versus slenderness ratio, λ, for different tapering angles (h/H), where H is the larger and h is the smaller section dimensions [2].

$$N_n = K\, X \beta_A A f_y / \gamma \qquad (1.0)$$

where;

N_n - buckling resistance of the tapered member [N]

K – Correction factor for tapered member

X – Correction factor for buckling mode

β_A – Correction factor for section formation

A – Smallest cross-sectional area [mm^2]

f_y – yield stress [Mpa]

γ – Material partial factor

The two most common modes of failure in steel structures are instability and yielding of the members.

Considering the buckling equations (1.1) and (1.2) as well as the buckling stress equation (1.3) for prismatic steel members with constant flexural rigidity. These equations cannot be applied to non-prismatic members whose flexural rigidity changes along the member longitudinal axis. Therefore, these equations for prismatic members need to be modified in order to incorporate the application of non-uniform steel members.

Euler buckling equation for column members

$$P_{cr} = \frac{\pi^2 EI}{(KL)^2} \quad \text{..... (1.1)}$$

where;

P_{cr} – critical buckling load [N]

EI – flexural rigidity [Nm^2]

KL – effective length [m]

Lateral-torsional buckling of beam members [51]

$$M_{xy} = \frac{\pi\sqrt{EI_y GJ}}{(KL)}\sqrt{1+\frac{\pi^2 EI_w}{(KL)^2 GJ}} \quad \text{..... (1.2)}$$

where;

I_w – warping section constant [m^6]

EI_y – flexural rigidity of minor axis [Nm^2]

GJ – torsional rigidity of beam [Nm^2]

EI_w – warping rigidity of beam [Nm^4]

KL – effective length [m]

Buckling stress for steel members in bending

$$F_e = \frac{F_{es} + F_{ez}}{2H}\left[1 - \sqrt{1 - \frac{4F_{es}F_{ez}H}{(F_{es} + F_{ez})^2}}\right] \quad \text{..... (1.3)}$$

$H = 1 - (x_o^2 + y_o^2)/r_o^2$

$r_o^2 = x_o^2 + y_o^2 + r_x^2 + r_y^2$

where;

$F_{es}F_{ez}$-Elastic flexural buckling stress [N/m^2]

H – Ratio of shear coordinates to radius of gyration

r_x, r_y –Radii of gyration about x and y axes [m]

x_o, y_o – Shear centre coordinates with respect to centurion [m]

For uniform members, every parameter in equations (1.1) to (1.3) is constant along or across the longitudinal axis of the member but once the section of the member becomes non-prismatic, parameters like second moment of area I, radius of gyration r, warping constant I_w, and torsional constant J, become variables as well. This makes the above equations inapplicable for non-prismatic members hence, there is the need to modify the above equations (1.1) to (1.3) to incorporate the application of non-prismatic members.

The effect of varying cross-sectional properties can be noted in the design procedures for non-uniform torsion, equation (1.4), which has the applied torque, M_t, which is directly related to the flexure and twist of the members. Torsion is non-uniform, if either one or both ends of the member are restrained from warping and there is axial strain in the longitudinal fiber or the applied torsional moment is non-uniform along the member. The equation (1.4) has two important design parameters such as second moment of area I, that is responsible for bending and torsional constant J, that is responsible for twisting.

If equation (1.4) is used in the analysis of prismatic members, it is quite difficult to predict the behaviour of the members by an analytical model if the members to be considered is non-prismatic because that will mean both the two key design parameters (I and J) will have to be treated as variable with respect to member's length.

$$M_t = C\frac{d\phi}{dz} - \mathrm{E}Ih^2\frac{d^3\phi}{2dz^3} \quad \text{..... (1.4)}$$

$$C = GJ$$

where;

J – Torsional constant and it a function of cross-sectional dimensions [m^4]

G – Shear modulus of the members [N/m^2]

C – Torsional rigidity of the members [Nm^2]

E – Modulus of elasticity [N/m^2]

I – Second moment of area [m^4]

h – Member section depth [m]

1.3 Objectives of the study

The main objective of this study is to investigate the general behaviour of non-prismatic steel members as compared to prismatic ones and their application in structural system. This will be achieved through numerous models of non-prismatic steel members under different degree of non-uniformity, steel sections, boundary and loading conditions which have not been considered in the previous research. As a result, this may lead to the modification of the available design guidelines of prismatic steel members to incorporate the design of non-prismatic members.

1.4 Hypothesis

It has been suggested by Muller [41] that non-prismatic steel members provide effective usage of materials by reducing wastage up to around 15%.

Saka [49] also observed that at least 10% weight reduction can be achieved and this will provide light weight structures. This is possible because most of the non-prismatic steel member's shapes are made in such a way that they closely follow the bending moment envelope hence, they have higher load bearing capacity. Non-prismatic steel members with smaller dimensions will support the same loading which would have been supported by prismatic members having larger volume and weight. Therefore, this results in an effective usage of the material and also increases in the load bearing capacity of steel members [65].

1.5 Scope of the study

This research will only be limited to the investigation of linear elastic behaviour of non-prismatic steel members under normal working conditions for steel as construction material. All the members under study are considered to be perfectly straight with no imperfections. Material nonlinearities will not be considered (e.g. material imperfections) as it requires a more detailed study of the materials properties of steel. Therefore, members and structures under investigation include; I, H, channel and angle beams, columns and few frame systems composed of various non-prismatic steel sections such as I and H.

1.6 Methodology

This Chapter highlights the steps taken to achieve the objective of the research. Therefore, for this research work, most of the results generated using numerical models because there are number of commercial computer packages with the ability to produce direct, fast and accurate results for structural analysis. For purposes of this research work, ADINA/M 8.4.2 was used.

Using steel of grade 350W and ADINA/M 8.4.2 package, numerical model which uses Finite Element Analysis (FEA) was used to investigate the behaviour of non-prismatic members under different boundary and loading conditions, member shapes, position and degree of non-uniformity.

However, some closed solutions were performed on prismatic members just for purposes of validity, accuracy and applicability of the results obtained from finite element method (FEM) since mesh density is a key in finite element models.

1.7 Structure of the thesis

This section briefly explains the thesis layout as outlined below;

- Introduction
- Literature review
- Methodology
- Results and discussion
- Conclusions and recommendations

The introduction gives the brief history of the research topic and the reasons as to why it is being conducted. Literature study explains the previous work done by other researchers and the pending issues which need to be dealt with. The methodology describes the procedure used to obtain the results discussed in Chapter 4. The last Chapter reports the findings and suggests further research if necessary.

1.8 Conclusion

This Chapter of the thesis is where the final say about the objective set at the beginning of work is made. It depends on both the literature viewed and the practical results obtained from the models. In addition, any recommendations will also be made in this section.

Chapter 2

Literature Review

2.1 Introduction

Non-prismatic or non-uniform steel members are made up of varying cross-sectional dimensions. They can be formed by fabricating different steel plates mainly through welding. The varying geometrical steel shapes are used to provide aesthetic features, weight reduction, which in turn leads to material cost reduction. Therefore, in the recent past, these types of steel members are being used widely in the construction industry, either for industrial or residential buildings. The methods available for the analysis and the design of prismatic steel members are well established. However, the analysis and design of non-prismatic steel members [49] are not well established

By making the shape of the members to closely follow the bending moment envelope, the weight of the members and material wastage can be significantly reduced. This is based on the fact in structural analysis stress is non-uniformly distributed along the member. Therefore, not all the material for prismatic steel member is used up in the support of the applied load. Steel members can be made non-uniform to provide the distribution of stress even so that the waste of steel material can be reduced though non-prismatic steel members tend to make analysis and design tedious. Presently, most architects are reported to prefer these types of steel members mainly because of the aesthetic features associated with the geometry.

Most design industries prefer tapered beams and columns in order to make the most use of structural materials. In many buildings, frames constitute the major part of the structural systems. Frames are made up of beams and columns. Beams are subjected to bending moments while columns and beam-columns to axial forces and bending moments. In most cases, these actions are generated by externally applied forces.

These forces can either be in the form of moment, axial or torsion. Since considerable proportions of members are also under torsion, design consideration should cater for all when developing the design guidelines for non-prismatic steel members.

The few researchers, who investigated closed section non-prismatic members, include Samir [52], Ramamurti and Karthikeyan [47], Dube and Dumir [17] and Yaozhi [66]. Yaozhi [66] studied the behaviour of non-prismatic steel members using circular hollow sections. This was adopted firstly from the 'water cube' in the National swimming centre of China for the 2008 Beijing Olympic Games.

In order to show the impact of having circular steel members whose ends are tapered as opposed to prismatic ones, Yaozhi [66] reports that some members have very low flexural and axial stresses. And they provide safer structures compared to those with prismatic end members. Therefore, it is reasonable to adopt structural members whose ends are tapered.

However, Yaozhi [66] in his findings overlooked different loading conditions, fixities of the members, tapering ratio, tapering position, torsional effect and the snap-through load for the framed structures made of tapered circular section. These factors need to be investigated further on the effect of tapered closed section members.

When compared to closed section non-prismatic members, most research is commonly done on welded thin-walled open sections such as tapered I-section columns because of their wide application in the construction industry. In addition, this may be due to the simplicity in their analysis and design. On the other hand, the minimal research level on tube members may partly be because there are fewer challenges due to their Centro-symmetric sections [66]. This enhances their torsional resistance. It could also be because there are fewer applications for tapered tubes compared to open sections. Structural engineers do prefer to use tapered tubes because of their excellent resistance to torsion and this has led to a rising interest in non-prismatic tube members [66].

As the procedures for analysis and the design of non-prismatic members, research reported indicates the use of dividing non-prismatic members into a number of uniform elements. This method is referred to as step representation. Although this method is highly cumbersome, it is not limited to stepped and linearly tapered members only. It is valid even for the most complicated geometrically varying sections since it divides members into finite uniform elements. Some computer software packages such as ABAQUS, ADINA, ANSYS, SOLID45 and NASTRAN can be used to analyse members with non-uniform sections.

2.2 Non-prismatic steel members

Non-prismatic steel members are made up of various shapes as presented by Timoshenko & Gere [61], Kee-Dong & Michael [34], Sapountzakis & Mokos [56] and Samir [52]. They can either be in the form of linearly tapered, haunches, stepped or elliptic depending on the designer's choice. However, most of the research reports linearly tapered members. Not much has been said about other geometrical shapes mentioned earlier except some few studies mentioned about stepped members [61]. This could be because of the difficulties in the analysis and time required for the computation.

However, there are various approaches employed by many researchers in the treatment of non-prismatic framed members, namely:

- Chebyshev polynomial approach [24]
- Power series approach [52]
- Bassel function [40]
- Rayleigh-Ritz method [3]
- Iteration procedure [18]
- Stochastic optimization [42]
- Runge-kutta method [39]

None of these methods used in the analysis of non-prismatic members considered the general structural behaviour of non-prismatic members in response to varying degree of non-uniformity.

2.2.1 Stepped column steel members

This is the type of steel members with cross-sectional dimension changes abruptly along the member axis. Its geometrical configuration resembles what is known as step representation. However, there has not been much attention paid to this type of non-prismatic steel members except in [61]. This may be because it can be analysed as long as the number of steps do not exceed a certain number for a specific fixity. For instance, Timoshenko & Gere [61] suggests that the maximum number of stepped section is one for a cantilever member with applied axial load at the free end while for pin ended support conditions, the maximum numbers of stepped sections are two.

The accuracy of this result is still questionable, since the numbers of steps used are so few and this may lead to a wide margin of error. Moreover, the critical buckling load is determined by trial and error, which may not be a reliable method of analysis. Therefore, in cases where the number of steps along the member increases, the method cannot be easily applied. To obtain a more accurate and general result, different boundary and loading conditions with higher number of steps should be investigated.

2.2.2 Reduced Beam Section (RBS)

This type of non-prismatic steel members can be distinguished from those of stepped, tapered or elliptic because they have no clear link in the positioning of the reduced beam section and beam's length. The positioning of the reduced beam section purely depends on the designer's choice. They are mainly used in the earthquake design and have been specified in some design standards such as (AISC 2005a, b; FEMA 2000). Kee-Dong and Michael [34] investigated the behaviour of reduced beam section connections in steel moment frames by the use of finite element method. They reported that by using 50% flange reduction in width at a localised region, the increase in the maximum storey drift ranges from 6 to 8% for typical moment frame buildings. However, when using 40% flange reduction, 4.5 to 6% increase in the maximum storey drift is achieved.

This is in contrary to 11% increase concluded by Chambers [12] and only about 5% increase in the storey drift reported by Grubbs [23] for the same 40% flange reduction in width.

The result obtained by Kee-Dong and Michael [34] shows a direct correlation between the flange reduction and the maximum increase storey drift of a typical moment frame building. The storey drift depends on the stiffness of the frame which is a function of the cross-sectional properties of the members, different connection types and loading conditions. It would have been more appropriate for Kee-Dong and Michael [34] to consider these factors in order to generalise the relationship between the reduced beam section and the corresponding maximum increase storey drift. According to the literature studied, there is still emerging interest to do further research on the overall reduced beam section in order to accurately quantify the effect of RBS on the elastic stiffness of the frames.

2.2.3 Analysis of tapered steel members

Tapered members are non-prismatic members with cross-sectional properties varying linearly along the member's length. Tapered members can either be used for beam, beam-column or framed system as a whole. There are various members types (closed or open), which can be used as tapered members; I, Z, W, circular, rectangular, angle and box sections. Most research done on non-prismatic or tapered members dealt with I-section tapered members.

Some of the I-section tapered members investigated are reported by Baptista & Muzeau [6], Saka [50], Sapalas [54], Rajasekaran [48], Siu [58], Jong-Dar [32], Andrade and Camotim [3] and Guo-Qiang and Jin-Jun [24]. An I-section member can either be tapered in the web, flange or both. Most designers prefer to taper the web, whether it is for static or dynamic analysis. However, there is no clear reason for such decision that has been mentioned in the published research.

Only Rajasekaran [48] and Siu [58] have so far considered tapering the flange in the stability analysis of beams. Siu [58] compared the effect of tapering the web on the same beam based on the fact that the web and the flanges are under different actions in beam.

Rajasekaran [48] investigated the effect of the tapering ratio on the member's behaviour but did not consider the effects of different boundary conditions except the simple and rigid supports, nor did he investigate different member sections apart from I-section. Kitipornchai and Trahair [35] investigated the flexural torsional buckling effect of a member by tapering the flange width or thickness but not both at the same time. Along the same line, O'Rourke [47] investigated columns while Shiomi and Kurata [57] investigated beams. Kitipornchai and Trahair [35] developed the idea from [37], which explained most of the research carried out on tapered members before 1972. Nethercot [45] investigated the effect of tapered cantilever beam on buckling of the members.

Researchers like Brown [9], Horne [26] and Lee [39] only narrowed their investigations on simply supported beams yet the stability of a member does not only depend on the cross-sectional properties of the member but also on the effective length of the member hence, different boundary conditions play a big role in the investigation of member's stability behaviour. None of the researchers mentioned above investigated the effect of tapering both the web and the flanges at the same time on the same beam under the same loading and boundary conditions.

Furthermore, not much has been published about the closed section tapered members however, the few reported are Ramamurti and Karthikeyan [49], Yaozhi [66] and Dube and Dumir [17]. Ramamurti and Karthikeyan [49] used tapered tube in the stress analysis while Yaozhi [66] used tapered-end members in the strength analysis and concluded that it is more sufficient to use tapered-end members without considering the effects of other factors such as different tapering angles, different tapering positions, different loading conditions and different boundary conditions because all these factors affect the strength of the members.

Dube and Dumir [17] used a more general approach in the dynamic analysis of the tapered tube in which different boundary conditions, different loading conditions and different thickness to length ratio were considered. Dube and Dumir [17] used a more general approach but other factors such as tapering angles and tapering position, which

affect the stiffness of the member, were over looked. For further research work, these factors should be considered.

Different researchers use different approaches in their analysis of tapered members. Most research reported considered the use of numerical model as opposed to experimental and analytical models. This could be as a result of the commercially available computer packages, which can handle nonlinear analysis. The difficulties in formulating the equations and boundary conditions of the tapered members and/ or it could be because of the high cost associated with the investigation of experimental models.

Some researchers like Saka [50], Siu [58] and Rajasekaran [48] used numerical method in the analysis of tapered members. Siu [58] used the Lagragian approach in the application of strain energy method. The process was simplified by using linear shape function and integration package such as Macsyma when deriving the element stiffness. On the other hand, Rajasekaran [48] used a unique element in such a way that the uses of an arbitrary system of axes passing through any reference point as reference system for lateral displacements and twist was considered. Saka [48] treated the depth of the section at each node as a design variable between the nodes. The depth is assumed to vary linearly while the width, the thickness of the flanges and the web were kept constant for simplicity.

After setting up the equations which could best describe the behaviour of a tapered member, Saka [50] developed an algorithm which can be used to determine the approximate solution of the problem by summing up the incremental results for each section of the members. When the incremental section sizes become smaller, the tapering effect also becomes negligible hence they are treated as uniform members within a section [50].

This method is not limited to the linearly tapered members only since it can also be applied to an arbitrary cross-section as long as the incremental section sizes are made smaller.

On the other hand, Sapalas [54] proposed a simpler procedure for the design of tapered members by applying the modification factors to the available design guidelines of

prismatic members. He narrowed his investigation on Euler buckling of column and lateral-torsional buckling of beam members. The buckling correction factors for non-prismatic members are determined by comparing the buckling expressions for prismatic members to the ones of non-prismatic members as seen in equation (2.1) and (2.2).

$$\left(\frac{\pi}{\mu_y L}\right)^2 EI_{tr} = \alpha_n \left(\frac{\pi}{\mu_y L}\right)^2 EI_{y2} \quad \text{.....(2.1)}$$

$$EI_Z\left(GI_{ttr} + \left(\frac{\pi}{\mu_\omega L}\right)EI_{\omega tr}\right) = \alpha_m{}^2 EI_Z\left(GI_t + \left(\frac{\pi}{\mu_\omega L}\right)EI_\omega\right) \quad \text{.....(2.2)}$$

where;

α_n - Correction factor for Euler buckling of non-prismatic columns.
α_m - Correction factor for lateral-torsional buckling of non-prismatic beams.
I_{tr} – Moment of inertia for a prismatic column [m^4]
$\mu_y L$ – Effective length of the column members [m]
I_{y2} - Moment of inertia for a non-prismatic column [m^4]
EI_z – Flexural rigidity of the beam members [Nm^2]
G – Shear modulus of elasticity [N/m^2]
I_w – Warping constant [m^6]

α_n and α_m were determined from numerous models carried out for different web tapering angles of I-section member having the same weight and boundary conditions. There are challenges associated with equations (2.1) and (2.2) because their development was based on cantilever H-section columns and pin ended I-section beams only.
On the other hand, the equation relating the moment of inertia I_x at any section along the axis of the steel member is given in (2.3), [61].

$$\mathbf{I_x} = \mathbf{I_c}\left(\frac{x}{\propto}\right)^n \quad \text{..... (2.3)}$$

Where $\mathbf{I_x}$ is the moment of inertia of the cross-section at a distance x from the origin and $\mathbf{I_c}$ is the moment of inertia of a cross-section at a distance α from the origin. This law governing equation is only limited to specific types of cross-sections.

As a check on the validity of expression (2.3) for determining the moment of inertia I_x at any cross-section along the axis of non-prismatic steel members, when the exponential variable n = 1, equation (2.3) results into the moment of inertia for a solid rectangular steel section. Furthermore, it can also be proved analytically that when n = 2, a box hollow section made up of four angle bars at its corners results [61].

Equation (2.3) has limitations because it is only applicable to steel sections that do not find wide application in construction industry. Therefore, there is the need to address the challenges for open non-prismatic steel sections like I, H, L & Z as well as closed sections steel like square, rectangular and circular hollow steel sections, which find wide applications in the construction industry.

Moreover, in the practical design procedures, it is very difficult to apply equation (2.3) because the second moment of area I_x is still a variable along the member and the challenge is to determine how a varying I can be used in design. Also, equation (2.3) can not be applied to another form of non-prismatic steel members, which do not have a linearly varying geometry, example includes stepped steel members. These types of steel members have constant cross-sectional dimensions for a specific segment and changes cross-sectional properties abruptly to new dimensions along the member. Equation (2.3) would have been a more general approach to the design of non-prismatic members if it catered for most of the open steel sections, which are used in practical design guidelines.

The law governing equation (2.3) for variation of the moment of inertia I_x along the axis of the bar developed by Timoshenko & Gere [60] was used by Ermopoulos [18] in the analysis of equivalent buckling length of non-prismatic members. The application of (2.3) is limited to members having constant or approximately constant cross-sectional areas. This makes equation (2.3) insufficient for design application since most practical steel members have open variable cross-sectional areas. Therefore, there is the need to update equation (2.3) to cover a wider application such that it can be included for the

design of non-prismatic members in the available design codes. The lack for modification of (2.3) shows that there has been little research work on the design of non-prismatic steel members since 1961.

According to Baptista & Muzeau [6], the design of tapered members can be extended from the known design guidelines of prismatic members in Euro code 3. In the design of prismatic compression members, the buckling resistance is determined by the use of equation (2.4).

$$N = X\beta_A A f_y / \gamma \quad \text{(2.4)}$$

where;

f_y - The yield stress of the member [N/m^2].

A - Cross-sectional area of smaller section of the member [m^2].

X - The reduction factor for the relevant buckling curve

β_A - The correction factor for the lateral torsional buckling curves for rolled sections.

γ - Material factor

The function (2.4) can be expanded to cater for non-prismatic steel members by including the correction factor K. The value of K is determined from the graph of K against slenderness ratio λ for different tapering ratio, (h/H), where h is the dimension of the member at the smaller section while H is the dimension of the member at the larger section of a tapered steel member.

The modified formula for non-prismatic (tapered) members is given in equation (1.0), in which, N_n is the buckling resistance of the tapered members and K is a coefficient taking into account the effect of tapering on the member buckling resistance. The value of K is determined only for the tapered members and the challenges still remain on how to update expression (1.0) in order to incorporate the application of K value to other form of non-prismatic steel sections.

However, Muller [43] applied the use of finite element method which considers elements with constant sections. The elements are defined by the cross-section at the ends of the

members. In determining the stiffness matrices, the assumption of linear elastic material behaviour and small deformation within the element was considered. The stiffness within the element is computed in the integration points of the actual cross-section. For the description of deformation behaviour perpendicular to the member (beam) axis, an approximation approach of 5th order and along the axis, an approach of 2nd order was applied. This function is flexible and can be used to model tapered members with one element. In addition, the problem of lateral-torsional buckling resistance is reasonably carried out by an optimised in-plane-design without using plastic capacities [42].

2.2.4 Analysis of arbitrarily non-prismatic steel members

The use of power series which is some times referred to as Maclaurin series has been employed by Samir [52] and Dube & Dumir [17] to solve the problem of analysis for non-prismatic members. Dube & Dumir [17] used the power series approach to solve for the buckling behaviour of steel members under elastic foundation and different degree of non-uniformity but overlooked different loading conditions and steel sections. Samir [52] used arbitrary axial loading and arbitrary non-prismatic members but did not consider the effect of different degree of non-uniformity and boundary conditions on the members which affect the stability of the members. Both Samir [52] and Dube & Dumir [17] developed their analysis from the general expression (2.5). Where, the variable moment of inertia **I**(x) of a general non-prismatic beam and or column can easily be presented in power series as seen in equations (2.5) to (2.8) in which X was also replaced by εL for simplicity of analysis.

$$P(x) = \sum_{i=0}^{ip} p_i x^i \quad \text{.....(2.5)}$$

$$\mathrm{I(x)} = \sum_{i=0}^{\infty} IiX^{\,i} \quad \text{..... (2.6)}$$

$$\frac{d^2}{dx^2}\left[EI(x)\frac{d^2y}{d^2x}\right] + p\frac{d^2y}{dx^2} = 0 \quad \text{.....(2.7)}$$

$$\frac{d^2}{d\varepsilon^2}\left[\left(\sum_{i=0}^{\infty} I_i L^i \varepsilon^i\right)\frac{d^2y}{d\varepsilon^2}\right] + \frac{pL^2 d^2 y}{Ed\varepsilon^2} = 0 \quad \text{.....(2.8)}$$

where;

I(x) - The variable moment of inertia [m^4]

I_i - The nodal moment of inertia [m^4]

X^i - The varying distance along the member [m]

i - An integer (0, 1, 2, 3….)

p(x) - Any variable quantity of the cross-section

P_i - An integer representing the number of terms in each series.

εL – Modified variable distance along the members [m]

ε – Tapering ratio of the members

From the power series, there is the need only to determine the terms I_i and X^i in order to approximate the moment of inertia of the element using the convergence theorem of the power series. Here, I_i is considered to be the sequential value and is determined at every node while X^i is the distance from the origin to the i^{th} node along the beam member [52]. The number of the sequential parameter I_i depends on the density of the mesh of the model but for more accurate results, a dense mesh is required.

Furthermore, Samir [52] suggested the use of non-dimensional variable ε, which is the ratio of variable distance x along the member to the total length L of the member. This eliminates the possible errors in units and also easier to deal with a constant length L than a variable parameter x all the times when applying the formula (2.5).

From the general fourth order differential equation for determining the deflection of a cantilever beam, the exact expression for the determination of displacements (rotation and translation) can be written. In this case, the value of the moment of inertia I for prismatic steel member is being replaced with the whole expression for power series (2.7), which makes it difficult for the analytical analysis of non-prismatic steel member hence, this procedure is only limited to numerical analysis.

Moreover, the difficult task is also on how to determine the nodal moment of inertia based on the fact that the more the nodes, the better the modal results but the more tedious the calculation is. Once, a simplified procedure of determining those nodal moment of inertia I_i is developed, the method of slope deflection can then be applied to

determine the stability function of non-prismatic (in terms of geometry along the member) steel member [52].

2.2.5 Arbitrary Cross-section

Steel members can also be non-prismatic with respect to cross-sectional geometry. This also raises a big challenge in structural design. For such members with no clear design guidelines which can be used for the computation of physical parameters like the second moment of area I, warping constant I_w and torsional constant J. These factors are easily computed for the design of uniform hot rolled cross-sections such as I, H, Z, & L, therefore, there is the need to investigate their behaviour. It has also been reported by Siu [57] that the shape of the cross section affects the stability of the members.

These types of cross-sectional shapes are very difficult to analyse analytically by direct integration hence, there is high demand on computer packages if these arbitrary steel shapes are to be put in practice. Therefore, in order to simplify the calculation of the physical parameters of the arbitrary cross-sections, the use of computer aided design (CAD) modellers and finite element method (FEM) analysers need to be employed to reduce the number of variables. This in turn leads to an inexpensive 2-D optimization as an alternative to costly 3-D shape optimization with multiple numbers of variables that may virtually be impossible for real life built up structures as derived by Apostol [4].
The multi-contour cross-section has to be descretized in elementary shapes, either triangles, rectangle etc. The cross-section velocity field defined [4] is used to relate the higher level shape variables with the lower levels. Vertex and control points used to define the cross-section contour. Once the design parametrization is known, the design sensitivities of the vertex coordinates with respect to the shape variables may easily be computed.

Apostol [4] and Siu [58] are so far the only researchers to have considered the design of arbitrary cross-sections. Siu [58] conducted two sets of experiments on a tapered H-section column and a tapered hexagonal beam. Siu [58] found out that buckling occurs at the mid-height of an H-section tapered column hence it has a higher buckling load compared to its counterpart prismatic one. While for the case of hexagonal tapered beam,

the buckling occurs at the apex and its buckling load is lower than that for prismatic members. This clearly demonstrates the effect of shape on the stability of steel members.

2.3 Buckling of non-prismatic steel members

Buckling is one of the most common failure modes associated with steel structures and it largely depends on the material and physical properties of the members. The most physical parameters which affect the buckling load of steel members are the cross-sectional dimensions, the shape and the effective length of the members. Buckling of steel members can either be global (both lateral and lateral torsional), local or both. The methods available for determining buckling load are energy method and equilibrium method which is mainly used for computer non-linear analysis. At the buckling load the equation of equilibrium reduces to (2.9);

$$KU - \lambda_l K_G U = 0 \quad \text{..... (2.9)}$$

Where K_G is initial or geometric stiffness matrix computed for reference load
λ_l is the load factor and U the buckled shape expressed in a relative sense [47]. Local buckling of a member mainly depends on the slenderness ratio (b/t) of the section.

The cross-sectional dimensions of the members are directly linked to the moment of inertia and the slenderness ratio which are in turn directly linked to the stability of the members. Changes in any of these parameters will affect the buckling resistance of the member drastically. Therefore, by having non-prismatic steel members, the problem of analysis and design of non-prismatic members for stability become more complicated. This is seen from Euler formulae of stability (1.1), the moment of inertia is the only physical parameter which can be determined by calculation and is considered to be a constant. As the cross-section of the element changes, the moment of inertia of the element changes as well since it depends on the cross-sectional dimensions. The complication arises as to which value of second moment of area to use in the determination of critical buckling load for a non-prismatic steel member if expression (1.1) is to be applied. However, Baptista & Muzeau [6] suggests that correction factor be

applied on equation (2.4) to cater for the changing second moment of area but the challenge still remains on how to determine the unique value for the correction factor.

An examination of the bending moment diagram for a buckled bar indicates that a bar of uniform cross-section is not the most economical form to carry compressive loads since not all the materials will be used in resisting the applied compressive load [61]. This can be demonstrated by the use of pinned ends compression members. Keeping the weight, volume and fixity constant but changing the section depth by removing the portion of material from the end and increasing the middle cross-section [61]. It is observed that there is an abrupt increase in the stability of the same member although the procedure for determining the buckling load is so cumbersome [61]. In addition, the global buckling load will be increased but the effect on the local buckling capacity of the section is not known since the member section changes from a lower stocky class to a higher class. Therefore, it is recommended that further investigations be carried out.

A straight forward and commonly used technique to analyse a tapered or non-prismatic beam-column is to divide the member into a number of uniform segments [58]. The challenge faced with this method is that it requires more number of elements in order to obtain an accurate solution in the analysis of the sharply tapered members.
Therefore, this results into heavy consumption of central processing unit (CPU) time, data preparation and manipulation efforts when the computer is used for the analysis. It also does not cater for wide range of boundary conditions, load applications and different tapering ratios that would eventually determine the optimum design conditions.

2.3.1 Snap-through

This is one of the most dangerous scenarios encountered by engineers since the structure does not go through a gradual failure process but snaps straight to collapse [58]. It is very difficult to monitor the snap-through failure mechanism in steel structures. It has been noted by Muller [42] and Siu [58] that non-prismatic steel members are more susceptible to snap-through failure mode. Therefore, it renders this type of members not suitable for the construction of space frame structures.

However, non-prismatic members will not reduce only the material cost, but also the dead weight of the structure and have higher stiffness due to smaller strain energy stored in them [58]. Non-prismatic members have number of challenges depending on the buckling modes. If the buckling occurs at a smaller section of the member, the snapping load will reduce as a result of reduction in the section's stiffness caused by removing part of the material to the central part of the member as compared to its uniform counterpart, rendering the member unsuitable for some structures like space frames.

2.3.2 Effective length factor for non-prismatic steel members

The effective length of any member affects its stability. At the moment, there are many methods used in determining the effective length factor for steel members. For the prismatic members, the most commonly used method is the column alignment charts.
These charts provide an easy and rapid route for design engineers in determining the effective length factor for both braced and un-braced frames. In order to use these charts, there is the need to calculate the parameters G_A and G_B which measure the restraints provided to the ends of the column under consideration.

G can be calculated as shown in equation (2.10);

$$G = \frac{\sum \mathrm{I}_c / L_c}{\sum \mathrm{I}_g / L_g} \qquad \text{.....(2.10)}$$

where;
∑(Ic/Lc) is the summation of the moment of inertia divided by length of all columns framing into the joint under consideration, and ∑(Ig/Lg) is the summation of the moment of inertia divided by length of all beams framing into the joint under consideration. The alignment charts used in the determination of effective length factors are shown in (Fig.2.1);

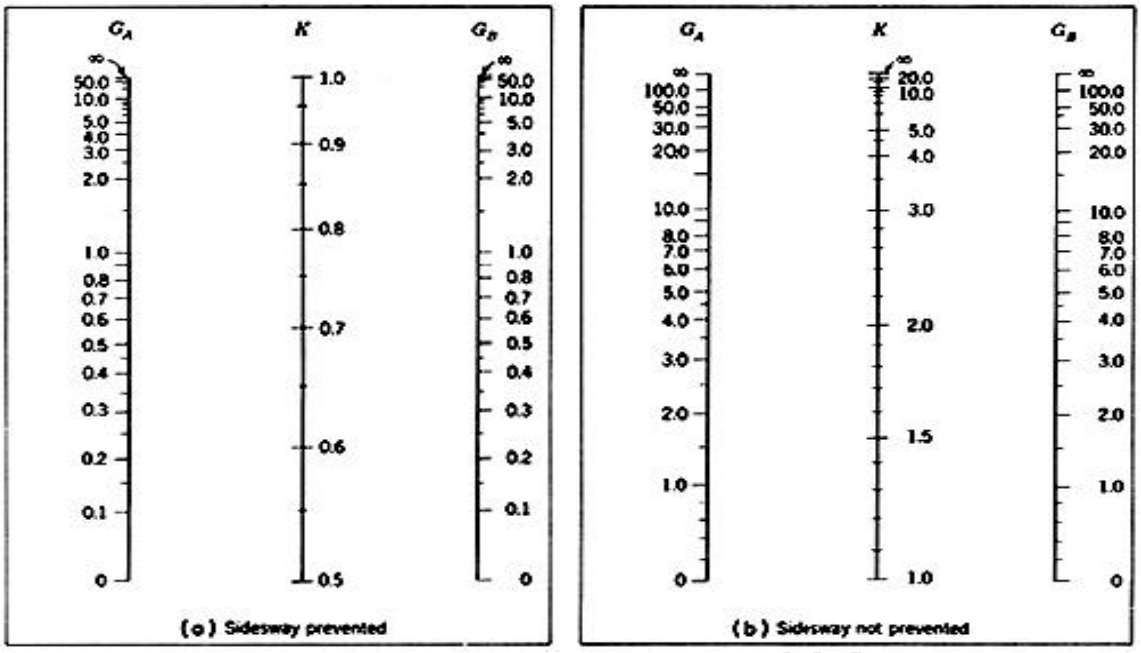

Figure 2.1 Design alignment charts [29]

The alignment chart is sometimes considered to be insufficient since its development is based on assumptions which are not satisfied in practical situation [21]. These assumptions are the following:

1. Behaviour is purely elastic.
2. All members have constant cross section.
3. All joints are rigid.
4. For braced frames, rotations at opposite ends of beams are equal in magnitude, producing single-curvature bending.
5. For un-braced frames, rotations at opposite ends of the restraining beams are equal in magnitude, producing reverse-curvature bending.
6. The stiffness parameter $L\sqrt{\frac{P}{EI}}$ is constant for all columns.
7. Joint restraint is distributed to the column above and below the joint in proportion to I/L of the two columns.
8. All columns buckle simultaneously.
9. No significant axial compression force exists in the girders.

If these assumptions are not satisfied in the design procedure, unrealistic estimates of effective length results from the design [11]. According to Assumption 2, the charts are only applicable to frames composed of prismatic members hence it cannot be applied to non-prismatic members. Assumptions 4 and 5, relating to equal end rotations of the restraining beams are not satisfied when the charts are applied to frames in which both the members and loadings are not symmetrical. The same applies to assumption 6 which is not often satisfied in actual practice. The assumption that all columns in a storey buckle simultaneously precludes the consideration of "stronger" columns assisting "weaker" or "leaner" columns when using the alignment charts. Because many of the above limitations are not often met, the use of alignment charts can frequently lead to unrealistic designs [11].

To address the limitations associated with the alignment charts, Chu & Chow [15] proposed a correction curve to modify the value of K obtained using the alignment charts. This method was proved by Johnston [31] as it is possible to be used when column sizes and loadings are not symmetrical but it still relies on the assumption that all columns in the frame reach their buckling load simultaneously. The method for determining the modified effective length factor is given in (2.11).

$$K_{modified} = \beta K \quad \text{.....(2.11)}$$

where;

$K_{modified}$ – Modified effective length factor

β - The correction factor determined from the tables.

K - The effective length factor determined from the alignment charts.

The alignment charts only use prismatic members but some researchers have extensively tried to modify them to incorporate the design of non-prismatic members [15]. One of the most widely known methods for calculating the effective length factor of non-prismatic columns was developed by Lee [39] and involved modifying the length of the member to obtain an "equivalent" prismatic member length which is also employed by Ermopoulos [42]. This "equivalent" member is based on the section properties of the smaller end of

the tapered member hence the design guideline is so conservative and therefore leaves room for modification [6]. The equation used by Lee [39] in determining the modification factor is given in (2.12).

$$P_{tapered} = \frac{\pi^2 EI_0}{(gl)^2} \quad \text{..... (2.12)}$$

Where $P_{tapered}$ is the critical elastic lateral buckling load of the tapered column, I_0 is the strong axis moment of inertia of the smaller end of the tapered members, and gl is the modified length of the tapered member pinned at both ends. The equation (2.12) can be rearranged to solve for the modification factor, g, (2.13).

$$g = \frac{\pi}{L}\sqrt{\frac{EI_0}{P_{tapered}}} \quad \text{..... (2.13)}$$

All the elements in this equation are known with the exception of $P_{tapered}$. Lee [39] used various lengths and degrees of tapering to determine the value of $P_{tapered}$ for each case. Using polynomial curve of best fit for the data, the equation of modification factor, g, can be obtained from expression (2.14).

$$g = 1 - 0.375\gamma + 0.08\gamma^2(1 - 0.0775\gamma) \quad \text{..... (2.14)}$$

Where;

$$\gamma = \frac{d_1}{d_0} - 1 \quad \text{..... (2.15)}$$

For the linearly tapered member, the depth at any distance z from the smaller end can be expressed as seen in equation (2.16).

$$d_z = d_0\left(1 + \frac{z}{L}\gamma\right) \quad \text{..... (2.16)}$$

Where d_1 is the section depth at the larger end of the member and d_o is the section depth at the smaller end of the member. These formulae can be verified, for instance if d_1 is

equal to d_0, the value of g is unity which conforms to the equation for prismatic column members with pinned- pinned joints.

The modification factor, g, was developed only for pinned ends connections therefore, to cater for members with different end connections, Lee [39] proposed a chart for determining Kγ which is the effective length factor for other end connections. The length of members framing in at a joint must be modified if the members are non-prismatic.

This can be done conveniently using the length modification factor; g. Equation (2.17) describes the use of this parameter.

$$G = \frac{I_{0c} / g_c L_c}{I_{0g} / g_g L_g} \quad \text{..... (2.17)}$$

where;
G is the joint restraint, I_{oc} and I_{og} are the moments of inertia at the smaller ends of the column and beams respectively; g_c and g_g are the length modification factors of the columns and beams, respectively, L_c and L_g are the actual lengths of the columns and beams, respectively. The values of G obtained for both ends of the column are then used in the charts to determine Kγ which is the modified effective length factors. However, there is still the need for more research to be done because the method described above heavily relies on charts and graphs which cannot be implemented in computer application [11].

The second procedure for determining the effective length factor which does not rely on correction curve and does not assume that all columns buckle simultaneously (2.18) was proposed by Cary [11].

$$K_i = \sqrt{\frac{\pi^2 I_i}{P_{ui}}\left[\frac{\sum P_u + \sum (C_L P_u)}{\sum (\beta I)}\right]} \quad \text{..... (2.18)}$$

K_i - The effective length factor for the i^{th} column in the storey under consideration

$\sum P_u$ - The sum of the vertical forces acting on the storey [N]

$\sum(C_L P_u)$ - The sum of $(C_L P_u)$ for each column in the storey [N]

$\sum(\beta I)$ - The sum of (βI) for all columns in the storey [m^4]

P_{ui} - The axial force in i^{th} column based on a first-order analysis [N]

I_i - The moment of inertia of the i^{th} column [m^4]

C_L - A stiffness correction factor to account for P-δ effects, and is defined as

$$C_L = \frac{K_n^{\,2}}{2} - 1 \quad \text{..... (2.19)}$$

Where K_n is the effective length factor as determined from the alignment charts, and β is a column end restraint coefficient defined as follows:

$$\beta = \frac{6(G_A + G_B) + 36}{2(G_A + G_B) + G_A G_B + 3} \quad \text{..... (2.20)}$$

Chen & Toma [13] suggested a more detailed investigation on the method proposed by Cary [11] citing that the method relies on the assumption that the quantity $L\sqrt{\frac{P}{EI}}$ (where L is the column length, P is axial load, and EI is flexural rigidity) is equal for all columns in a storey which is unrealistic in practical situations.

Cary [11] used SAP90 [51] computer package in the modification of the equation (2.18) for prismatic members to incorporate the application of tapered members. The fact that this method does not rely on many of the restricting assumptions incorporated in the derivation of the alignment charts, it can be assumed to give accurate results for the frames in which members and loadings are not symmetrical. In addition, the method does not assume that all columns in a storey reach their buckling load simultaneously.

Because this method does not rely on the use of charts or iterative solutions, it lends itself suitable for computerized solution and makes it an ideal candidate for modification of frames with non-prismatic members where it allows accurate estimation of column effective length factors.

SAP90 [51] has the ability to allow for the presentation of moment of inertia of tapered members. The equation (2.21) is used by SAP90 [51] to describe parabolic variation in moment of inertia along the length of the member [11].

$$I = I_0\left[1+\left(\left(\frac{I_L}{I_0}\right)^{1/2}-1\right)y\right]^2 \quad \text{.....(2.21)}$$

where;

I is the moment of inertia at the point of interest, I_L is the moment of inertia at the larger end of the member, I_0 is the moment of inertia at the small end of the member, and y is the ratio of the distance to the point of interest (measured from the smaller end) divided by the length of the member [11]. Cary [11] proposed a formula for determination of K-factor as given in equation (2.22). The detailed derivation is not included here. According to Cary [11], the moment magnification factor, A_F, is given in equation (2.22).

$$A_F = \frac{1}{\left(1-\frac{\sum P/L}{5\sum \eta}\right)-\sum\left(\frac{p}{L}\right)\left(\frac{\Delta_1}{\sum H}\right)} \quad \text{.....(2.22)}$$

And according to Chen [13], it is given in equation [2.23].

$$\left(A_F\right)_i = \frac{1}{1-\frac{P_i}{\left(P_{ek}\right)_i}} \quad \text{.....(2.23)}$$

where;

$$\left(P_{ek}\right)_i = \pi^2 EI_i \Big/ \left(K_i L_i\right)^2 \quad \text{.....(2.24)}$$

Equating the two expressions for moment magnification factor, yields the proposed effective length factor for non-prismatic members [11].

$$K_i = \sqrt{\left(\frac{\pi^2 EI_0}{P_i L^2{}_i}\right)\left[\left(\sum P/L\right)\left[\frac{1}{5\sum \eta}+\frac{\Delta_1}{\sum H}\right]\right]} \quad \text{.....(2.25)}$$

where;

$$\eta = \frac{\left(3 + 4.8m + 4.2m^2\right)EI}{L^3} \quad \text{..... (2.26)}$$

m is the ratio of the smaller to larger end moments of the members. EI_i and L_i are the flexural rigidity and length of the member, respectively. P_i is the axial force in the member, $\sum(P/L)$ is the sum of the axial force to length ratio of *all* members in a storey, $\sum H$ is the storey lateral loads producing Δ_I, Δ_I is the first-order inter-storey deflection, and η is the member stiffness index [11].

In the procedure developed by Cary [11], the optimisation of the tapering ratio would have been considered to allow the use of a dimensionless parameter (ratio of the smaller moment of inertia to the larger one) instead of using the moment of inertia of the smaller section of the member which renders the design highly conservative. And also, the assumption of the $\sum H$ which is not the actual lateral load applied to the frame but the fraction of the gravity load. The question here is how much fraction of the gravity load one should apply as lateral load in order to obtain a meaningful result?

2.4 Equivalent non-prismatic steel members

The analysis and design of non-prismatic steel members can be obtained by application of correction factors to the design guidelines for prismatic members. This approach has mainly been employed for stability analysis. Sapalas [54] proposed equations (2.1) and (2.2) while Baptista & Muzeau [6] proposed equation (1.0) for buckling analysis of non-prismatic members. For this approach, the critical buckling load of non-prismatic members is expressed in terms of the critical buckling load of the prismatic members.

The buckling length of non-prismatic members can also be expressed in a similar way as for buckling load but so far only Ermopoulos [18] is reported to have considered that treatment.

For both simplicity and errors minimisation, Ermopoulos [18] preferred to use dimensionless parameters in expressions (2.27) to (2.31) in his investigation but the detailed derivation is not included here.

$$\Gamma = \frac{L_c}{\alpha} \quad \text{.....(2.27)}$$

$$\overline{P}_m = \frac{PL^2{}_c}{E\,\mathrm{I_m}} \text{.....(2.28)}$$

$$\overline{P}_{cr} = \frac{P_{cr}L^2{}_c}{E\,\mathrm{I_m}} \text{.....(2.29)}$$

$$\mu = \sqrt{\frac{P\alpha^2}{EI_c} - \frac{1}{4}} \rangle 0 \text{.....(2.30)}$$

$$\mathrm{K} = \frac{\pi}{\sqrt{\overline{P}_{cr}}} \text{.....(2.31)}$$

where;

L_c - The length of the tapered bar [m]

α - The distance from the reference origin to the point in question along the member [m]

P - The external axial compressive force [N]

P_{cr} - The critical buckling load [N]

E - The modulus of elasticity [N/m^2]

$I_{c,}\, I_{1c}$ - The moment of inertia of the tapered bar at the two ends; say A and B [m^4]

I_m - The moment of inertia at the middle of the tapered bar [m^4]

K - The equivalent buckling length ratio

$\overline{P}_m$ - The external load [N]

In order to determine the equivalent buckling length ratio k of the non-prismatic member, the critical load $\overline{P}_{cr}$ of this member has to be established first.

In Ermopoulos [18], the determination of $\overline{P}_{cr}$ was done by iteration processes and the equivalent buckling load was evaluated from (2.31). From equations (1.1) and (2.28) to (2.30), the equivalent buckling ratio k is obtained by the expression (2.31) and depends on the distribution factor of the constant, I_m. Ermopoulos [18] over looked the types of shape, the cross-section must bear in order to fulfil the relationship of non-uniformity used in proposed guidelines.

The length correction factor K, for prismatic members is always determined either from alignment chart or from equation (2.20) for which the development of alignment chart is based on in order to use (1.1). This is applied in (EC3, Annex E) but can be extended to tapered members by use of equivalent buckling length. The equivalent buckling length can be determined through the manipulation of critical buckling load for both non-prismatic and prismatic members. In this way, a non-dimensional constant can be derived through graphical method. This constant is termed, the correction factor. Although this relationship can be applied to analyse the problem of non-uniform members, it is only limited to specific types of load cases, boundary conditions and shapes of the members from which the correction factor was derived. Therefore, it requires a more detailed investigation of the equivalent factor procedures to cover arbitrary loading cases, different boundary conditions and various members' shapes.

2.5 Stresses

Stresses can either be bending, shear, torsional or axial stress which results from the applied actions to the structures. They are both internal and external effects to the structural members and can be considered as the intensity of the action applied to the member over a specified area. Stress is considered to be crucial in the design of steel members because it is the main cause of strength failure in steel structures through yielding of the section if the localised applied stress exceeds the bearing capacity of the cross-section. For axially loaded tapered columns, the critical stress will always occur at the smaller end and decreases towards the larger section. This is because the cross-sectional area increases from smaller end to the larger section and simultaneously stress decreases from larger end to smaller section.

2.5.1 Shear deformation

Shear deformation has been verified to significantly influence the structural behaviour of prismatic steel members with I-section under certain conditions [24]. This can be extended to tapered members as well. It is possible that the effect of shear deformation acting in tapered members reduces its stiffness [24].

2.5.2 Bending stresses

The flexural formula gives reasonably accurate values for the bending stress in non-prismatic beams whenever the changes in the cross-sectional dimensions are gradual. In prismatic beams, the section modulus S (measure of flexural strength of a beam) is constant; therefore, the stresses vary in direct proportion to the bending moment M. However, in non- prismatic beams, the section modulus also varies along the longitudinal axis hence, the maximum stresses cannot be assumed to occur at the section with the largest bending moment [22]. Therefore, there is the need to develop functions which relate the distance along the axis and the corresponding depth at any point and which can be used to maximise the expression for bending stress in order to determine the maximum stress as reported in [22]. For detailed analysis, consider the beam shown in Fig. 2.2 with a rectangular solid section.

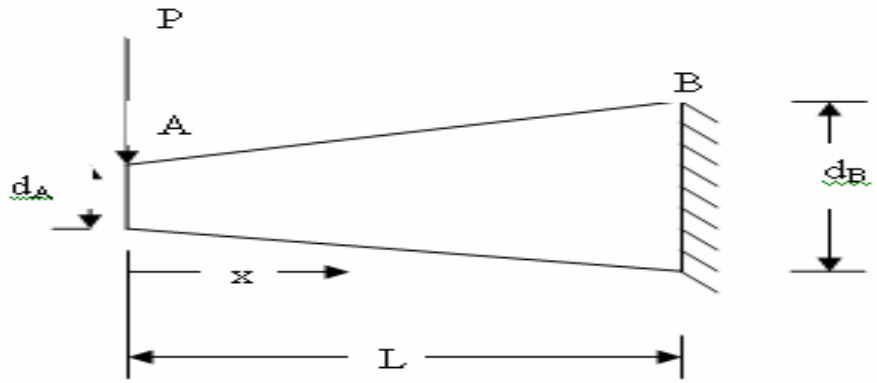

Figure 2.2 Tapered cantilever beam with a rectangular solid section

where;

d_A – Cross-sectional depth at the smaller section of the cantilever beam [m]

d_B – Cross-sectional depth at the larger section of the cantilever beam [m]

d_x – Variable cross-sectional depth along the cantilever beam [m]

P – Applied point load [N]

Assuming,

$$\frac{d_B}{d_A} = 2$$

$$d_x = d_A + (d_B - d_A)\frac{x}{L} \quad \text{.....(2.32)}$$

Therefore,

$$S_x = \frac{\pi d_x^{\,3}}{32} = \frac{\pi}{32}\left(d_A + (d_B - d_A)\frac{x}{L}\right)^3 \quad \text{.....(2.33)}$$

And stress σ_1 can then be formulated as shown in equation (2.34)

$$\sigma_1 = \frac{M_x}{S_x} = \frac{32px}{\pi\left[d_A + (d_B - d_A)\left(x/L\right)\right]^3} \quad \text{.....(2.34)}$$

Maximum stress at fixed sport B

When x = L

$d_B = 2d_A$

Upon substitution for d_B, equation (2.34) can be reduced to equation (2.35).

$$\sigma_B = \frac{4pL}{\pi d_A^{\,3}} \quad \text{.....(2.35)}$$

Maximum stress at a distance *x*

$$\sigma_1 = \frac{32px}{\pi d_A^{\,3}\left(1 + x/L\right)^3} \quad \text{.....(2.36)}$$

Optimisation of flexural stress of beam element requires determination of the location for which the maximum stress occurs.

To determine the location of the cross-section having the largest bending stress in the beam, take the derivative of $\frac{d\sigma_1}{d_x}$ and equating it to zero. After solving the equation, the value of *x* that makes σ_1 a maximum is L/2.

Upon substitution,

$$\sigma_{\max.} = \frac{128pL}{27\pi d_A^{\,3}} = 4.741\frac{PL}{\pi d_A^{\,3}} \quad \text{.....(2.37)}$$

$$S = \frac{bd_x^{\,2}}{6} \quad \text{.....(2.38)}$$

To justify the economical use of non-prismatic steel members, consider an I-section under flexural action shown in Fig.2.3**,** [38].

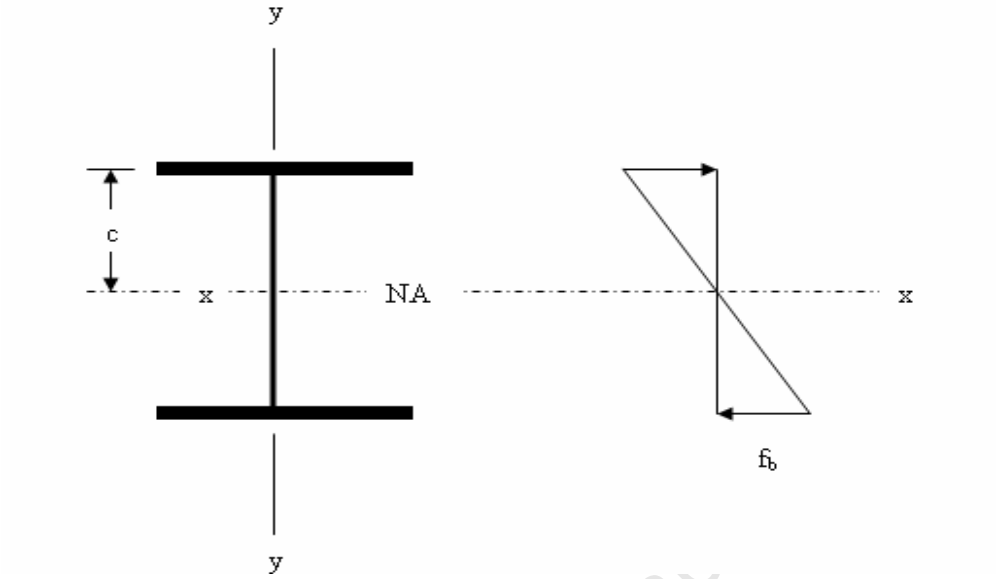

Figure 2.3 An I-section steel member showing stress distribution under bending moment.

Assuming the bending moment provided, M, the distance from the centroidal neutral axis, x, to the extreme fiber is, c, and the moment of inertia for a section is I, the formula for determining the flexural stress σ_b is given by (2.39).

$$\sigma_b = \frac{Mc}{I} = \frac{M}{S} \quad \text{.....(2.39)}$$

And section modulus, S, is given by function (2.40)

$S = I/c$ .....(2.40)

For a given bending moment, M, the minimum section modulus required of a beam is, $S = M/\sigma_b$.

From the formula (2.39) above, it can be seen that flexural stress of a member is directly proportional to the applied bending moment and inversely proportional to the section modulus. The smaller the bending moment, the smaller the section modulus is required in order to provide a uniform distribution of stress throughout the member. In this sense, the effective usage of material is achieved.

When considering a case of a solid circular cantilever beam in which the applied load varies as the cross-section does so along the members' axis, thus Fig. 2.4a. The incremental stresses at any point along the member can be determined.

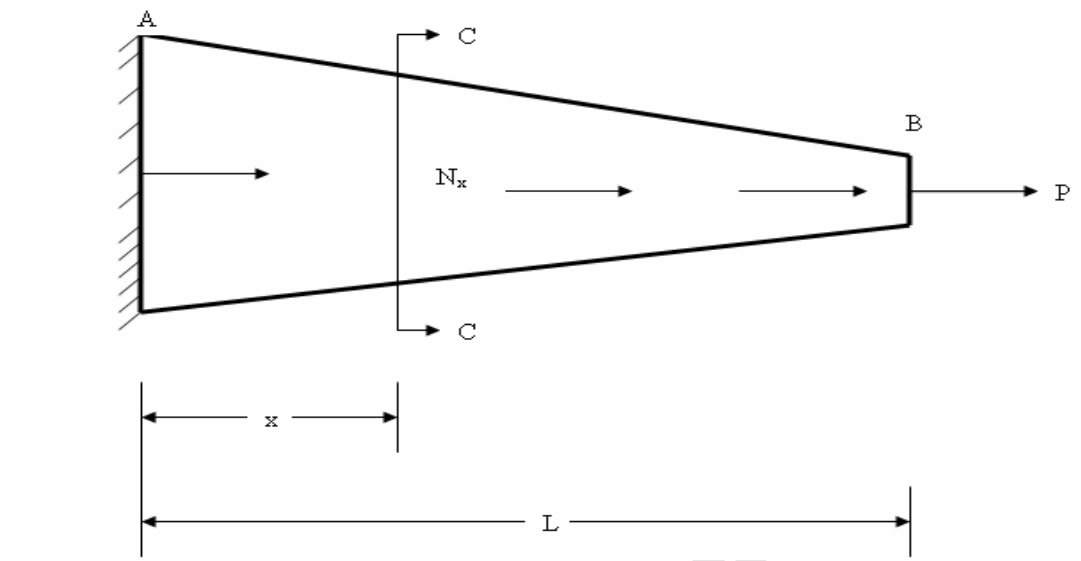

Figure 2.4a Tapered solid circular cantilever beam

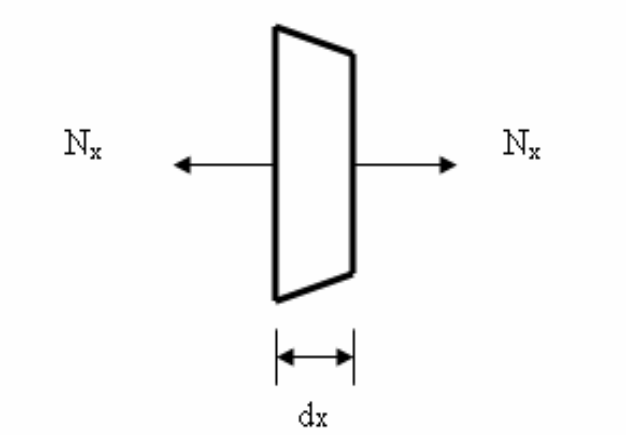

Figure 2.4b. An exploded slice of section c-c
Where p is the distributed varying applied force along the axis

To determine the total stress, it is necessary to consider the change in the length of a differential element of the bar and then integrate over the length of the bar as shown in equation (2.43).

$$d\sigma = \frac{N(x)d_x}{EA(x)} \quad \text{.....(2.41)}$$

$$\sigma = \int_0^L d\sigma \quad \text{.....(2.42)}$$

$$\sigma = \int_0^L \frac{N(x)d_x}{EA(x)} \quad \text{.....(2.43)}$$

where;

σ – Axial stress in the beam member [N/m^2]

N(x) – Variable internal axial forces [N]

A(x) – Variable cross-sectional area [m^2]

E – Modulus of elasticity [N/m^2]

2.6 Deflection of beam elements

Structural members, ranging from frame components to large bridge beams, could be non-prismatic or prismatic but their deflections are an important design consideration [5]. The deformations can either be obtained by the use of beam deflection theory or numerical methods such as the finite strip application, direct numerical integration of the governing equations and finite element methods.

The deflection is derived by the use of Bernoulli-Euler beam theory as shown in equation (2.44). To apply this formula, the beam element must be slender in order to hold the assumptions of Bernoulli-Euler beam theory of the cross-section remains plane before and after deformation.

$$EI(x)\frac{d^2u}{dx^2} = -m(x) \quad \text{.....(2.44)}$$

where;

EI is the flexural rigidity, u the deflection and m(x) the bending moment of the member.

However, it is Implicit in the use of this expression because of the assumption that the beam is sufficiently slender so that the variations in the cross-section do not affect shallow beam behavior i.e. small deflections and rotations, and linear direct strain across the beam [5].

For a linearly tapered cantilever beam with a uniformly distributed line load (UDL) from [52], equation (2.44) can be expressed as shown in (2.45).

$$EI(L)\left[\overline{K} + K\frac{x}{L}\right]u'' = \frac{qx^2}{2} \quad \text{.....(2.45)}$$

$$\overline{K} = 1 - K \quad \text{.....(2.46)}$$

where;

K - The ratio of the depth at the free end to the depth at the fixed end of the cantilever beam.

EI - Beam flexural rigidity [Nm^2].

q - The uniformly distributed line load (UDL), [N/m]

L – Length of the beam [m]

The deflection of a cantilever beam is reduced when cross-section of the fixed end is increased while for the free end is reduced as reported by Samir [52]. This is in close agreement with what was expected due to the effect of weight reduction at the free end. Therefore, there will be a shift in the center of gravity towards the clamped end. According to Baker [5], it is only for the span-to-depth ratio of less than 5 and the $\overline{K}$ of less than 0.5 does the tapering of the beam have significant effect on the maximum deflection at the tip of a cantilever beam with a solid rectangular section.

He also noted that as the tapering angle increases, the deflection decreases and this explains the hypothesis of effective increase in the stiffness at the fixed end of a cantilever beam.

After a number of empirical results, Baker [5] formulated the relationship between the maximum deflections of a prismatic steel member and non-prismatic steel members as seen in equation (2.47).

$$u_{tapered} = \frac{u_{prismatic}}{\sqrt{\overline{K}}} \quad \text{.....(2.47)}$$

Equation (2.47) suggested by Baker [5] may not be valid because in order to make the deflection for tapered members equal to the one of prismatic members, the ratio of the depth at free end to the depth at the fixed end must be one. From the expression (2.46), the value of $\overline{K}$ equals to zero when the tapering ratio K is unity and upon substitution for the value of $\overline{K}$ into equation (2.47), the resulting deflection of the tapered beam is infinity which is trivial.

It is only if $\overline{K}$ is replaced with K then the expression (2.47) relating the deflection of a tapered member with the prismatic members suggested by Baker [5] is valid for solid rectangular members. Therefore, further investigation may be required to correct and modify equation (2.47) in order to incorporate the application of open sections, different fixity and different loading conditions.

2.7 Effect of using non-prismatic steel members

Using non-prismatic steel members does not only provide benefit to the structures but has some challenges as well. As reported by Timoshenko & Gere [61], the computation of critical buckling load is more tedious for non-prismatic members as compared to that of uniform members. In addition, this may lead to higher degree of error occurrence. On the other hand, material saving, weight reduction and aesthetic appearance are observed [42]. For the same members under the same fixity, it was found that approximately 10% weight reduction can be achieved when using non-uniform members as opposed to uniform members [50].

2.8 Conclusion

The studies reported considered mainly linearly tapered I-section steel members under axial applied forces for stability analysis. None of them considered the effect of varying degree of tapering (tapering ratio) on the stability of the tapered members.

The applied actions like torsion, bending moment, etc and their resulting effects on the structures made up of non-prismatic members were not considered. Therefore, in this investigation, the effects of different tapering ratios, member classes, section types, boundary and loading conditions, which were not considered in the previous research, will be reported.

Chapter 3

Theoretical framework for numerical models of non-prismatic steel members

3.1 Introduction

Structural steel is made up of elements such as iron, carbon, vanadium, aluminium, chromium, molybdenum, copper, niobium and manganese. Steel members like any other construction materials exhibit unique structural behaviour which is quite different from other elements. For example, as can be seen in Fig.3.1, it is a ductile material. Moreover, it has high strength to volume ratio hence, it is lighter in comparison to concrete. Steel is very strong in tension as opposed to concrete which is very strong in compression. Yield strength of steel usually ranges from 200MPa to 1500MPa and it is very susceptible to fire since it loses its strength at the temperatures around 600^{o}C. It can be hot rolled and/ or fabricated to various shapes and forms such as I, H, Z, channel, angle etc sections, thus Fig. 3.2.

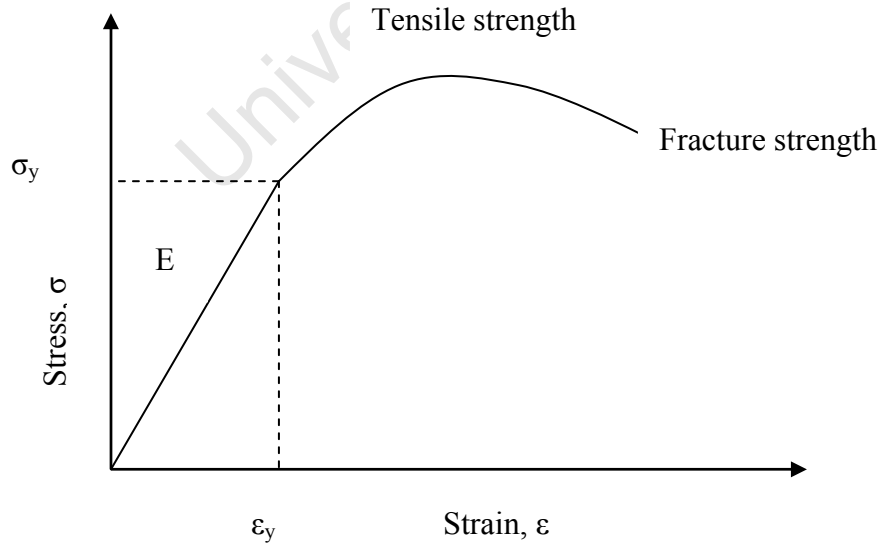

Figure 3.1. The engineering stress-strain curve

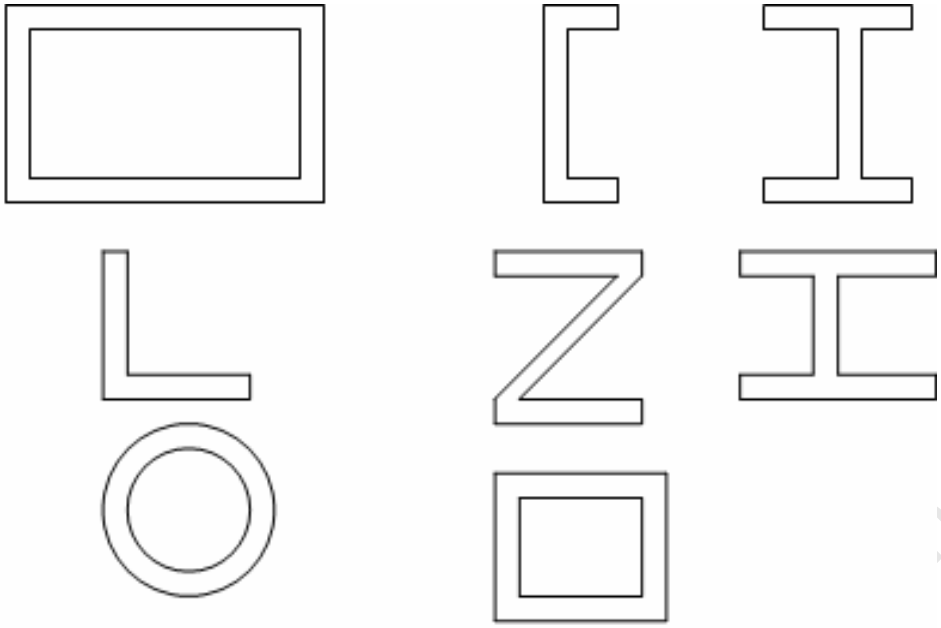

Figure 3.2. Various steel sections

3.2 Structural analysis of steel members

Of the three major design criteria for steel members, instability is the crucial one for thin-walled structures compared to strength and serviceability. A steel member loses its stability and buckles when the applied load exceeds a certain value known as critical buckling load. This value (critical buckling load) is unique for every member. On the other hand, strength analysis is based on the behaviour of member changing from elastic to plastic. Therefore, when the applied stress exceeds the section capacity of the steel members, the section's property changes its behaviour from elastic to plastic as a result there is a reduction in its load bearing capacity. At the point of elastro-plastic, the stress value is known as yield stress.

3.2.1 Displacement Analysis for steel members

Displacement is used to describe both translational and rotational movements taking place within the structures. These movements could be in-plane, out-plane or both on a member. Therefore, the derivation of these two actions is considered as follows;

- **Euler-Bernoulli Beam Theory**

This theorem is based on the assumption that plane section remains plane during and after deformation which is not applicable to thin-walled structure when analyzed for stability [43]. Nevertheless, this research work is limited to Euler-Bernoulli beam theorem. The un-deformed beam section used in the derivation of displacement formula (3.1) is shown in Fig. 3.3.

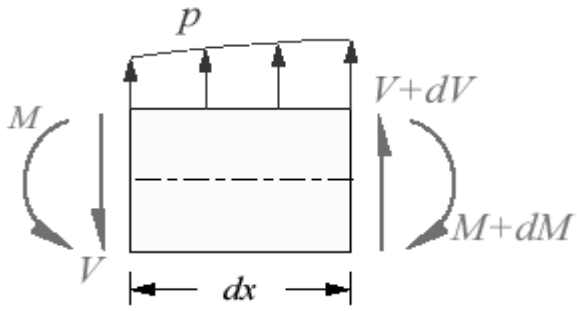

Figure 3.3 Beam section under uniformly distributed load, *p*

The derivation of out of plane displacement is based on equilibrium principle regardless of whether the member is prismatic or non-prismatic. Considering Fig. 3.3 to 3.5, the summation of all the shear forces, V, in the y-direction in equation (3.1) and the summation of all the moment at any point in expression (3.2) will eventually yield the displacement equations (3.3) and (3.8) for beams.

Also, the consideration of other conditions such as; kinematics, constitutive and resultants are important in the derivation of equation (3.6)

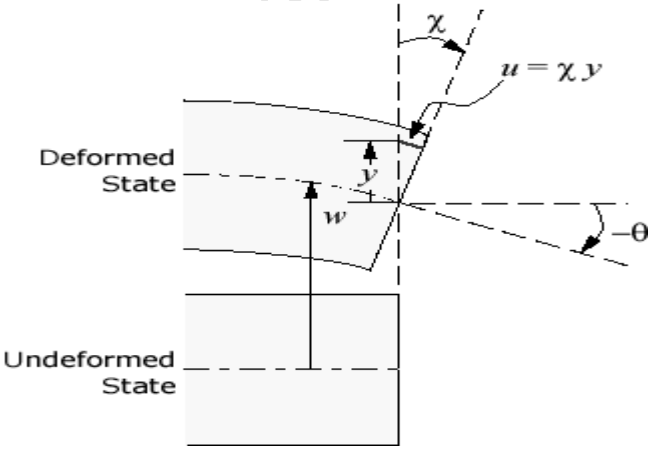

Figure 3.4 Deformed and un-deformed beam section

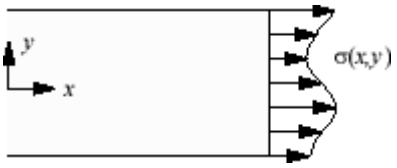

Figure 3.5. Axial stresses on a beam cross-section

$$\frac{dV}{dx} = -p \quad \text{(3.1)}$$

$$\frac{dM}{dx} = V \quad \text{(3.2)}$$

$$\theta = \frac{dw}{dx} \quad \text{(3.3)}$$

$$\sigma(x, y) = E \cdot \varepsilon(x, y) \quad \text{(3.4)}$$

$$M(x) = \iint y \cdot \sigma(x, y) d_x d_y \quad \text{(3.5)}$$

$$V(x) = \iint \sigma_{xy}(x, y) \cdot d_y d_x \quad \text{(3.6)}$$

$$\frac{d^2}{dx^2}\left[EI \frac{d^2 w}{dx^2} \right] = p \quad \text{(3.7)}$$

$$EI \frac{d^4 w}{dx^4} = p \quad \text{(3.8)}$$

where;

w - Coordinate normal to the beam's neutral axis [m]

EI – Flexural rigidity of the beam members [Nm^2]

P – Uniformly distributed applied line load [N]

x – Coordinate along the beam neutral axis [m]

V – Shear force [N]

θ –Rotational angle [radians]

σ – Flexural stresses [N/m^2]

ε – Strain in the beams

M – Bending moment of the beams [Nm]

E – Modulus of elasticity [N/m^2]

It is only when EI is constant then the equation of deflection (3.7) can be simplified to (3.8). In addition, equation (3.8) cannot easily be solved by analytical means when EI becomes variables and therefore it requires numerical analysis to be employed or a modification factor to be introduced in order to incorporate the analysis of non-prismatic members.

- **Saint-Venant's torsional Principle**

When the applied moment acts about the axis of the structural member, it produces torsional effects. This results into deformation which may be in form of twist and warping depending on the restraint conditions of the members leading to uniform or non-uniform torsion. In addition, torsion always produces shear deformation due to shear stresses. For free warping of members at the ends, the angle of twist is given in equation (3.9). However, when the end of the cross-section of the member is restrained from warping, bending action occurs in combination with torsional action, thus (3.10) is developed. This means, the displacements of members depend on both twisting and bending effect.

$$\phi = \frac{T\ell}{JG} \quad \text{.....(3.9)}$$

where;

ℓ = length [m]

ø = Angle of twist [rad/m]

G = Shear modulus [N/m^2]

J = torsional constant [m^4]

T = applied torques [Nm]

$$M = EI\frac{d^2u}{dz^2} \quad \text{.....(3.10)}$$

where;

I = moment of inertia [m^4]

u = lateral displacement [m]

An open section is more affected by the torsional effect than closed sections. Therefore, for thin-walled prismatic sections, the torsional constant, J, can easily be determined from the available design guidelines [59]. But, this is only possible for prismatic members. Once the member becomes non-prismatic, the equations (3.9) and (3.10) will not hold hence, they need to be modified to incorporate the application of varying cross-sectional dimensions.

3.2.2 Strength Analysis of steel Members

Steel members are mainly designed against yield stress for which the load bearing capacity of the member reduces, thus Fig. 3.1. Stress can also be defined as the intensity of force within a localised area as seen in equation (3.11). This either results from applied shear, moment or axial force. Their variation depends on the sectional dimensions. Equation (3.11) proves, the stress is only constant for the case of prismatic members under axial load but for all the other cases, it varies depending on the cross-sectional geometry, boundary and loading conditions of the members.

$$\sigma = \frac{P}{A} \qquad \text{.....(3.11)}$$

where;

σ – Stresses of the members [N/m^2]

P – Applied load [N]

A – Cross- sectional area [m^2]

The boundary and loading conditions affect the bending moment distribution in the members as seen in Fig. 3.6a, b. Therefore, this in turn affects the bending capacity of the members and uniforms members seem not to be the best for structural assemblage.

$$\sigma(x, y) = \frac{My}{I} \qquad \text{.....(3.12)}$$

where;

σ – Flexural stresses of the beam members [N/m^2]

M – Bending moment of the beams [Nm]

y – The distance between the neutral axis and the outer most part of the beam's cross-section [m]

I – Moment of inertia [m^4]

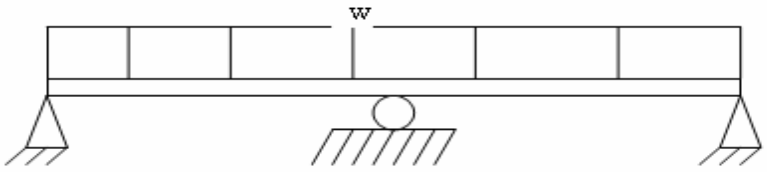

Figure 3.6a. Two span beam with uniformly distributed line load (udl), w.

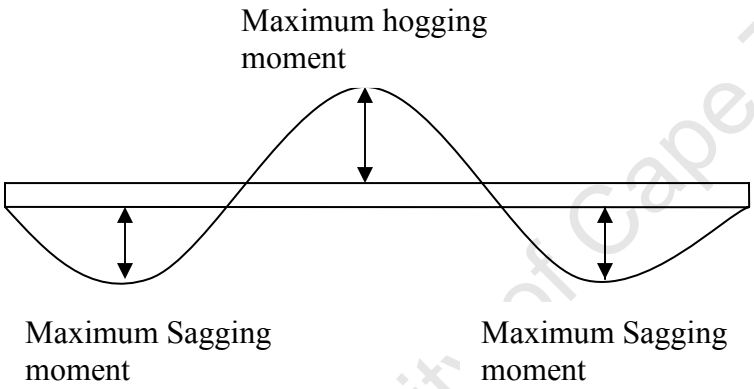

Figure 3.6b. Bending moment distribution for a two span beam element under (udl)

Stress is not only considered in strength analysis but also in stability analysis since it manifests itself as early as the bifurcation point whenever buckling occurs. There are always shearing forces acting on the cross-sections of the bar and if the cross-section becomes variable, the analysis gets even more complicated.

Therefore, the effect of these forces on the critical load should not be ignored. The shearing forces V acting on an element of length *dx* between two cross sections due to applied compressive force p is given in equation (3.13).

$$V = p\frac{dy}{dx} \quad \text{.....(3.13)}$$

The change in the slope produced by the shearing force is nV/AG, from [61], where A is the total cross-sectional area of the column, G the shear modulus and n, a numerical factor depending on the shapes of the cross section. This shows how cross-section determines the magnitude of shearing forces. However, for the case of non-prismatic members, there is a quest to modify this analysis procedure to incorporate the varying cross-sectional behaviour.

3.2.3 Instability Analysis of steel members

Instability in structural analysis is defined as the state for which structure loses its load carrying capacity. At this point, for small applied load, there is large deflection resulting. The two main types of instability associated with steel members are global and local buckling. Therefore, open sections are more susceptible to either local or global buckling than closed sections. In addition, local buckling mainly occurs in thin-walled structures depending on their slenderness ratio. It is a localized effect for which only the small portion of members under compressive force is distorted and manifests itself mainly in plate elements compared to beam elements. Global buckling is a situation in which the whole member fails at the same time. Global buckling on the other hand can still be broken down into lateral and lateral-torsional buckling. However, Euler buckling occurs when the member only moves through translation while lateral-torsional buckling occurs during both translational and rotational movements of the structural members. Cross-sectional properties are the main factor for determining the buckling capacity of the members but there are other factors such as support conditions, initial imperfection and loading conditions that affect the instability of the steel members as well.

3.2.3.1 Buckling of Column members

Columns are structural members subjected to compressive force. A cantilever prismatic column in Fig. 3.7 has a critical buckling load equation (1.1) according to Euler method but this equation can be modified to cater for critical buckling load of non-prismatic members.

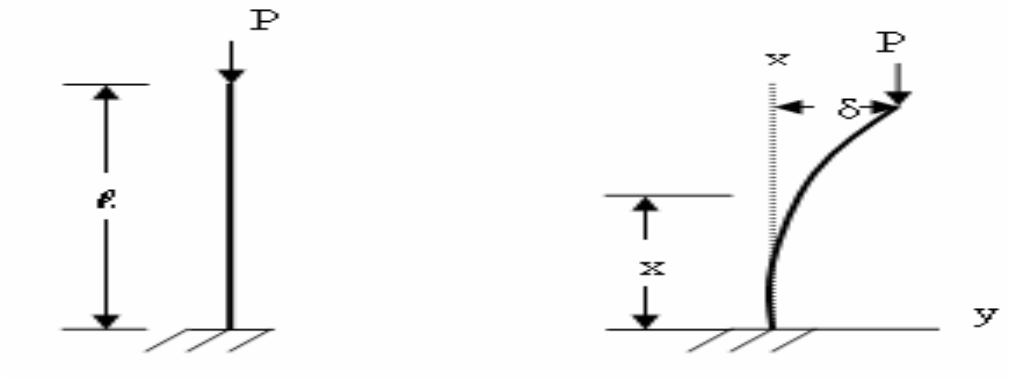

Figure 3.7. Buckling configuration of a cantilever column

Considering bending moment in (3.14) at any section along the longitudinal column's axis in the *x*-direction, the differential equation (3.15) can be developed. Making the substitution for k into (3.15), equation (3.16) can be derived and it has a solution of the ordinary differential equation (3.18).

$$M = -P(\delta - y) \quad \text{.....(3.14)}$$

$$EI\frac{d^2y}{dx^2} = P(\delta - y) \quad \text{.....(3.15)}$$

$$\frac{d^2y}{dx^2} + k^2 y = k^2\delta \quad \text{.....(3.16)}$$

$$k^2 = \frac{P}{EI} \quad \text{.....(3.17)}$$

$$y = A\cos kx + B\sin kx + \delta \quad \text{.....(3.18)}$$

Boundary conditions;

$$x = y = \frac{dy}{dx} = 0 \quad \text{.....(3.19)}$$

First Critical buckling load;

$$P_{cr} = \frac{\pi^2 EI}{4\ell^2} \quad \text{.....(3.20)}$$

Theoretical representation of buckling mechanism of a perfectly straight column member

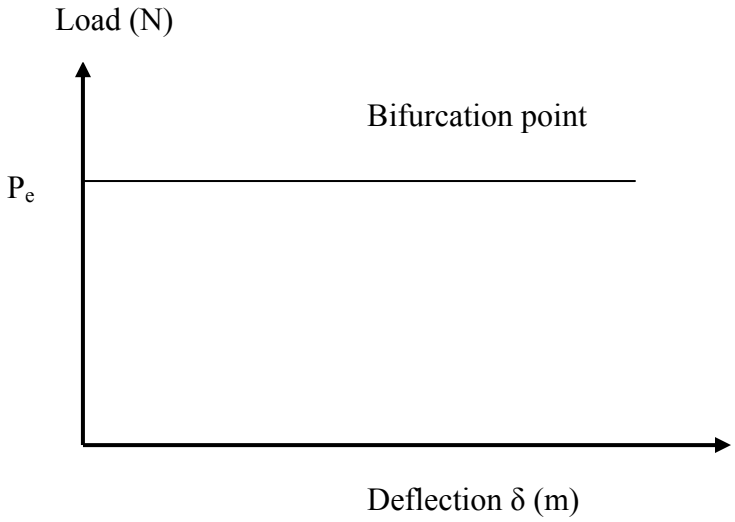

Figure 3.8. Bifurcation point for column members

When the boundary conditions in (3.19) are applied to equation (3.18), the constant A and B can be determined. Upon substitution of the constants, equation (3.20) is derived. But this equation is only valid for prismatic members. However, the same analytical mean used to determine critical buckling load for prismatic members can be extended for stepped members of Fig. 3.9 a, b.

In the same way, equation (3.21) can be developed from Fig. 3.9a by applying boundary conditions at the ends of the columns and continuity conditions in the middle of the column. In that sense, the k value in (3.21) and (3.22) is the same as for (3.17).

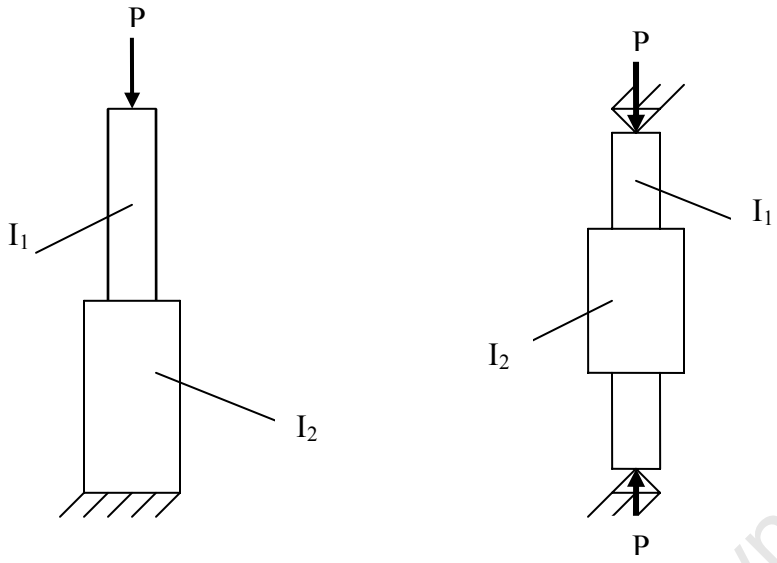

(a) Cantilever Stepped Column (b) Pin ended Stepped Column

Figure 3.9. Stepped column members

Critical buckling load for non-prismatic (stepped column) members can be calculated as shown in equations (3.21) and (3.22).

$$\tan k_1 \ell_1 \tan k_2 \ell_2 = \frac{k_1}{k_2} \quad \text{.....(3.21)}$$

$$P_{cr} = \frac{mEI_2}{\ell^2} \quad \text{.....(3.22)}$$

where;

l – Total length of the columns [m].

k – Ratio of critical buckling load to flexural rigidity of the column members [m^{-2}]

m - The numerical factor depending on the ratio of the half middle length to the total length and the two second moment of area

EI – Flexural rigidity of the column members [Nm^2]

By dividing the column member in Fig.3.9b into halves and substituting the half length of the middle part in equation (3.21) to replace the length of the bottom part of Fig.3.9a while keeping all the other parameters constant, and the boundary together with the conditions of continuity are applied, equation (3.22) can be derived.

As the number of steps in the cross-section increases, derivation of equation (3.22) becomes even more complicated hence it is advisable to use one of the approximation methods [61]. One of the advantages of these approximation methods is that they can easily be implemented in computer program.

3.2.3.2 Buckling of beam members

The ideal definition of beams can be considered as structural members under bending action. The structures must always be arranged in such a way as to allow in-plane bending. Therefore, the applied load must act through shear centre but the practical situation is not the case due to lateral instability of the lateral unrestrained members hence the lateral-torsional buckling often induced. Therefore, the resulting coupled twist together with lateral deformation make the situation more complicated in beams than in columns. Nevertheless, beam members can be classified according to fixity as cantilever, pin ended, fix ended, fix-pin ended, semi-fix ended, etc.

Instability analysis of thin-walled beam members can become more complicated with the consideration of different fixities and load application because, for every section of thin-walled members, there are seven degrees of freedom (three rotations, three translations and warping). Fig. 3.10 shows various fixities for Steel members.

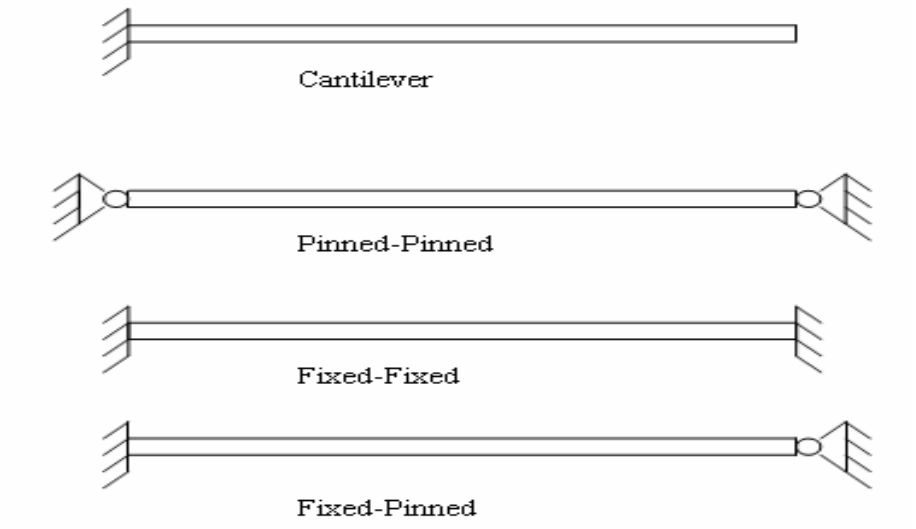

Figure 3.12 Members under different fixities

Nethercot [45] suggested the use of effective length factor K for beams as that one used in columns to provide a more conservative design guideline but concluded that it can only be used for most of the common boundary conditions known. However, the general expression for determining the critical bending moment for a prismatic beam is shown in (3.23). To show the effect of boundary conditions on the critical buckling load of beam members, consider equation (2.14) which is developed from a prismatic cantilever beam.

Looking at these two equations (3.23) and (3.24), the value of K can be taken as two.

$$M_{ocr} = \frac{\pi}{KL}\sqrt{EI_y GJ}\sqrt{\left(1+\frac{\pi^2 EI_w}{(KL)^2 GJ}\right)} \quad \text{.....(3.23)}$$

$$M_{ocr} = \frac{\pi}{2L}\sqrt{EI_y GJ}\sqrt{\left(1+\frac{\pi^2 EI_\omega}{4L^2 GJ}\right)} \quad \text{.....(3.24)}$$

where;

M_{ocr} - Critical bending moment [Nm]

K - Effective length factor

EI_y - flexural rigidity [Nm^2]

GJ - Torsional rigidity [Nm^2]

I_w - warping constant [m^4]

Equation (3.23) is only applicable to prismatic beam members. Therefore, in order to use equation (3.23) in the analysis and or design of non-prismatic members, a geometrical correction factor must be applied. This, therefore, raises a big challenge since most of the parameters in (3.23) depend on the geometrical configuration of the members. Sapalas [54] developed equation (2.2), which has the general correction factors. However, its derivation was based on tapered I-section members only and the consideration of different tapering ratios, boundary and loading conditions were not included. For a better analysis and design of non-prismatic members, a further investigation is required.

3.3 Finite element analysis

Before the advent of computers, it was quite difficult for engineers to decide on what type of elements to be used in modelling of the structures. But now with the availability of computer finite element method (FEM) packages in the market, the engineers' task has been made much easier. Therefore, the finite element modelling package used in this study is ADINA/M 8.4.2 version which has the ability to produce non-linear analysis of any form of structures since it is a FEM program. It was developed by Klaus-Jurgen Bathe and is now registered under ADINA R & D, Inc.

3.3.1 ADINNA/M 8.4.2

ADINA is comprised of ADINA structure, ADINA-F, ADINA-T, ADINA-AUI, ADINA-FSI and ADINA-TMC. It is used for finite element analysis of structures, heat transfer and CFD. However, for this investigation, only ADINA structure was used. ADINA/M 8.4.2 structure has one major challenge in its compatibility with other (FEM) packages. For instance, it is only compatible to (FEM) packages such as Nastran and ANSYS.

3.3.2 ADINA/M 8.4.2 structures

For the purpose of this research work, only ADINA/M 8.4.2 was used because it has the ability to directly produce the displacement, collapse, stress, both dynamic implicit and explicit, modal and stability analysis of any form of structures. However, the output results are stored in the porthole file which can only be viewed through post processing. The steps for modelling in ADINA/M 8.4.2 are summarised below:

- Geometry definition
- Element definition
- Application of restraints
- Load application
- Mesh definition
- Analysis set up
- Post processing

3.3.2.1 Geometry definition

ADINA uses linear analysis system in which the geometry definition is based on the centreline of the elements. However, there are two categories of geometry in AUI. There is a simple and ADINA-M geometry types. The simple model geometry type can be defined by using the vector points which are used to define lines which in turn are also used to define surfaces or volumes. On the other hand, ADINA-M model geometry type can be defined by the use of vector coordinates, which define the edges of the surfaces and consequently the body. However, the new geometry can be formed from the original ones by transformation. For complicated geometry in most cases, a separate batch file is written and uploaded in the current directory.

3.3.2.2 Element definition

This is a command used to define the type of elements to be used on the model analysis. They can be specified as truss, 2-D solid, 3-D solid, Beams, Isobeams, plates, shells, pipes, springs and general for structural analysis. These types of elements are already available in the program library. They are mainly chosen based on the geometry of the model definition.

3.3.2.3 Application of restraints

For the models to be effective, the degree of rigid body movement needs to be restricted by applying restraint conditions. ADINA program does not include warping degree of freedom for most of the analyses except in thin-walled plates hence every point in space has six degree of freedom. The restraint is applied by setting the boundary conditions on either points, lines, edges or surfaces depending on the type of models. It is to fix all or certain degree of freedom on the models. For instance, a pin support has all translations fixed and all rotations free while clamped support all translations and rotations fixed. However, ADINA has two predefined condition in the program library; all, for which all the degrees of freedom are fixed and none, for which all the degrees of freedom are free. Therefore, any other restraints conditions need to be specified by the users.

3.3.2.4 Load application

The loads are classified as; force, moment, displacement, pressure, distributed line load, centrifugal, mass proportional, electromagnetic, etc. The type of load applied depends on the element group definition. For instance, distributed line load is applied on lines/edges of beams, isobeams, pipes and shell elements while pressure loading is applied on surfaces and or faces of 3-D solid, 2-D solid and shell elements. The simplified steps for load application are summarised below:

- Select the type of load to be applied
- Select previously defined load if it is the same load being applied or select a new load
- Select the geometry type to which the load is to be applied

The load can be specified as constant or variable time function. This is used to control variation in loading. Variable time function can be classified as step or automatic time function.

3.3.2.5 Mesh generation

The mesh can be defined as the assemblage of elements joined together by nodal points and element edges to form the whole structure. The process of meshing requires that the element's size and orientation be determined by the modellers. It is therefore, a crucial stage of modelling because it requires a lot of engineering intuition. At this point, the user decides on the size of the element to be used in the model analysis, bearing in mind that the finer the element sizes, the more accurate the solution will be, but the more the central processing unit (CPU) time required for the computational processes. For simple structure, the mesh is always coarse since the structure does not have too much discontinuity in the geometry.

In ADINA, the element size can be determined either by choosing the number of division per model edge, the minimum element size at the end of model edge or the actual element size along the model edge. The structure can also be meshed as a whole or as a part depending on the mesh density required for each part. Therefore, it can also be deleted and regenerated depending on the model requirements.

3.3.2.6 Analysis set up

For the analysis to be effective, restraint conditions have to be set up depending on the analysis types. For example, static, linearised buckling and collapse analysis etc. Because the output results of these analyses are different, their analysis conditions must also be different. Consider a linearised buckling analysis whose buckling load factor must fall between 1 and 500.

The applied load must also fall within a certain range since the load bearing capacity of the structure is constant. On the other hand, the displacement must be specified as large while strain as small, the number of buckling load, buckling analysis method, method of generating starting vectors, convergence tolerance, number of iteration vectors used simultaneously and maximum number of iteration per eigenpair used must also be specified. This is not the case for collapse analysis where only the maximum displacement must be specified for the first solution and for static analysis where only the type of load application is specified. Therefore, for every buckling analysis, different magnitudes of load are applied in order to obtain convergence for a linearised buckling analysis. ADINA/M uses subspace iteration method and the critical buckling load factor, λ, is only allowed to fall in between 1 and 500. Nevertheless, ADINA/M executes the buckling analysis in two ways; either by secant formulation (3.25) or classical formulation (3.26);

$${}^{t_1}K\phi_i = \gamma_i K\phi_i \quad \text{.....(3.25)}$$

$\gamma_i > 0$

ϕ_i Is the eigenvector

The classical formulation is given as;

$${}^{t_1}K\phi_i = \gamma_i \left({}^{t_1}K - {}^{t_1}K_{NL}\right)\phi_i \quad \text{.....(3.26)}$$

$\gamma_i > 0$

${}^{t_1}K_{NL}$ Is the geometrically nonlinear part of ${}^{t_1}K$ and this type of formulation is considered to give more accurate result since the model had non-linear geometrical configuration (non-prismatic)

The critical buckling load coefficient λ is calculated from (3.27);

$$\lambda_i = \frac{1}{1-\gamma_i} \quad \text{.....(3.27)}$$

λ_i is the critical load factor and γ_i is an eigenvalue.

The critical load vector is evaluated from (3.28);

$$R_{cri} = {}^{t_0}R + \lambda_i \left({}^{t_1}R - {}^{t_0}R \right) \quad \text{.....(3.28)}$$

${}^{t_1}R \& {}^{t_0}R$, are the externally applied load vectors at the time t_0 & t_1 and the first critical load factor λ_1 must fall within the range; $1 < \lambda_1 < 500$ otherwise the ADINA program will stop running.

The convergence check of eigenvalue γ_i is measured using $\frac{\gamma_i^{(k+1)} - \gamma_i^{k}}{\gamma_i^{(k+1)}} \leq SSTOL$; i =1, N

where;

K - The iteration counter

SSTOL - User specified convergence tolerance

N - The number of Eigenmodes requested.

Generally, the stability problem of thin-walled members become even more complicated if the members become non-prismatic however small it may be because of the warping phenomena of their cross-sections.

ADINA is designed in such a way that when the model is run, the output result is automatically saved into the user-specified folder or program temporary folder. The user can specify the folder to which the output files must be stored by saving the whole model in that same folder before running the model analysis. In that way, by default, when the analysis is run, the output files will be saved in the same folder or the user can also specify the predefined folder during the actual model analysis run in.

3.3.2.7 Post processing

When ADINA has finished analysing the models, the output files can only be viewed through post processing. The output results can either be displayed as graphs, band plots or digit numerals depending on the types of analyses requested.

Any modification to the displayed results such as text insertion, load and boundary display, magnification factor etc can still be done in ADINA post processing. The original mesh of the model can also be displayed on request.

The output files must be saved as a Bitmap or vector snapshot and then they can be transferred in any other computer program such as Microsoft words, Microsoft excel, etc for further modification. Finally, the output result can also be printed directly from the ADINA program.

Chapter 4

Comparative Analysis of Non-prismatic Steel Members

4.1 Introduction

There are many factors which affect the general behaviour of non-prismatic steel members and frame systems composed of non-prismatic members. Steel members can either be made non-prismatic along or across the member's longitudinal axis. Therefore, to provide a reliable and accurate conclusion on the behaviour of non-prismatic members, both longitudinal and cross-sectional non-prismatic members must be simulated under the same restraint conditions.

Very little has been mentioned about non-prismatic steel members under different geometrical configurations. However, Siu [58] reported the effect of arbitrary cross-section on the stability of steel members in which he chose to use a hexagonal shape and compared the results with that of square ones. He concluded that for a hexagonal shape, failure occurs at the apex of the column while for a square shape, failure occurs at mid-height of the column for the same tapering ratio. This behaviour can be attributed to the fact that changes in the cross-sectional geometry affect the stability of the members. This in turn affects the critical buckling load. Therefore, cross-sectional geometry is a key factor in determining the feasibility of non-prismatic steel members and frame systems composed of non-prismatic members in this study.

In this study, the effect of different member types, span length, boundary conditions, tapering ratio (h/H), loading conditions, member classes and sections on non-prismatic members were investigated. The resulting deflections, stress distributions, bending moment, critical buckling load, angle of twist and sway were presented in the form of graphs, pictures and tables. These results were used in the comparative analysis of non-prismatic steel members.

Numerical method was used in the investigation of member's behaviour based on the fact that there are available FEM packages in the market. The main software used for the numerical modelling was ADINA/M 8.4.2 version.

The selection of steel sections and dimensions for model analysis was based on their applicability in the construction industry. Therefore, the sections mainly used were I, T, channel, angle and H. In addition, the members simulated ranges from stocky class one to slender class four, which were subjected to different loading types under various fixities. Member's fixities play a big role in determining the general behaviour of any structural members.

For every varying degree of geometrical non-uniformity, the following results; the first critical buckling load, maximum deflections, angles of twist and maximum stress distribution were recorded.

4.2 Material properties used in the model Analysis

Steel members as any other construction materials have both varying and constant physical properties. In this study, only the constant material properties were considered since the objective of the research was to investigate the effect of varying geometrical property on the structural behaviour of the steel members. Therefore, the varying material properties like coefficient of thermal expansion, moment of inertia, torsional constant etc were not considered in the list below;

Density of steel (**ρ**)	7850 kg/m^3
Poison's ratio (**υ**)	0.30
Young's modulus of Elasticity (**E**)	2.05E5 MPa
Shear modulus of Elasticity (**G**)	77E3 MPa
Yield strength /steel grade (δ_y)	350 MPa

4.3 Members in bending

These are structural elements which can be classified as beams or beam-columns. They are mainly subjected to either transverse loading or bending moment. Furthermore, these members are classified according to their fixities. Examples include cantilever, pin ended, fix ended and pin-fix ended beams. The steel sections which are mainly used for beams or beam-columns are I, T, H or channel.

4.3.1 Cantilever Tapered beams

These are members fixed at one end and free at the other end. They are either under transverse loading or applied bending moment. There are various steel sections which can be used as cantilever beams. However, in this study only I, T and channel section under different classes and span length were simulated. The results recorded were maximum displacements, bending moment, stress distribution and critical buckling load.

I and T-section steel members are always designated as h x b x m where h is the height, b is the width and m is the mass per unit length. Channel sections on the other hand are designated as h x b where h and b have the same meaning as for I and T-sections. Therefore, there are various geometrical properties of I and T-section members which can be made non-prismatic, i.e. web depth, web thickness, flange width, flange thickness, etc. However, in this study, only the web depth and flange width were made non-prismatic. Both point load and uniformly distributed line load (UDL) were applied but at different interval. The detailed model procedures and the output data are presented below:

a) Web tapered cantilever 3metre 203 x 133 x 30 I-section beam members under 50kN point load at the free end

Firstly, a 3 metre span cantilever beam was subjected to a 50kN point load at the free end. Starting from a tapering ratio of unity (h/H =1) as seen in Fig. 4.1 for undeformed and deformed shapes, keeping all the other geometrical parameters constant, the web depth at the free end of the member was reduced gradually at 10mm increment, and at the same time, the web depth at the fixed end was increased gradually by the same amount in order to keep the weight and volume constant.

Secondly, the weight of the beam was varied by keeping all the dimensions at the fixed end constant while reducing the web depth at the free end gradually by 10mm increment.

For every change in the tapering ratio of either member with constant or varying weight, the resulting deflections, stress distribution and the first critical lateral-torsional buckling moment were recorded as seen in Table 4.1 to 4.5.

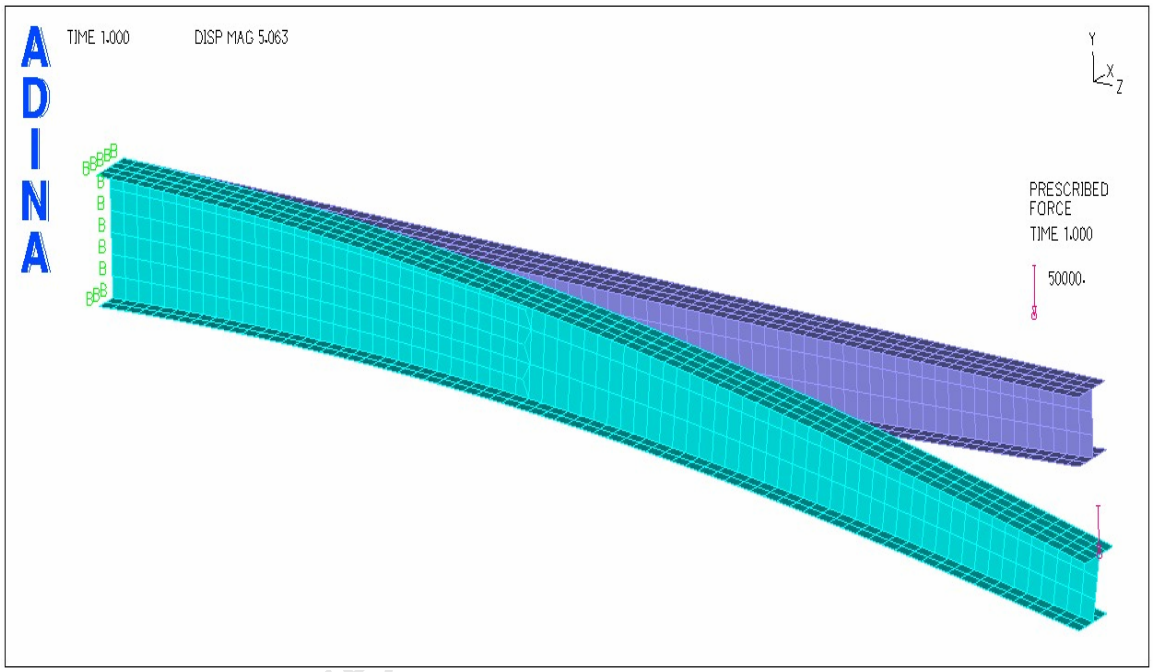

Figure 4.1. Deflected and the original shape for a web tapered cantilever I-section beam

Table 4.1**. Maximum deflection of a web tapered 203 x 133 x 30 I-section cantilever beam with constant weight under 50kN point load at the free end**

Web depth at the fixed end, H_w (mm)	Web depth at the free end, h_w (mm)	Tapering ratio (h_w/H_w)	Maximum deflections at the free end, Δ_{max} (mm)	% decrease in the maximum deflections
193.4	193.4	1.00	82.4	0.0
203.4	183.4	0.90	78.1	5.2
213.4	173.4	0.81	74.3	9.8
223.4	163.4	0.73	70.9	14.0
233.4	153.4	0.66	67.9	17.6
243.4	143.4	0.59	65.3	20.8
253.4	133.4	0.53	62.9	23.7
263.4	123.4	0.47	60.9	26.1
273.4	113.4	0.41	59.1	28.3
283.4	103.4	0.36	57.5	30.2
293.4	93.4	0.32	56.2	31.8
303.4	83.4	0.27	55.1	33.1
313.4	73.4	0.23	54.2	34.2
323.4	63.4	0.20	53.6	35.0

Table 4.2. **Maximum deflections of a web tapered 203 x 133 x 30 I-section cantilever beam with varying weight under 50kN point load at the free end**

Web depth at the fixed end, H_w (mm)	Web depth at the free end, h_w (mm)	Tapering ratio (h_w/H_w)	Maximum deflections at the free end, Δ_{max} (mm)	% increase in the maximum deflections
193.4	193.4	1.00	82.4	0.0
193.4	183.4	0.95	84.7	2.8
193.4	173.4	0.90	87.1	5.7
193.4	163.4	0.84	89.7	8.9
193.4	153.4	0.79	92.5	12.3
193.4	143.4	0.74	95.6	16.0
193.4	133.4	0.69	98.9	20.0
193.4	123.4	0.64	106.4	29.1
193.4	113.4	0.59	106.4	29.1
193.4	103.4	0.53	115.6	40.3
193.4	93.4	0.48	115.6	40.3
193.4	83.4	0.43	127.2	54.4
193.4	73.4	0.38	127.2	54.4
193.4	63.4	0.33	134.0	62.6

Generally, under constant weight and volume, from Table 4.1**,** as the tapering ratio (h_w/H_w) decreases, the maximum deflection at the free end of a web tapered cantilever beam under a point load decreases. This behaviour can be attributed to an increase in the flexural rigidity of the member at the fixed end as the cross-sectional dimension increases. In addition, there will be a total reduction in the effective weight of the member at the free end, which results into a decrease in the maximum deflections since deflections of a cantilever beam is a function of effective gravity load.

There is a different in the behaviour for web tapered cantilever beam with varying weight as seen in Table 4.2, where a decrease in the tapering ratio results in an increase in the maximum deflections. This effect might be due to a reduction in the effective stiffness of the member resulting from removing some materials from the free end of the beam hence, a reduction in the section capacity.

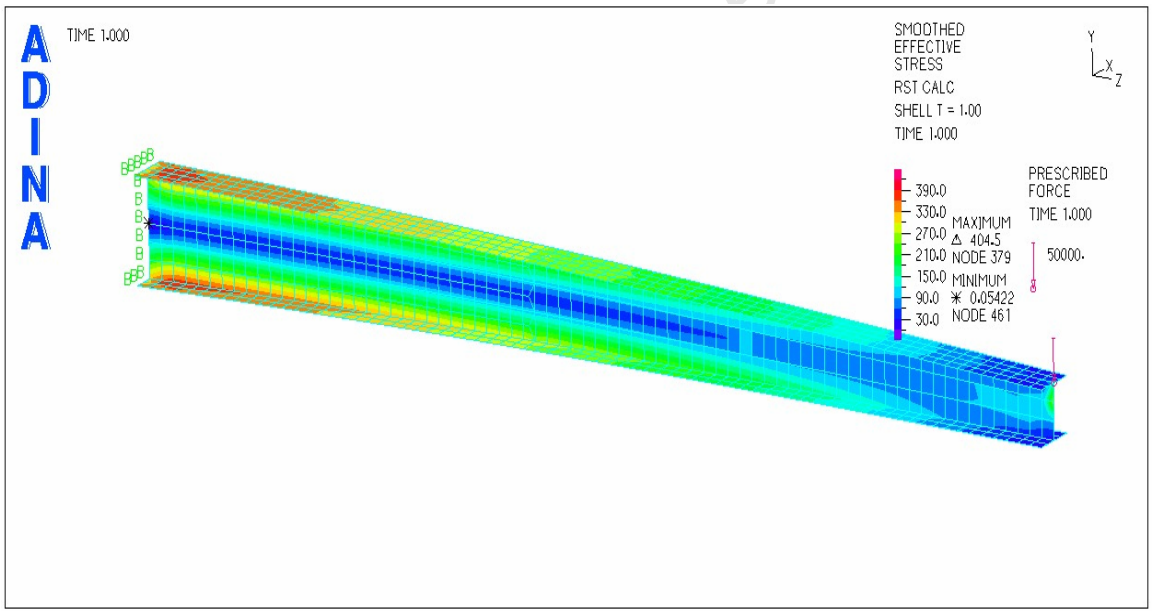

Figure 4.2 Flexural stress distributions for a web tapered cantilever I-section beam

Flexural stress for a web tapered cantilever beam decreases from the fixed end towards the free end as seen in Fig. 4.2. However, the neutral axis of the cantilever beam experiences minimal flexural stress as compared to all the other sections of the beam element. The outer most fibres of the fixed end experience the highest flexural stresses.

Table 4.3. **Maximum flexural stress of a web tapered 203 x 133 x 30 I-section cantilever beam with constant weight under 50kN point load at the free end**

Web depth at the fixed end, H_w (mm)	Web depth at the free end, h_w (mm)	Tapering ratio (h_w/H_w)	Maximum flexural stresses at the fixed end, σ_{max} (N/mm^2)	% decrease in the flexural stress
193.4	193.4	1.00	533	0.0
203.4	183.4	0.90	505	5.3
213.4	173.4	0.81	479	10.1
223.4	163.4	0.73	455	14.6
233.4	153.4	0.66	433	18.8
243.4	143.4	0.59	414	22.3
253.4	133.4	0.53	395	25.9
263.4	123.4	0.47	379	28.9
273.4	113.4	0.41	363	31.9
283.4	103.4	0.36	349	34.5
293.4	93.4	0.32	335	37.1
303.4	83.4	0.27	322	39.6

It can be observed from Table 4.3 that as the web tapering ratio (h_w/H_w) decreases, the maximum flexural stress at the fixed end of the cantilever beam decreases. This result conforms to equation (3.12), where flexural stress is a function of section modulus of the beam. Decrease in the web tapering ratio results into an increase in the section modulus at the fixed end of the beams and consequently a decrease in the flexural stress.

Table 4.4. **Maximum flexural stress of a web tapered 203 x 133 x 30 I-section cantilever beam with a variable weight under 50kN point load at the free end**

Web depth at the fixed end, H_w (mm)	Web depth at the free end, h_w (mm)	Tapering ratio (h_w/H_w)	Maximum flexural stresses at the fixed end, σ_{max} (N/mm^2)	% increase in the flexural stress
193.4	193.4	1.00	533	0.0
193.4	183.4	0.95	534	0.2
193.4	173.4	0.90	535	0.4
193.4	163.4	0.84	536	0.6
193.4	153.4	0.79	537	0.8
193.4	143.4	0.74	538	0.9
193.4	133.4	0.69	539	1.1
193.4	123.4	0.64	540	1.3
193.4	113.4	0.59	541	1.5
193.4	103.4	0.53	543	1.9
193.4	93.4	0.48	543	1.9
193.4	83.4	0.43	545	2.3

A decrease in the tapering ratio results in an increase in the maximum flexural stress as shown in Table 4.4. This is contrary to what was expected since the results of Table 4.3 show a gradual decrease in the maximum flexural stress under the same loading conditions as the tapering ratio decreases. This behaviour can be attributed to a reduction in the effective section modulus as some portion of the member is removed.

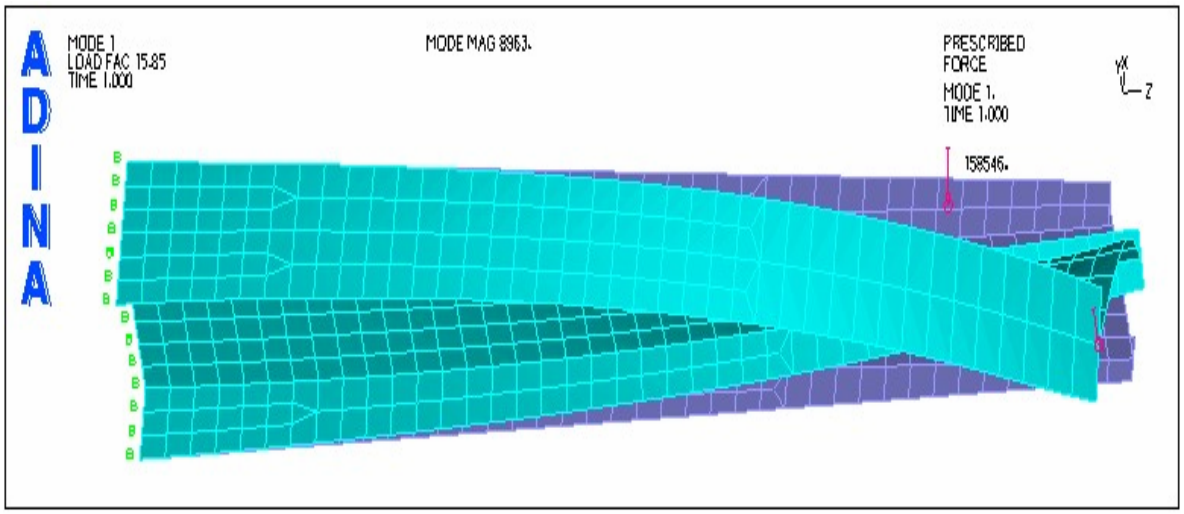

Figure 4.3. Lateral-torsional buckling of a cantilever tapered I-section beam together with the original mesh

Table 4.5. **Lateral-torsional buckling moment of a web tapered 203 x 133 x 30 I-section cantilever beam**

Web depth at the fixed end, H_w (mm)	**Web depth at the free end, h_w (mm)**	**Tapering ratio (h_w/H_w)**	**Critical buckling moment M_{cr} (kNm)**	**% increase in the critical buckling moment**
193.4	193.4	1.00	89.3	0.0
203.4	183.4	0.95	92.3	3.4
213.4	173.4	0.90	95.9	7.4
223.4	163.4	0.84	99.8	11.8
233.4	153.4	0.79	106.9	19.7
243.4	143.4	0.74	112.6	26.1
253.4	133.4	0.69	119.3	33.6
263.4	123.4	0.64	127.0	42.2
273.4	113.4	0.59	136.0	52.3
283.4	103.4	0.53	146.4	63.9
293.4	93.4	0.48	158.6	77.6
303.4	83.4	0.43	172.5	93.2
313.4	73.4	0.38	188.3	110.9
323.4	63.4	0.33	205.5	130.1

Table 4.5 shows an increase in the load bearing capacity of the web tapered cantilever beam as the tapering ratio decreases. A decrease in the tapering ratio (h_w/H_w) increases the sectional dimensions at the fixed support and reduces the one at the free end. This arrangement leads to an increase in the flexural rigidity at the support and also increase in the torsional rigidity at the free end. Therefore, the critical buckling moment of the member will be increased according to equation (3.23).

b) Analysis of a web tapered 3m, 203 x 133 x 30 I-section cantilever beam members under 17kN/m UDL

In a similar manner as for the web tapered cantilever beam members under 50kN point load, a 17kN/m UDL was applied to the cantilever beam as shown in Fig. 4.4 in order to investigate the effect of different loading conditions on a web tapered cantilever beams. Therefore, starting with prismatic cantilever beam (h_w/H_w =1), the web depth at the free end was reduced gradually at 10mm increment. At the same time, the web depth at the fixed end was increased by the same amount. For every change in the web tapering ratio, the resulting deflections, flexural stress and the critical buckling moment were recorded as shown in Table 4.6 to 4.8.

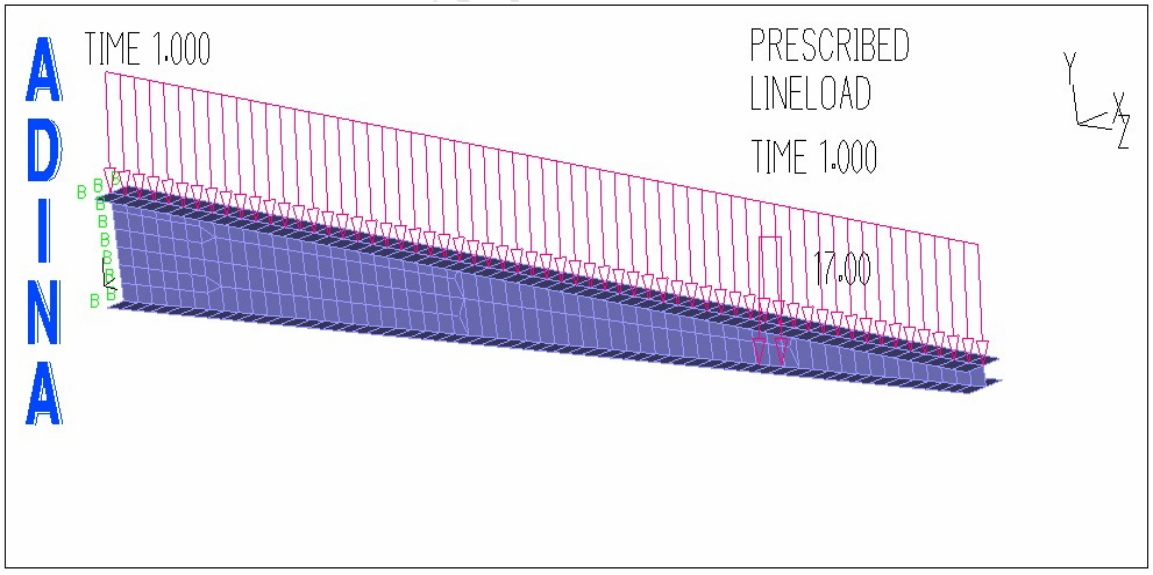

Figure 5.4. Web tapered cantilever I-section beam member under UDL

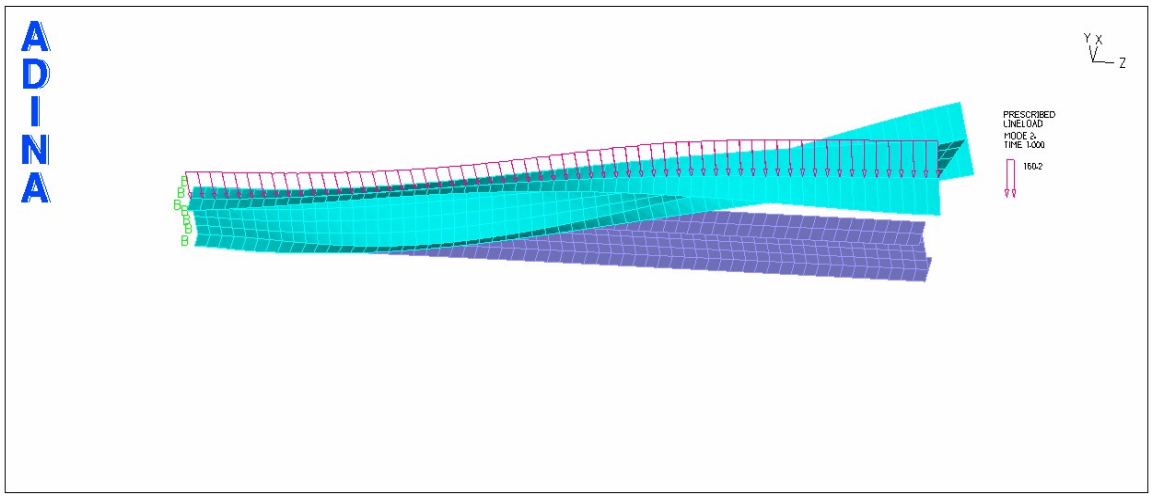

Figure 4.5. Lateral-torsional buckled together with the original model of a cantilever tapered I-section beam

From Table 4.5 and 4.8, it can be observed that there is no significant difference in the load bearing capacity of the web tapered cantilever beams under point load and UDL. Therefore, it can be concluded that point load and UDL have no significant effect on lateral-torsional buckling of a web tapered cantilever beam members. This result closely agreed with the expression (1.2).

Table 4.6. **Maximum deflections of a web tapered 203 x 133 x 30 I-section cantilever beam under 17kN/m UDL**

Web depth at the fixed end, H_w (mm)	**Web depth at the free end, h_w (mm)**	**Tapering ratio (h_w/H_w)**	**Maximum deflections at the free end, Δ_{max} (mm)**	**% decrease in the maximum deflections**
193.4	193.4	1.00	31.7	0.0
203.4	183.4	0.95	29.7	6.3
213.4	173.4	0.90	28.0	11.7
223.4	163.4	0.84	26.4	16.7
233.4	153.4	0.79	24.9	21.5
243.4	143.4	0.74	23.7	25.2
253.4	133.4	0.69	22.5	29.0
263.4	123.4	0.64	21.5	32.2
273.4	113.4	0.59	20.5	35.3
283.4	103.4	0.53	19.7	37.9
293.4	93.4	0.48	18.9	40.4
303.4	83.4	0.43	18.2	42.6
313.4	73.4	0.38	17.6	44.5
323.4	63.4	0.33	17.0	46.4

As the tapering ratio (h_w/H_w) decreases, the maximum deflections of a web tapered cantilever beam under UDL decreases, thus Table 4.6. This is the same behaviour experienced by web tapered cantilever beam under point load, thus Table 4.1. Therefore, point load and UDL can be considered to have no significant effect on the deflections of a web tapered cantilever beams. This can be verified using Euler-Bernoulli Beam Theorem where behaviour of a beam does not depend on the type of load applied.

Table 4.7. **Maximum flexural stress of web tapered 203 x 133 x 30 I-section cantilever beam under 17kN/m UDL**

Web depth at the fixed end, H_w (mm)	**Web depth at the free end, h_w (mm)**	**Tapering ratio (h_w/H_w)**	**Maximum flexural stresses at the fixed end, σ_{max} (N/mm^2)**	**% decrease in the flexural stress**
193.4	193.4	1.00	271.1	0.0
203.4	183.4	0.95	258.8	4.5
213.4	173.4	0.90	244.9	9.7
223.4	163.4	0.84	232.4	14.3
233.4	153.4	0.79	221.0	18.5
243.4	143.4	0.74	210.5	22.4
253.4	133.4	0.69	200.8	25.9
263.4	123.4	0.64	191.9	29.2
273.4	113.4	0.59	183.7	32.2
283.4	103.4	0.53	176.2	35.0
293.4	93.4	0.48	169.1	37.6
303.4	83.4	0.43	162.6	40.0
313.4	73.4	0.38	156.4	42.3
323.4	63.4	0.33	150.7	44.4

Table 4.7 shows a similar trend as in Table 4.2 for maximum flexural stress of web tapered cantilever beam as the tapering ratio decreases. Where decrease in the tapering ratio results into a decrease in the maximum flexural stress**.** Therefore, the application of either point load or UDL does not influence the effect tapering ratio on the distribution of flexural stress of a web tapered cantilever beam. This result agreed with the closed form solution of equation (3.12).

Table 4.8. **Lateral-torsional buckling moment of a web tapered 203 x 133 x 30 I-section cantilever beam**

Web depth at the fixed end, H_w (mm)	**Web depth at the free end, h_w (mm)**	**Tapering ratio (h_w/H_w)**	**Critical buckling moment M_{cr} (kNm)**	**% increase in the critical buckling moment**
193.4	193.4	1.00	164.5	0.0
203.4	183.4	0.95	170.6	3.7
213.4	173.4	0.90	177.4	7.8
223.4	163.4	0.84	184.8	12.3
233.4	153.4	0.79	193.1	17.4
243.4	143.4	0.74	202.3	23.0
253.4	133.4	0.69	212.6	29.2
263.4	123.4	0.64	224.5	36.5
273.4	113.4	0.59	237.2	44.2
283.4	103.4	0.53	250.8	52.5
293.4	93.4	0.48	265.8	61.6
303.4	83.4	0.43	282.0	71.4
313.4	73.4	0.38	301.6	83.3
323.4	63.4	0.33	319.1	94.0

The critical buckling moment of the web tapered cantilever beam under UDL increases as the tapering ratio (h_w/H_w) decreases. This may result from the increase in the effective stiffness of the cantilever beam as the cross-sectional dimensions at the support of the beam increases, described in *section 4.3.1a*. Both Tables 4.5 and 4.8 show an increase in the critical buckling moment. Therefore, the application of either point load or UDL does not influence the effect of tapering ratio on the bearing capacity of a web tapered cantilever beam. This can also be justified by the use of equation (1.2), where the stability of beams does not depend on the type but the position of load application.

c) Behaviour of a flange tapered 203 x 133 x 30 I-section cantilever beam members under 50kN point load at the free end

In order to effectively investigate the impact of tapering ratio on an I-section cantilever beam members, the beam flanges were tapered at the same incremental rate under constant weight as for web tapered cantilever beams described earlier. The resulting deflections, stress distribution and lateral-torsional buckling moment were tabulated and compared with those of web tapered members. Table 4.9, 4.10 and 4.11 show the results of flange tapered I-section cantilever beams under different tapering ratios.

Table 4.9. **Maximum deflections of a flange tapered 203 x 133 x 30 I-section cantilever beam under 50kN point load at the free end**

Flange width at the fixed end, W_f (mm)	Flange width at the free end, w_f (mm)	Tapering ratio (w_f/W_f)	Maximum deflections at the free end, Δ_{max} (mm)	% decrease in the maximum deflections
133	133	1.00	82.4	0.0
143	123	0.86	80.0	2.9
153	113	0.74	77.7	5.7
163	103	0.63	75.7	8.1
173	93	0.54	73.8	10.4
183	83	0.45	72.2	12.4
193	73	0.38	70.6	14.3
203	63	0.31	69.3	15.9
213	53	0.25	68.0	17.5
223	43	0.19	66.8	18.9
233	33	0.14	65.8	20.1
243	23	0.09	64.9	21.2

For decreasing tapering angles, the maximum deflection of a flange tapered cantilever beam decreases as shown in Table 4.9. This is the same effect as for web tapered cantilever beam members in Table 4.1. This behaviour is expected since deflection is a function of effective stiffness of the member [18]. Therefore, different positioning of taper has no impact on the effect of tapering ratio on an I-section cantilever beam.

Table 4.10. **Maximum flexural stress of a flange tapered 203 x 133 x 30 I-section cantilever beam under 50kN point load at the free end**

Flange width at the fixed end, W_f (mm)	Flange width at the free end, w_f (mm)	Tapering ratio (w_f/W_f)	Maximum stress at the fixed end, σ_{max} (N/m^2)	% decrease in the flexural stress
133	133	1.00	533.1	0.0
143	123	0.86	502.3	5.8
153	113	0.74	474.8	10.9
163	103	0.63	450.1	15.6
173	93	0.54	427.9	19.7
183	83	0.45	407.8	23.5
193	73	0.38	390.3	26.8
203	63	0.31	374.3	29.8
213	53	0.25	359.6	32.5
223	43	0.19	346.2	35.1
233	33	0.14	333.8	37.4
243	23	0.09	322.4	39.5

For a cantilever beams with a constant point load at the free end, the maximum flexural stress occurs at the fixed support as seen in Fig. 4.2. Therefore, either increasing the web depth or the flange width at the fixed support will increase the section modulus hence, a reduction in maximum flexural stress. This is shown in Table 4.3 and 4.10 where, a decrease in either web or flange tapering ratio led to a decrease in the maximum flexural stress.

Table 4.11. **Lateral-torsional buckling moment of a flange tapered 203 x 133 x 30 I-section cantilever beam with constant weight**

Flange width at the fixed end, W_f (mm)	Flange width at the free end, w_f (mm)	Tapering ratio (w_f/W_f)	Critical buckling moment M_{cr} (kNm)	% increase in the critical buckling moment
133	133	1.00	89.3	0.0
143	123	0.86	92.9	4.0
153	113	0.74	94.8	6.2
163	103	0.63	96.2	7.7
173	93	0.54	97.2	8.8
183	83	0.45	97.7	9.4
193	73	0.38	97.5	9.2
203	63	0.31	96.6	8.2
213	53	0.25	94.9	6.3
223	43	0.19	92.1	3.1
233	33	0.14	88.1	-1.3
243	23	0.09	82.6	-7.5

Table 4.11 above, shows a unique behaviour of a flange tapered cantilever beam members. As the tapering ratio decreases, the critical buckling moment increases up to a point, say (w_f/W_f = 0.45), then the critical buckling moment starts decreasing as the tapering ratio decreases, which is different from the behavioural trend observed. This behaviour can be attributed to the fact that flanges and web are under different action. Therefore, different tapering position on the cantilever I-section beams influence the effect of tapering ratio, thus Table 4.5 and 4.11.

d) The effect of tapering ratios (h/H) on a web tapered 2metre 356 x 171 x 45 I-section cantilever beam members

To compare the effects of different tapering ratios on different classes of I-section steel members, 356 x 171 x 45 I-section, which is a class two member, was simulated under the same conditions as 203 x 133 x 30 I-section, which is a class one member. The resulting deflections, stress distribution and lateral-torsional buckling moment for the two different classes of I-section steel members were tabulated and compared.

Table 4.12. **Maximum deflections of a flange tapered 356 x 171 x 45 I-section cantilever beam under 100kN point load at the free end**

Flange width at the fixed end, W_f (mm)	Flange width at the free end, w_f (mm)	Tapering ratio (w_f/W_f)	Maximum deflections at the free end, Δ_{max} (mm)	% decrease in maximum deflections
171	171	1.00	12.2	0.0
181	161	0.89	11.9	2.5
191	151	0.79	11.7	4.1
201	141	0.70	11.5	5.7
211	131	0.62	11.3	7.4
221	121	0.55	11.1	9.0
231	111	0.48	10.9	10.7
241	101	0.42	10.8	11.5
251	91	0.36	10.6	13.1
261	81	0.31	10.5	13.9
271	71	0.26	10.4	14.8
281	61	0.22	10.3	15.6
291	51	0.18	10.2	16.4
301	41	0.14	10.1	17.2

For a constant weight and volume, the maximum deflection decreases as the tapering ratio decreases as shown in Table 4.12. This behaviour here is the same as the one observed for class one member in Table 4.9. Therefore, I-section steel members of class one and two experience the same effect of different tapering ratios on maximum deflection of cantilever beams.

Table 4.13**. Maximum stress of a flange tapered 356 x 171 x 45 I-section cantilever beam under 100kN point load at the free end**

Flange width at the fixed end, W_f (mm)	Flange width at the free end, w_f (mm)	Tapering ratio (w_f/W_f)	Maximum stress at the fixed end, σ_{max} (N/mm^2)	% increase in flexural stress
171	171	1.00	541.1	0.0
181	161	0.89	542.1	0.2
191	151	0.79	543.2	0.4
201	141	0.70	545.0	0.7
211	131	0.62	548.0	1.3
221	121	0.55	544.6	0.6
231	111	0.48	546.2	0.9
241	101	0.42	548.0	1.3
251	91	0.36	550.0	1.6
261	81	0.31	552.3	2.1
271	71	0.26	555.0	2.6
281	61	0.22	558.2	3.2
291	51	0.18	562.1	3.9

It can be observed from Table 4.10 and 4.13 that class two I-section steel member experiences less effect of different tapering ratios on flexural stress distribution compared to class one. Table 4.13 shows negligible effect in the maximum flexural stress i.e. the maximum flexural stress increased by 3.9% for the decrease in tapering ratio from 1 to 0.18. Therefore, class one and two I-section steel members experience different effect of tapering ratio on flexural stress distribution.

Table 4.14. **Lateral-torsional buckling moment of a flange tapered 356 x 171 x 45 I-section cantilever beam with constant weight.**

Flange width at the fixed end, W_f (mm)	Flange width at the free end, w_f (mm)	Tapering ratio (w_f/W_f)	Critical buckling moment M_{cr} (kNm)	% increase in the buckling moment
171	171	1.00	242.4	0.0
181	161	0.89	256.2	5.7
191	151	0.79	269.0	11.0
201	141	0.70	281.4	16.1
211	131	0.62	301.8	24.5
221	121	0.55	300.8	24.1
231	111	0.48	308.8	27.4
241	101	0.42	313.4	29.3
251	91	0.36	316.4	30.5
261	81	0.31	317.0	30.8

Table 4.14 shows gradual increase in the critical buckling moment of a 356 x 171 x 45 I-section flange tapered cantilever beams as the tapering ratio (w_f/W_f) decreases. This is in contrary to the behaviour exhibited by 203 x 133 x 30 I-section flange tapered cantilever beam in which the critical buckling moment initially increases up to 0.45 tapering ratio then starts decreasing as the tapering ratio decreases. Therefore, class one and two of I-section and flange tapered cantilever beams experience different effects of tapering ratios on the load carrying capacity. This behaviour could be based on the fact that class one and two of I-section steel members experience different load carrying capacity.

e) Effect of tapering ratio on a 2metre web tapered 103 x 133 x 30 T-section cantilever beam

Under constant weight and volume, the tapering ratio (h/H) was varied and the web depth at the fixed end was increased gradually at 10mm interval. At the same time, the web depth at the free end was reduced by the same amount while keeping all the other dimensions constant in order to keep the weight and volume constant as seen in Fig.4.6. The lateral-torsional buckling configuration is shown in Fig.4.7. A 50kN point load was applied at the free end and the resulting deflections, stress distribution and critical buckling moment were recorded in Table 4.15 to 4.17.

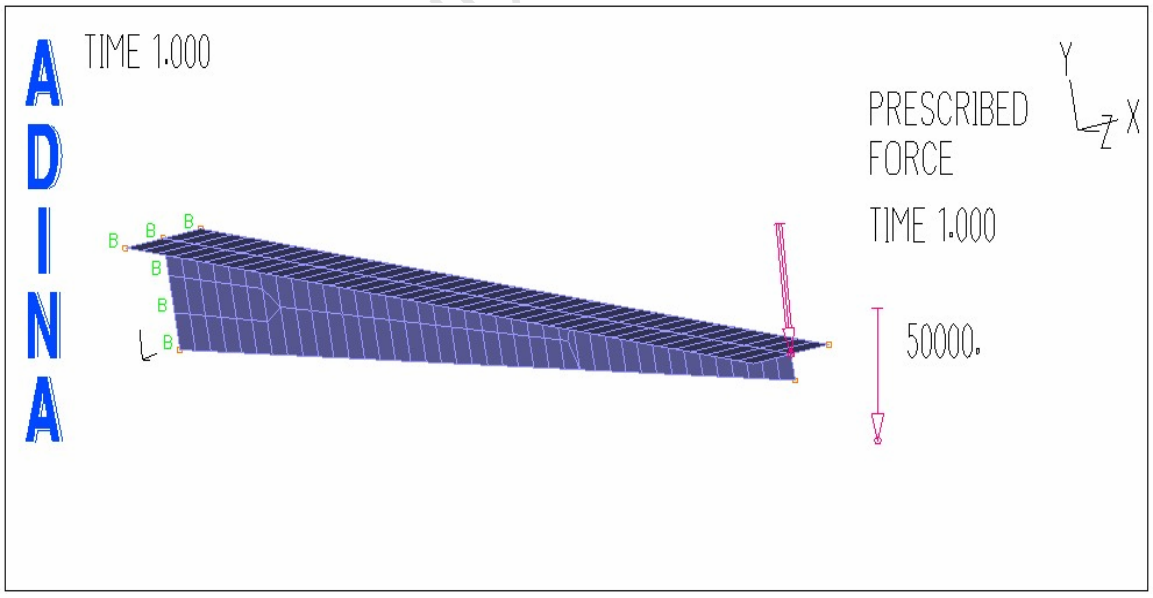

Figure 4.6. Web tapered cantilever T-section beam member under point load

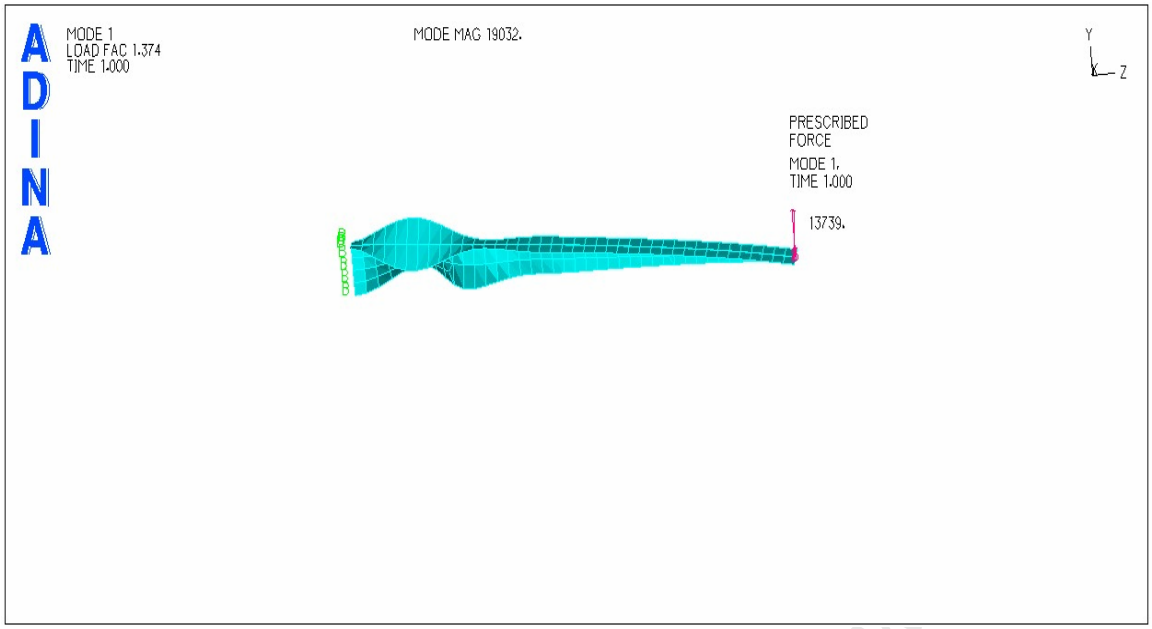

Figure 4.7. Lateral-torsional buckling of a cantilever web tapered T-section beam

Table 4.15**. Maximum deflections of a web tapered 102 x 133 x 30 T-section cantilever beam under 50kN point load at the free end**

Web depth at the support, H_w(mm)	**Web depth at the free end, h_w(mm)**	**Tapering ratio (h_w/H_w)**	**Maximum deflection at the free end, Δ_{max} (mm)**	**% decrease in the deflections**
102	102	1.00	455	0.0
112	92	0.82	399	12.3
122	82	0.67	358	21.3
132	72	0.55	327	28.1
142	62	0.44	305	33.0
152	52	0.34	291	36.0
162	42	0.26	285	37.4
172	32	0.19	287	36.9
182	22	0.12	302	33.6

The maximum deflection of a web tapered T-section decreases as the tapering ratio decreases up to 0.26, when the applied action has reached the section capacity (yield strength) of the smaller section of the member then the deflection starts increasing with decreasing tapering ratio, thus Table 4.15. Therefore, it is evident that tapering ratio has different effect on the deflection of different steel section with web tapered cantilever beam under the same boundary conditions.

Table 4.16. **Maximum flexural stress at the support of a web tapered 102 x 133 x 30 T-section cantilever beam under 50kN point load at the free end**

Web depth at the support, H_w(mm)	Web depth at the free end, h_w(mm)	Tapering ratio (h_w/H_w)	Maximum stress of the cantilever, σ_{max} (N/mm^2)	% decrease in the flexural stress
102	102	1.00	4799.8	0.0
112	92	0.82	3997.0	16.7
122	82	0.67	3382.3	29.5
132	72	0.55	3083.7	35.8
142	62	0.44	2679.6	44.2
152	52	0.34	2426.2	49.5
162	42	0.26	2517.2	47.6
172	32	0.19	2692.9	43.9
182	22	0.12	3184.3	33.7

Initially as the tapering angle decreases, the maximum stress decreases due to increase in the section modulus up to a tapering ratio (h_w/H_w), of 0.34. Thereafter, the stress increases with a decrease in the tapering ratio as shown in Table 4.16. Therefore, different types of steel sections experienced different effect of tapering ratio on stress distribution.

Table 4.17. **Critical buckling moment of a web tapered 102 x 133 x 30 T-section cantilever beam with a constant weight**

Web depth at the support, H_w(mm)	Web depth at the free end, h_w(mm)	Tapering ratio (h_w/H_w)	Critical buckling moment M_{cr} (kNm)	% decrease in the buckling moment
102	102	1.00	27.50	0.0
112	92	0.82	27.46	0.1
122	82	0.67	27.44	0.2
132	72	0.55	27.44	0.2
142	62	0.44	27.40	0.4
152	52	0.34	27.38	0.4
162	42	0.26	27.39	0.4
172	32	0.19	27.42	0.3
182	22	0.12	27.48	0.1

The same behaviour of stress distribution is experienced in the stability analysis of a cantilever T-section beam. Initially, the critical buckling moment decreases as the web tapering ratio decreases to 0.34 then the critical buckling moment starts increasing as the tapering ratio decreases due to a change in the buckling mode, thus Table 4.17.

Therefore, different tapering ratios affect the load bearing capacity of different steel sections differently since the case for I-section shows an increase in the load carrying capacity of the member as the tapering ratio decreases, thus Table 4.14.

f) Effect of tapering ratio on 1metre web tapered 100 x 50 channel section cantilever beam

Keeping the weight and volume constant, the web depth at the fixed end was gradually increased at 10mm increment while reducing the web depth at the free end by the same amount under 50kN applied point load as seen in Fig.4.8. For every change in the tapering angle, the resulting deflections, stress distribution and critical buckling load were tabulated.

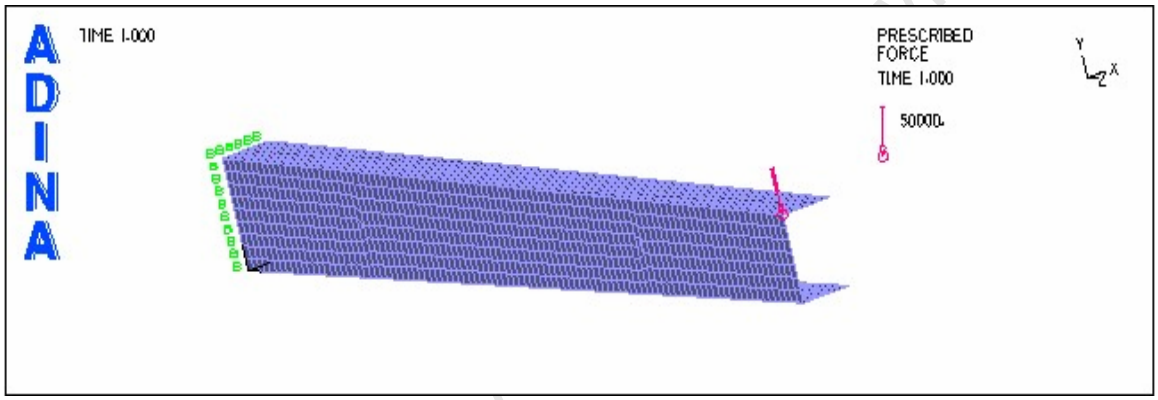

Figure 4.8. Web tapered cantilever channel section beam member under a point load

Table 4.18. **Maximum deflections of a web tapered 100 x 50 channel section cantilever beam under 50kN point load at the free end**

Web depth at the fixed end, H_w(mm)	**Web depth at the free end, h_w(mm)**	**Tapering ratio (h_w/H_w)**	**Maximum deflection at the free end, Δ_{max} (mm)**	**% decrease in the deflections**
100	100	1.00	85.2	0.0
110	90	0.82	71.0	16.7
120	80	0.67	59.9	29.7
130	70	0.54	51.0	40.1
140	60	0.43	43.7	48.7
150	50	0.33	37.8	55.6
160	40	0.25	36.0	57.7
170	30	0.18	37.4	56.1
180	20	0.11	41.8	50.9

The maximum deflection decreases as the tapering ratio (h_w/H_w) decreases up to 0.25 then the deflection starts increasing with decreasing tapering ratio as seen in Table 4.18. This effect can be attributed to the reduction in the section capacity of the cantilever beam, which results from excessive reduction in the flexural stiffness at the free end of the beam. The effect is the same as for T-section web tapered cantilever members, thus Table 4.15.

Table 4.19. **Maximum flexural stress of a web tapered 100 x 50 channel section cantilever beam under 50kN point load at the free end**

Web depth at the support, H_w(mm)	**Web depth at the free end, h_w(mm)**	**Tapering ratio (h_w/H_w)**	**Maximum stress of the cantilever σ_{max} (N/mm^2)**	**% decrease in the flexural stress**
100	100	1.00	1587	0.0
110	90	0.82	1322	16.7
120	80	0.67	1115	29.7
130	70	0.54	951	40.1
140	60	0.43	896	43.5
150	50	0.33	881	44.5
160	40	0.25	928	41.5
170	30	0.18	1132	28.7

Table 4.19 shows initial decrease in the flexural stress up to a tapering ratio of 0.33 then the maximum stress starts increasing with decreasing tapering ratio. Therefore, for design purposes, the optimum tapering ratio for channel section is 0.33. This same behaviour is exhibited by web tapered T-section cantilever beams, thus Table 4.16.

Table 4.20. **Critical buckling moment of a web tapered 100 x 50 channel section cantilever beam**

Web depth at the support, H_w(mm)	**Web depth at the free end, h_w(mm)**	**Tapering ratio (h_w/H_w)**	**Critical buckling moment M_{cr} (kNm)**	**% increase in the buckling moment**
100	100	1.00	36.12	0.0
110	90	0.82	40.56	12.3
120	80	0.67	44.90	24.3
130	70	0.54	54.35	50.5
140	60	0.43	57.10	58.1
150	50	0.33	64.10	77.5
160	40	0.25	71.85	98.9
170	30	0.18	79.60	120.4

For any decrease in the tapering ratio, there is an increase in the load bearing capacity of the web tapered cantilever beam as seen in Table 4.20. This behaviour is in agreement with that of I-section cantilever beams but not T-section cantilever beams. Therefore, different tapering ratios affect load bearing capacity of different steel sections differently.

4.3.2 Single Span Tapered beam members

Single span beam members can either be fix ended, pin ended or fix-pin ended and made up of different sections; I, T, channel, etc. However, in this study, the geometry of the single span beam members was mainly modelled to follow the bending moment envelope. Therefore, different loading conditions required different geometrical configuration of the beam members.

4.3.2.1 Fix ended 203 x 133 x 30 I-section non-prismatic beam members

The 203 x 133 x 30 I-section having web thickness, t_w = 6.4mm, flange thickness, t_f = 9.6mm and span length, L = 3m can be made non-prismatic in the web depth or web thickness and flange width or flange thickness separately or together. However, in this study, only the web depth and flange width were made non-prismatic under constant volume and weight.

a) Behaviour of a web tapered 203 x 133 x 30 I-section fix ended beam members.

A fix ended 203 x 133 x 30 I-section beam member of web thickness, t_w = 6.4mm, span length, L = 3m and flange thickness, t_f = 9.6mm was simulated for the effect of tapering ratio on beam deflection, flexural stress and lateral-torsional buckling. A 50kN point load was applied in the middle of the beam and the web depth at the fixed supports and at the point of load application was increased gradually at 10mm increment. At the same time, the web depth between the fixed supports and the point of load application were reduced by the same amount in order to keep the weight and volume of the beam constant, thus Fig. 4.9. The resulting deflections, flexural stress distribution and critical buckling moment were tabulated below.

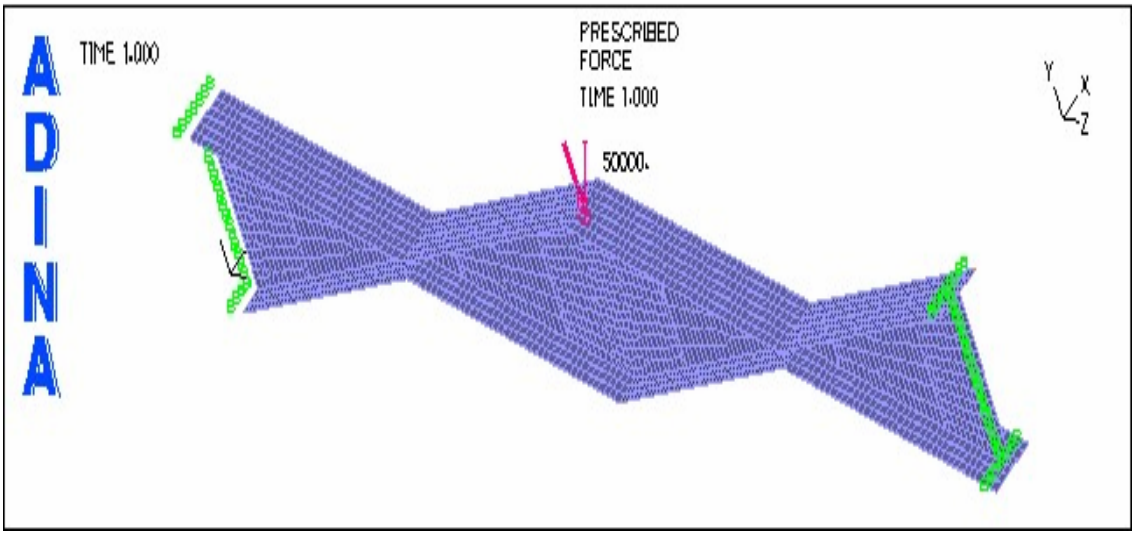

Figure 4.9. Web tapered fix ended I-section beam member under point load.

Table 4.21. **Maximum deflections at mid-span of a web tapered 203 x 133 x 30 I-section fix ended beams**

Web depth at supports, H_w(mm)	Web depth at the smaller section, h_w(mm)	Tapering ratio (h_w/H_w)	Maximum deflection, Δ_{max} (mm)	% decrease in the deflections
193.4	193.4	1.00	1.87	0.0
203.4	183.4	0.90	1.75	6.4
213.4	173.4	0.81	1.65	11.8
223.4	163.4	0.73	1.57	16.0
233.4	153.4	0.66	1.50	19.8
243.4	143.4	0.59	1.44	23.0
253.4	133.4	0.53	1.42	24.1
263.4	123.4	0.47	1.36	27.3
273.4	113.4	0.41	1.32	29.4
283.4	103.4	0.36	1.29	31.0
293.4	93.4	0.32	1.26	32.6
303.4	83.4	0.27	1.24	33.7
313.4	73.4	0.23	1.21	35.3
323.4	63.4	0.20	1.18	36.9
333.4	53.4	0.16	1.16	38.0
343.4	43.4	0.13	1.14	39.0

Generally, as the web tapering ratio decreases, the maximum deflection decreases, thus Table 4.21**.** Therefore, it is evident that web tapering ratio has the same effect on the deflections of I-section fix ended beam members as of cantilever beam members, thus Table 4.1.

Table 4.22. **Maximum stresses of a web tapered 203 x 133 x 30 I-section fix ended beams**

Web depth at supports, H_w(mm)	Web depth at the smaller section, h_w(mm)	Tapering ratio (h_w/H_w)	Maximum flexural stress, σ_{max} (N/mm^2)	% decrease in the flexural stress
193.4	193.4	1.00	178.5	0.0
203.4	183.4	0.90	173.3	2.9
213.4	173.4	0.81	169.4	5.1
223.4	163.4	0.73	166.3	6.8
233.4	153.4	0.66	163.4	8.5
243.4	143.4	0.59	160.6	10.0
253.4	133.4	0.53	158.8	11.0
263.4	123.4	0.47	154.2	13.6
273.4	113.4	0.41	151.4	15.2
283.4	103.4	0.36	148.8	16.6
293.4	93.4	0.32	146.1	18.2
303.4	83.4	0.27	143.6	19.6
313.4	73.4	0.23	142.1	20.4
323.4	63.4	0.20	143.2	19.8
333.4	53.4	0.16	144.1	19.3

As the tapering ratio decreases, the flexural stress at the fixed supports decreases to tapering ratio, (h_w/H_w = 0.23), then the stress at the smaller section of the beam, which increases steadily with the decreasing tapering ratio as shown in Table 4.22, controls the design. The unique behaviour of fix ended beam can be attributed to the fact that the smaller cross-section of the member yields beyond a tapering ratio of 0.23. Therefore, fixities play a major role on the effect of tapering ratio regarding stress distributions.

Table 4.23. **Critical buckling moment of a web tapered 203 x 133 x 30 I-section fix ended beams**

Web depth at supports, H_w(mm)	Web depth at the smaller section, h_w(mm)	Tapering ratio (h_w/H_w)	Critical buckling moment, M_{cr} (kNm)	% decrease in buckling moment
193.4	193.4	1.00	171.8	0.0
203.4	183.4	0.90	154.4	10.1
213.4	173.4	0.81	136.7	20.4
223.4	163.4	0.73	119.8	30.3
233.4	153.4	0.66	104.3	39.3
243.4	143.4	0.59	90.65	47.2
253.4	133.4	0.53	78.90	54.1
263.4	123.4	0.47	68.90	59.9
273.4	113.4	0.41	60.70	64.7

It can be observed from Table 4.23 that as the tapering ratio decreases, the critical buckling moment decreases. This effect might result from a steady reduction in the flexural stiffness of the two smaller cross-sections. Therefore, web tapered beam members with different fixities experience different effect of tapering ratio on their load bearing capacity.

b) Behaviour of a flange tapered 203 x 133 x 30 I-section fix ended beam members

In order to compare the effect of tapering ratio on different tapering positions, a fix ended 203 x 133 x 30 I-section beam member of web thickness t_w = 6.4mm, flange thickness, t_f = 9.6mm and span length, L = 3m was simulated for beam deflections, flexural stress and lateral-torsional buckling. A 50kN point load was applied in the middle of the beam and the flange width at the fixed supports and at the point of load application was increased gradually at 10mm increment. Under the same conditions, the flange width between the fixed supports and the point of load application was reduced gradually by the same amount as seen in Fig. 4.10. The resulting deflections, flexural stress and critical buckling moment for every change in the tapering ratio are shown in Tables 4.24 to 4.26

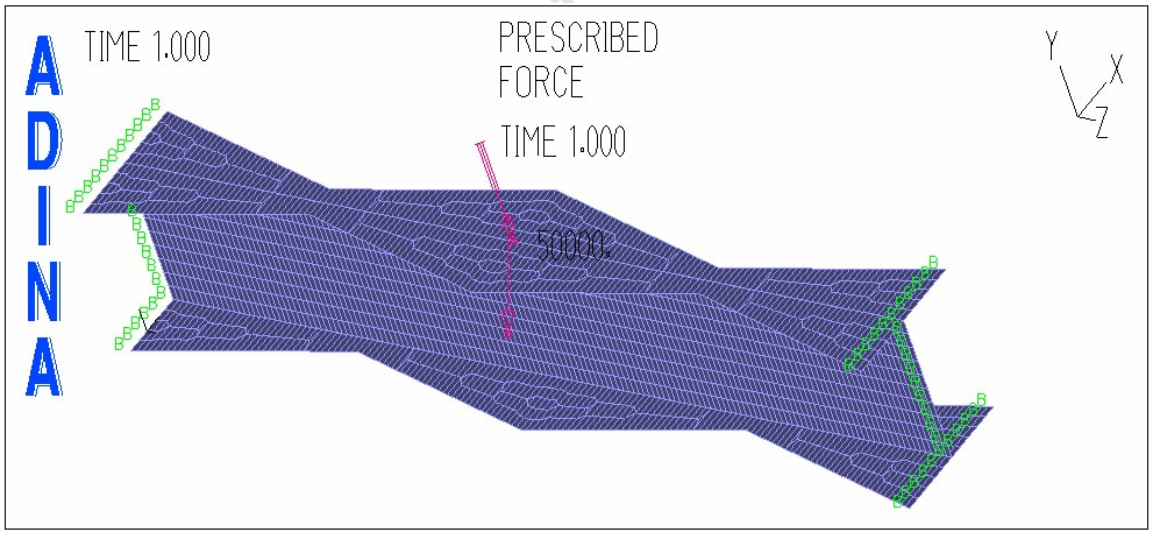

Figure 4.10. Flange tapered fix ended I-section beam member under a point load in the mid-span

Table 4.24. **Maximum deflections of a flange tapered 203 x 133 x 30 I-section fix ended beams**

Flange width at supports, W_f (mm)	Flange width at the smaller section, w_f (mm)	Tapering ratio (w_f/W_f)	Maximum deflection, Δ_{max} (mm)	% decrease in the deflections
133	133	1.00	1.87	0.0
143	123	0.86	1.84	1.6
153	113	0.74	1.82	2.7
163	103	0.63	1.80	3.7
173	93	0.54	1.79	4.3
183	83	0.45	1.78	4.8
193	73	0.38	1.77	5.3
203	63	0.31	1.76	5.9
213	53	0.25	1.76	5.9
223	43	0.19	1.76	5.9
233	33	0.14	1.76	5.9

A decrease in the flange tapering ratio (w_f/W_f) results in a decrease in the maximum deflections of a fix ended I-section beam members when a point load is applied in the middle of the beam as shown in Fig. 4.10**.** However, the resulting numerical maximum deflections are recorded in Table 4.24. Therefore, different positioning of taper has no effect on the maximum deflections of a fix ended beam since the same effect is experienced by both web and flange tapered members.

Table 4.25. **Maximum flexural stress of a flange tapered 203 x 133 x 30 I-section fix ended beams**

Flange width at supports, W_f (mm)	Flange width at the smaller section, w_f (mm)	Tapering ratio (w_f/W_f)	Maximum flexural stress, σ_{max} (N/mm^2)	% decrease in the flexural stress
133	133	1.00	178.5	0.0
143	123	0.86	178.0	0.3
153	113	0.74	177.0	0.8
163	103	0.63	175.9	1.5
173	93	0.54	175.9	1.5
183	83	0.45	176.1	1.3
193	73	0.38	176.3	1.2
203	63	0.31	176.4	1.2
213	53	0.25	176.4	1.2
223	43	0.19	176.7	1.0
233	33	0.14	176.8	1.0

As the tapering ratio, (w_f/W_f) decreases initially to 0.54, the maximum flexural stress decreases due to increase in the section modulus at the section with the highest bending moment as seen in equation (2.34). However, after tapering ratio (w_f/W_f = 0.54), the maximum flexural stress of the fix ended beam starts increasing with decreasing tapering ratio. This behaviour can be attributed to the extreme lost of the section capacity of the smaller cross-sectional dimensions. This behaviour is almost the same as that for web tapered beam, thus Table 4.22. Therefore, the effect of tapering ratio on flexural stress for a fix ended beams is the same regardless of tapering position.

Table 4.26. **Critical buckling moment of a flange tapered 203 x 133 x 30 I-section fix ended beams**

Flange width at supports, W_f (mm)	**Flange width at the smaller section, w_f (mm)**	**Tapering ratio (w_f/W_f)**	**Critical buckling moment, M_{cr} (kNm)**	**% increase in the buckling moment**
133	133	1.00	27.9	0.0
143	123	0.86	31.7	13.6
153	113	0.74	31.7	13.6
163	103	0.63	74.4	166.7
173	93	0.54	74.4	166.7
183	83	0.45	74.4	166.7
193	73	0.38	74.4	166.7
203	63	0.31	74.5	167.0
213	53	0.25	105.1	276.7
223	43	0.19	167.3	499.6
233	33	0.14	194.8	598.2

Table 4.26 shows increase in load bearing capacity of the fix ended flange tapered beam as the tapering ratio, (w_f/W_f) decreases. This is contrary to the results obtained in Table 4.23 for web tapered fix ended beam where the load bearing capacity decreases as the tapering ratio decreases. Therefore, different tapering positions on fix ended beams have different effect on the load carrying capacity of the same member. This behaviour might be based on the fact that the flange and web are under different action. It can also be concluded that the optimum position of tapering the fix ended beam is the flange.

4.3.2.2 Pin ended 203 x 133 x 30 I-section non-prismatic beam members

Pin ended beam members have zero bending moment at their supports and maximum bending moment in the middle of the beams. Therefore, if their geometry is to closely resemble the bending moment envelope, the beams must have larger section dimensions in the middle as compared to the ones at the supports for either web or flange non-prismatic members.

a) Effect of tapering ratio on a web tapered 203 x 133 x 30 I-section pin ended beam members

The pin ended 203 x 133 x 30 I-section beam members with web thickness, t_w = 6.4mm, flange thickness, t_f = 9.6mm and span length, L = 3m under constant volume and weight, was simulated for the effect of different tapering ratios on beam deflections, flexural stress and lateral-torsional buckling moment. Therefore, in order to keep the weight and volume constant, the web depth in the middle of the beam was increased at 10mm interval and at the same time, the web depth at the supports were reduced by the same amount, thus Fig. 4.11. A 50kN point load was applied in the middle of the beam and the resulting deflections, flexural stress and critical buckling moment were recorded in Tables 4.26 to 4.28**.**

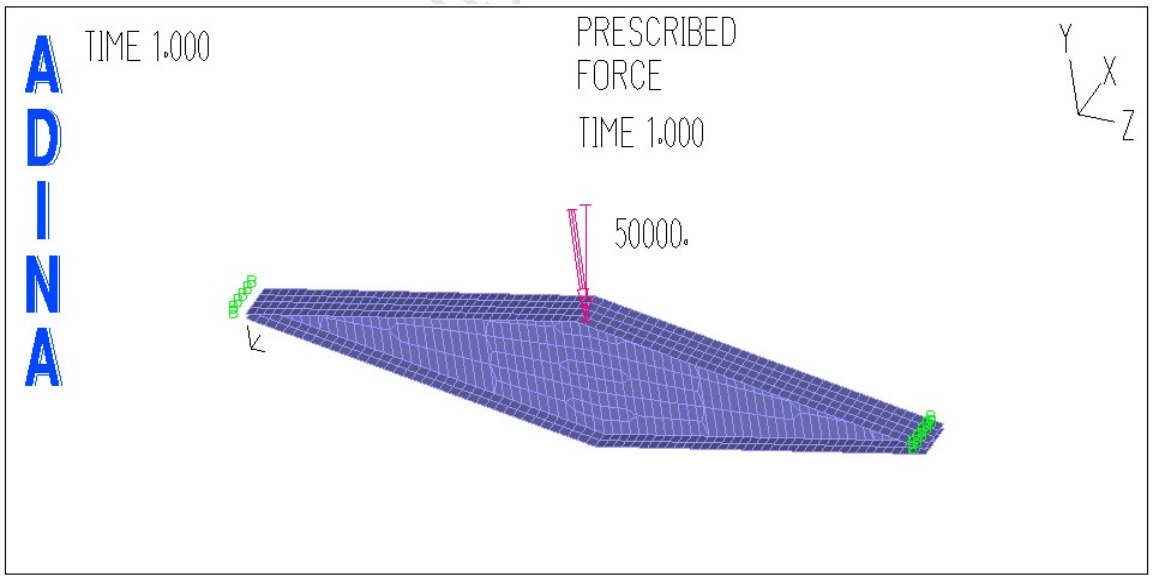

Figure 4.11. A single span web tapered I-section pin ended beam member under a point load

Table 4.27. **Maximum deflections of a web tapered 203 x 133 x 30 I-section pin ended beams**

Web depth at the supports, H_w(mm)	Web depth at mid-span, h_w(mm)	Tapering ratio (h_w/H_w)	Maximum deflections, Δ_{max} (mm)	% increase in the deflections
193.4	193.4	1.00	1.65	0.0
183.4	203.4	1.11	1.66	0.6
173.4	213.4	1.23	1.67	1.2
163.4	223.4	1.37	1.68	1.8
153.4	233.4	1.52	1.70	3.0
143.4	243.4	1.70	1.73	4.8
133.4	253.4	1.90	1.76	6.7
123.4	263.4	2.13	1.79	8.5
113.4	273.4	2.41	1.84	11.5
103.4	283.4	2.74	1.89	14.5
93.4	293.4	3.14	1.95	18.2
83.4	303.4	3.64	2.02	22.4

For a pin ended web tapered I-section beam members under a point load as seen in Fig. 4.11, the maximum deflection increases with decreasing tapering ratios, thus Table 4.27**.** This behaviour can be attributed to a reduction in flexural rigidity at the supports concurrently with the increasing effective weight in the middle of the beams. Therefore, different fixities experienced different effects of tapering ratio on beams deflections since the results in Table 4.27 are not the same as those of Table 4.1 and 4.21 for web tapered cantilever and fix ended beam members under 50kN.

Table 4.28. **Flexural stress of a web tapered 203 x 133 x 30 I-section pin ended beams**

Web depth at the supports, H_w(mm)	Web depth at mid-span, h_w(mm)	Tapering ratio (h_w/H_w)	Maximum flexural stress, σ_{max} (N/mm^2)	% increase in the flexural stress
193.4	193.4	1.00	69.0	0.0
183.4	203.4	1.11	70.0	1.4
173.4	213.4	1.23	70.1	1.6
163.4	223.4	1.37	73.2	6.1
153.4	233.4	1.52	75.8	9.9
143.4	243.4	1.70	78.8	14.2
133.4	253.4	1.90	82.2	19.1
123.4	263.4	2.13	86.8	25.8
113.4	273.4	2.41	92.1	33.5
103.4	283.4	2.74	98.2	42.3
93.4	293.4	3.14	105.2	52.5
83.4	303.4	3.64	113.5	64.5

Table 4.28 shows a continuous increase in the flexural stress of the pin ended web tapered beam members as the tapering ratio decreases. This is due to a reduction in section's modulus at the supports of the members. However, this behaviour is different from the ones observed in Tables 4.3 and 4.22 with a decrease in flexural stress as the tapering ratio decreases for cantilever and fix ended beams. Therefore, different fixities experiences different effects of tapering ratio on web tapered beam stress distribution.

Table 4.29. **Critical buckling moment of a web tapered 203 x 133 x 30 I-section pin ended beams**

Web depth at the supports, H_w(mm)	**Web depth at mid-span, h_w(mm)**	**Tapering ratio (h_w/H_w)**	**Critical buckling moment, M_{cr} (kNm)**	**% decrease in the buckling moment**
193.4	193.4	1.00	340.2	0.0
183.4	203.4	1.11	324.6	4.6
173.4	213.4	1.23	309.6	9.0
163.4	223.4	1.37	294.8	13.3
153.4	233.4	1.52	280.9	17.4
143.4	243.4	1.70	267.2	21.5
133.4	253.4	1.90	254.4	25.2
123.4	263.4	2.13	242.6	28.7
113.4	273.4	2.41	231.7	31.9
103.4	283.4	2.74	221.6	34.9
93.4	293.4	3.14	212.5	37.5
83.4	303.4	3.64	204.2	40.0

From Table 4.29, the critical buckling moment of a pin ended beam member decreases as the tapering ratio increases. This may result from the reduction in the stiffness of the beams at the supports. Therefore, a pin ended beam member reduces its load bearing capacity with an increasing tapering ratio. This is an evident that different beam fixities influence the effect of web tapering ratio on load bearing capacity of the beam, since this result is not the same as the ones observed in Table 4.5 and 4.23 for web tapered I-section cantilever and fix ended beam members.

b) Effect of tapering ratio on a flange tapered 203 x 133 x 30 I-section pin ended beam members

Keeping the weight and volume constant, a flange tapered 203 x 133 x 30 I-section pin ended beam member with web thickness, t_w = 6.4mm, flange thickness, t_f = 9.6mm and span length, L = 3m was simulated for deflections, stress distribution and lateral-torsional buckling load. The model aimed at comparing the effects of different flange tapering ratios with that of web on the same beam under the same boundary and loading conditions.

In order to make the model geometry closely resemble the bending moment envelope for a 50kN point load applied in the middle of a beam, starting from flange tapering ratio of unity, (w_f/W_f = 1), the flange width at the supports were reduced at 10mm interval and at the same time, the flange width in the middle were increased by the same magnitude as shown in Fig. 4.12. The resulting deflections, flexural stress and buckling moment for every change in the flange tapering ratio were tabulated.

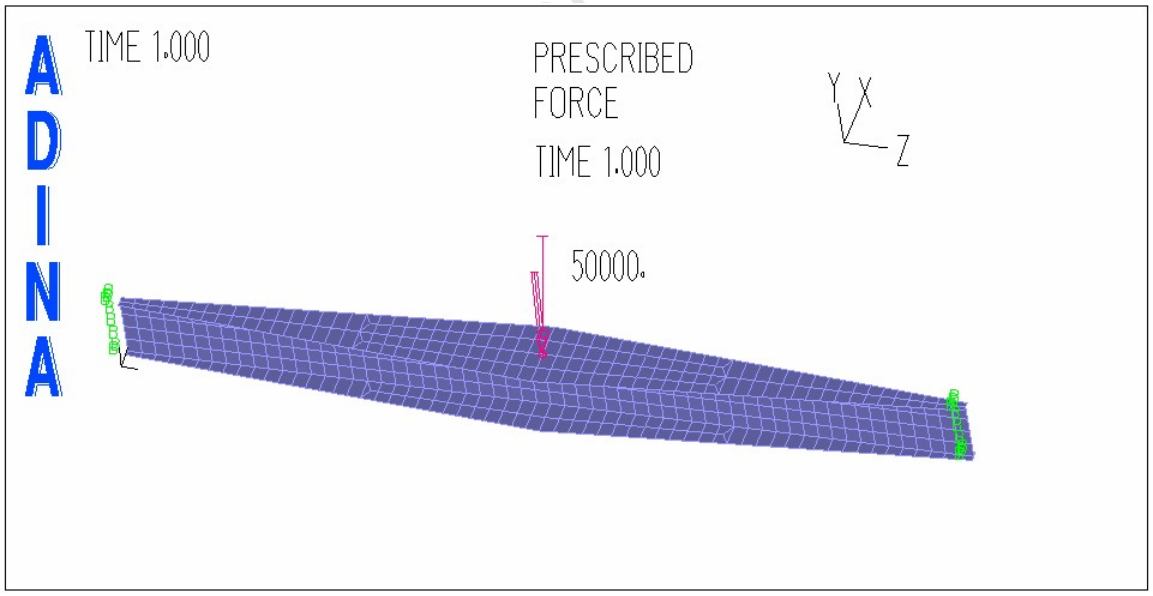

Figure 4.12. A single span flange tapered pin ended I-section beam member under point load

Table 4.30**. Maximum deflections of a flange tapered 203 x 133 x 30 I-section pin ended beams**

Flange width at the supports, W_f (mm)	Flange width at the mid-span, w_f (mm)	Tapering ratio (w_f/W_f)	Maximum deflection, Δ_{max} (mm)	% increase in the deflections
133	133	1.00	1.70	0.0
123	143	1.16	1.70	0.0
113	153	1.35	1.71	0.6
103	163	1.58	1.72	1.2
93	173	1.86	1.73	1.8
83	183	2.20	1.74	2.4
73	193	2.64	1.76	3.5
63	203	3.22	1.79	5.3
53	213	4.02	1.81	6.5
43	223	5.19	1.85	8.8
33	233	7.06	1.90	11.8

It is clearly observed from Table 4.30, as the flange tapering ratio w_f/W_f increases, the maximum deflection of a pin ended I-section beam members increases. Therefore, different tapering ratios for either web or flange have the same effect on deflection of a single span I-section pin ended beam with applied point load in the middle. However, this is not the same behaviour with fix ended and cantilever beams. This implies that different fixities experience different effects of flange tapering ratio on the beam deflection.

Table 4.31**. Maximum flexural stress of a flange tapered 203 x 133 x 30 I-section pin ended beams**

Flange width at the supports, W_f (mm)	Flange width at the mid-span, w_f (mm)	Tapering ratio (w_f/W_f)	Maximum flexural stress, σ_{max} (N/mm^2)	% decrease in the flexural stress
133	133	1.00	111.6	0.0
123	143	1.16	111.1	0.4
113	153	1.35	110.7	0.8
103	163	1.58	110.4	1.1
93	173	1.86	110.1	1.3
83	183	2.20	109.9	1.5
73	193	2.64	109.7	1.7
63	203	3.22	109.6	1.8
53	213	4.02	109.5	1.9
43	223	5.19	112.7	-1.0
33	233	7.06	125.7	-12.6

Table 4.31 shows a negligible impact of flange tapering ratio on flexural stress of a pin ended beam as compared to web tapering ratio of the same beam, thus Table 4.28**.** This behaviour can be attributed to the fact that web of an I-section is under shear while flange is under bending action. Therefore, changes in the depth of the web affect stress distribution of the I-section beam member more than that from changes in the width of the flanges.

Table 4.32**. Critical buckling moment of a flange tapered 203 x 133 x 30 I-section pin ended beams**

Flange width at the supports, W_f (mm)	**Flange width at the mid-span, w_f (mm)**	**Tapering ratio (w_f/W_f)**	**Critical buckling moment, M_{cr} (kNm)**	**% decrease in the buckling moment**
133	133	1.00	344.9	0.0
123	143	1.16	344.6	0.1
113	153	1.35	343.9	0.3
103	163	1.58	342.6	0.7
93	173	1.86	340.0	1.4
83	183	2.20	333.1	3.4
73	193	2.64	323.5	6.2
63	203	3.22	311.2	9.8
53	213	4.02	295.8	14.2
43	223	5.19	277.0	19.7
33	233	7.06	253.9	26.4

As the flange tapering ratio, w_f/W_f, increases, the lateral-torsional buckling moment of a pin ended I-section single span beam member decreases. This behaviour can be attributed to a reduction in the flange flexural stiffness at the supports. This same behaviour is also experienced by both web and flange tapered pin ended beams. Therefore, for stability design purposes it is not recommended to taper the pin ended beams as it is evident from Table 4.29 and 4.32 that as the tapering angle increases, the load bearing capacity of the member decreases.

4.4 Behaviour of steel members in compression

These members can be classified as cantilever, pin ended, fix ended or pin-fix ended columns, depending on the boundary conditions applied. In practical applications, H and I-sections are mainly used for column members but in this study, for comparative analysis of different tapering ratios on different steel sections under compressive loading, channel and angle sections were simulated in addition to H and I-sections for load bearing analysis.

4.4.1 *Global buckling analysis of cantilever columns.*

Different types of steel sections were modelled as cantilever columns for stability analysis. The weight and volume were kept constant by varying the dimensions of the two extreme end of the member simultaneously. In addition, the thicknesses were kept constant throughout the model analysis.

4.4.1.1 Effect of different tapering ratios on 152 x 152 x 23 H-section cantilever columns

A column made up of 152 x 152 x 23 H-section and other dimensions as web thickness, t_w = 6.1mm, flange thickness, t_f = 6.8mm and the height of 3m was modelled for stability analysis under various geometrical arrangements.

a) Web tapered 152 x 152 x 23 H-section cantilever columns

Firstly, the column's web depth at the free end was decreased gradually at 10mm interval. However, the web depth at the fixed end was increased by the same amount while keeping every other dimension constant as seen in Fig.4.13**.** A constant load was applied at the free end and the first critical buckling load for every different tapering ratio was recorded, thus Table 4.33**.**

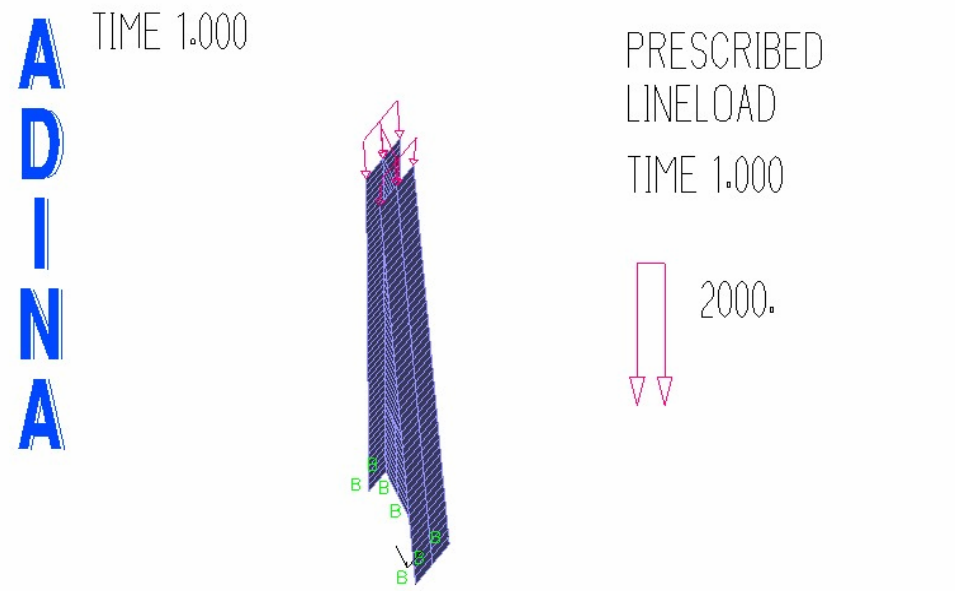

Figure 4.13a Web tapered H-section cantilever column member with larger dimensions at the fixed support

Table 4.33a**. Global first critical buckling load of a web tapered 152 x 152 x 23 I-section cantilever columns with larger dimensions at the fixed support**

Web depth at fixed support, H_w (mm)	Web depth at free end, h_w (mm)	Tapering ratio (h_w/H_w)	Critical buckling load, P_{cr} (kN)	% increase in the critical buckling load
145.2	145.2	1.00	201	0.0
155.2	135.2	0.87	203	1.0
165.2	125.2	0.76	203	1.0
175.2	115.2	0.66	203	1.0
185.2	105.2	0.57	203	1.0
195.2	95.2	0.49	203	1.0
205.2	85.2	0.42	206	2.5
215.2	75.2	0.35	206	2.5
225.2	65.2	0.29	206	2.5
235.2	55.2	0.23	206	2.5
245.2	45.2	0.18	206	2.5
255.2	35.2	0.14	206	2.5

Table 4.33a shows slight increase in the load bearing capacity as the tapering ratio, (h_w/H_w), of the web tapered cantilever column with larger section's dimensions at the fixed end, having constant weight and volume decreases. This behaviour may be attributed to the slow increase in the stiffness at the columns support. Therefore, the effect of tapering an H-section cantilever column with the kind of arrangement such as the one in Fig.4.13a can be considered insignificant.

Secondly, in order to compare the effect of web tapering position, the web depth at the free end was increased gradually at 10mm interval. At the same time, the web depth at the fixed end was decreased by the same interval while keeping every other dimension constant as seen in Fig.4.13b**.** The critical buckling load was recorded against different tapering ratios, thus Table 4.33b.

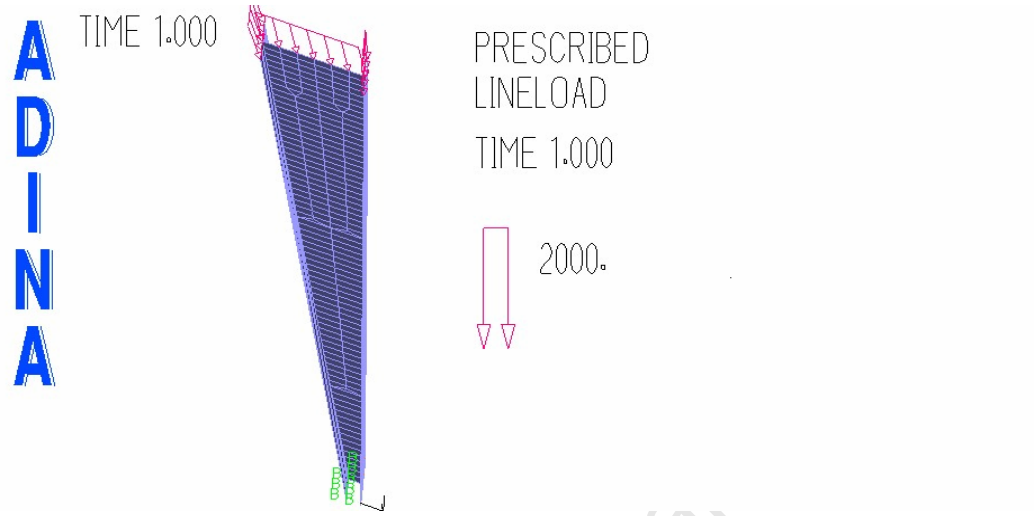

Figure 4.13b. Web tapered H-section cantilever column members with larger section at the free end

Table 4.33b**. Global first critical buckling load of a web tapered 152 x 152 x 23 I-section cantilever columns with larger dimensions at the free end**

Web depth at fixed end, H_w (mm)	**Web depth at free end, h_w (mm)**	**Tapering ratio (h_w/H_w)**	**Critical buckling load, P_{cr} (kN)**	**% increase in the critical buckling load**
145.2	145.2	1.00	201	0.0
135.2	155.2	1.15	207	3.0
125.2	165.2	1.32	207	3.0
115.2	175.2	1.52	207	3.0
105.2	185.2	1.76	207	3.0
95.2	195.2	2.05	206	2.5
85.2	205.2	2.41	206	2.5
75.2	215.2	2.86	206	2.5
65.2	225.2	3.45	206	2.5
55.2	235.2	4.26	206	2.5
45.2	245.2	5.42	184	-8.5
35.2	255.2	7.25	137	-31.8

Generally, the first critical buckling load in Table 4.33b decreases as the tapering ratio, (h_w/H_w), increases.

This is evident, increasing the section dimensions at the free end reduces the stiffness of the columns at the support and the members become less stable. Table 4.33a shows a clear increase in the buckling load as tapering ratio decreases as opposed to Table 4.33b, which shows general decrease in the buckling load for the same member under different geometrical arrangement, shown in Fig. 4.13b. This result is in close agreement with the conclusion made in [61].

b) Flange tapered 152 x 152 x 23 H-section cantilever columns

Keeping weight, volume and thickness constant, the flange width was reduced at 10mm increment at the free end while increasing at the fixed end by the same amount as seen in Fig. 4.14a. The first critical buckling load was recorded against every varying tapering ratio, thus Table 4.34a.

Following similar procedures, flange width at the fixed end was reduced at 10mm interval while increasing the one at the free end by the same interval as seen in Fig. 4.14b**.** The resulting critical buckling load for every incremental flange changes was recorded in Table 4.34b.

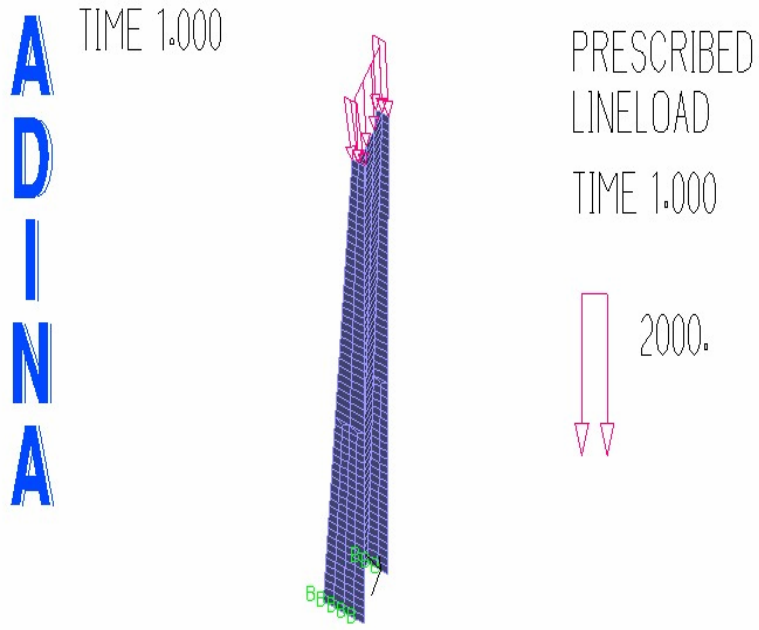

Figure 4.14a. Flange tapered H-section cantilever column members with larger dimensions at the fixed support

Table 4.34a**. First critical buckling load of a flange tapered 152 x 152 x 23 I-section cantilever columns with larger dimensions at the fixed end.**

Flange width at the fixed end, W_f (mm)	Flange width at the free end, w_f (mm)	Tapering ratio (w_f/W_f)	Critical buckling load, P_{cr} (kN)	% increase in the critical buckling load
152	152	1.00	201	0.0
162	142	0.88	223	10.9
172	132	0.77	237	17.9
182	122	0.67	249	23.9
192	112	0.58	258	28.4
202	102	0.50	265	31.8
212	92	0.43	268	33.3
222	82	0.37	267	32.8
232	72	0.31	263	30.8
242	62	0.26	253	25.9
252	52	0.21	237	17.9
262	42	0.16	216	7.5

The critical buckling load of flange tapered column increases rapidly as the tapering ratio changes which is not the case with web tapered column. Therefore, it is evident that tapering the flange has more impact on the column stability compared to web tapering ratio. This can be attributed to the fact that buckling of a laterally unrestrained column occurs about the weaker axis. Furthermore, after flange tapering ratio ($w_f/W_f = 0.43$), the load bearing capacity of the column starts decreasing due to a change in the buckling modes.

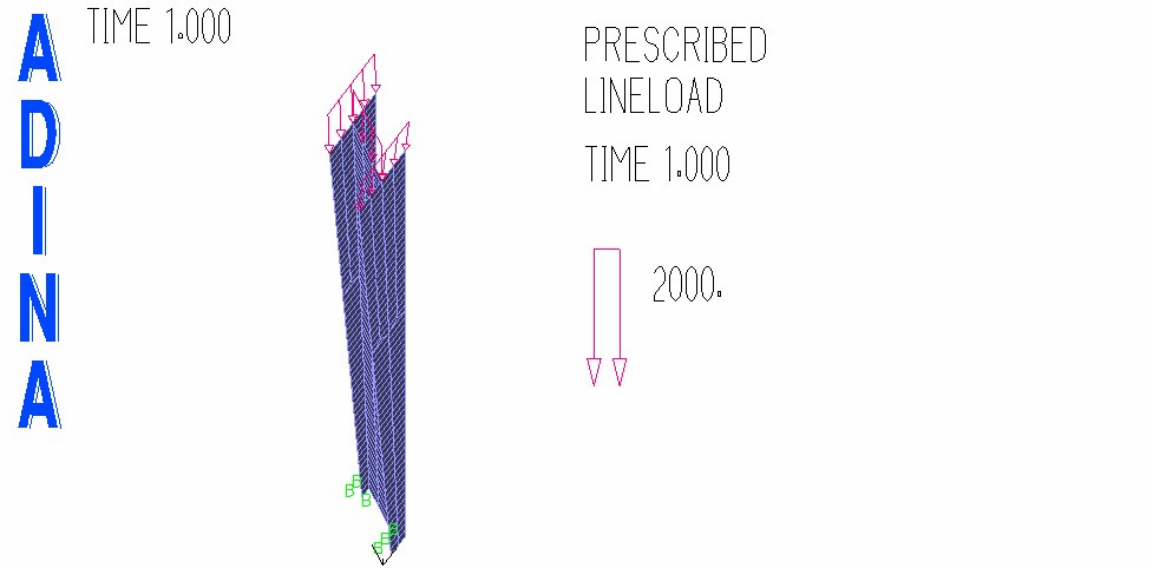

Figure 4.14b. Flange tapered H-section cantilever column members with larger dimensions at the free end

Table 4.34b**. Global buckling load of a flange tapered 152 x 152 x 23 I-section cantilever columns with larger dimensions at the free end**

Flange width at the fixed end, W_f (mm)	Flange width at the free end, w_f (mm)	Tapering ratio (w_f/W_f)	Critical buckling load, P_{cr} (kN)	% decrease in the critical buckling load
152	152	1.00	201	0.0
142	162	1.14	190	5.5
132	172	1.30	172	14.4
122	182	1.49	154	23.4
112	192	1.71	135	32.8
102	202	1.98	116	42.3
92	212	2.30	98	51.2
82	222	2.71	81	59.7
72	232	3.22	65	67.7
62	242	3.90	50	75.1

There is a gradual decrease in the load bearing capacity of flange tapered cantilever column as the tapering ratio (w_f/W_f) increases. This behaviour can be attributed to a gradual decrease in the column stiffness at the support as the tapering ratio increases. Increase in column sectional dimension at the free end reduces the flexural rigidity of the member at the support, which results into a reduction in member stability (Fig. 4.34b).

4.4.1.2 Behaviour of 25 x 25 x 5 angle section cantilever column member

A column member with angle cross-sectional dimensions; 25 x 25 x 5, leg thickness, t = 5mm and a height of 1m was modelled for comparative analysis of the effect of tapering ratio on different types of steel sections used as cantilever columns. Starting with the uniform members, the width of both legs at the free end of the column was reduced gradually at 2mm interval while the width of both legs at the fixed supports was increased by the same amount in order to keep the volume and weight constant, thus Fig.4.15. Thereafter, the cross-sectional dimensions at the top of the cantilever column were increased by 4mm interval while the bottom cross-sectional dimensions were reduced gradually by the same interval as shown in Fig. 4.16**.** The first critical buckling load for both cases was recorded.

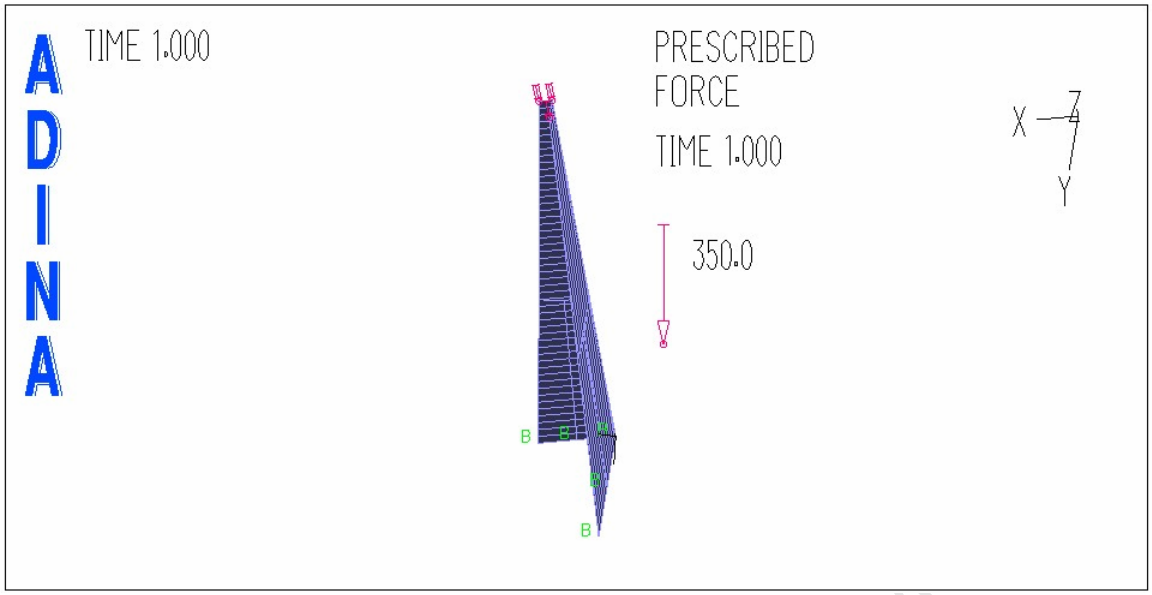

Figure 4.15. Tapered angle section cantilever column member with smaller dimensions at the free end

Table 4.35**. The critical buckling load of 25 x 25 x 5 angle section non-prismatic cantilever column**

Section dimensions at the support, H (mm)	Section dimensions at the free end, h (mm)	Tapering ratio (h/H)	Critical buckling load, P_{cr} (kN)	% increase in the critical buckling load
25	25	1.00	2465.1	0.0
27	23	0.85	2708.1	9.9
29	21	0.72	2915.1	18.3
31	19	0.61	3075.0	24.7
33	17	0.52	3177.0	28.9
35	15	0.43	3204.0	30.0
37	13	0.35	3150.0	27.8
39	11	0.28	2994.3	21.5
41	9	0.22	2727.9	10.7
43	7	0.16	2340.3	-5.1

As the tapering ratio decreases in Table 4.35, the critical buckling load increases. This is due to the initial increase in the stiffness of the column at the support up to a tapering ratio, (h/H = 0.43), then as the buckling configuration changes, the load bearing capacity of the member starts decreasing with decreasing tapering ratio. This behaviour may be due to a decrease in stiffness of the member at the support after (h/H = 0.43).

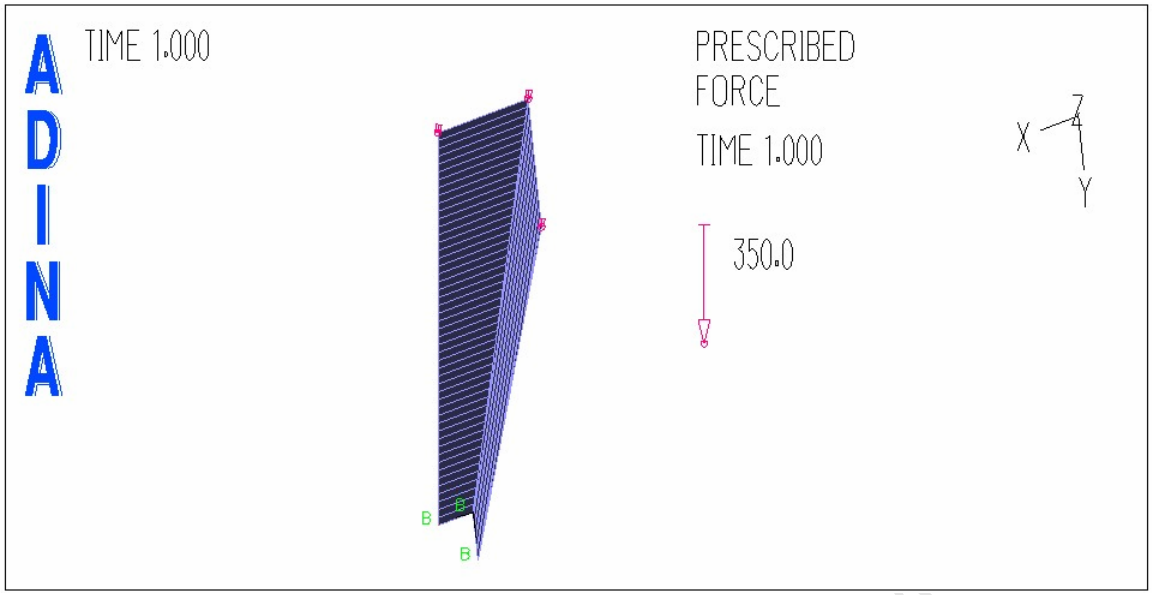

Figure 4.16. Tapered angle section cantilever column member with larger dimensions at the free end

Table 4.36. **Critical buckling load of a tapered cantilever angle section column with larger dimensions at the free end**

Section dimensions at the support, H (mm)	Section dimensions at the free end, h (mm)	Tapering ratio (h/H)	Critical buckling load, P_{cr} (N)	% decrease in the critical buckling load
25	25	1.00	2465.1	0.0
23	27	1.17	2197.2	10.9
21	29	1.38	1914.3	22.3
19	31	1.63	1624.5	34.1
17	33	1.94	1338.9	45.7
15	35	2.33	1065.3	56.8
13	37	2.85	810.3	67.1
11	39	3.55	584.7	76.3
9	41	4.56	393.9	84.0

The buckling load decreases as the tapering ratio (h/H) increases. This is the same result observed for H-section cantilever column in Table 4.33b. Therefore, for this kind of geometrical arrangement, the load bearing capacity of the column decreases with decreasing tapering ratio regardless of the section type.

4.4.1.3 Behaviour of *C76 x 38* channel section cantilever column members

A channel section cantilever column can either be made non-prismatic in the web depth, flange width or web and flange thicknesses. However, for this study, the web and flange thicknesses were kept constant throughout the simulation processes.

a) Web tapered cantilever C76 x 38 channel section columns

Cantilever column member of cross-sectional dimensions; C76 x 38 with web thickness, t_w = 5.1mm, flange thickness, t_f = 6.8mm and a height of 1m were modelled for stability analysis under various tapering ratios. The web depth at the fixed end was increased gradually by 2mm interval. At the same time, the web depth at the free end was reduced by the same amount in order to keep the weight and volume constant as seen in Fig. 4.17**.** The resulting critical buckling load for every change in web tapering ratio, was recorded, thus Table 4.37.

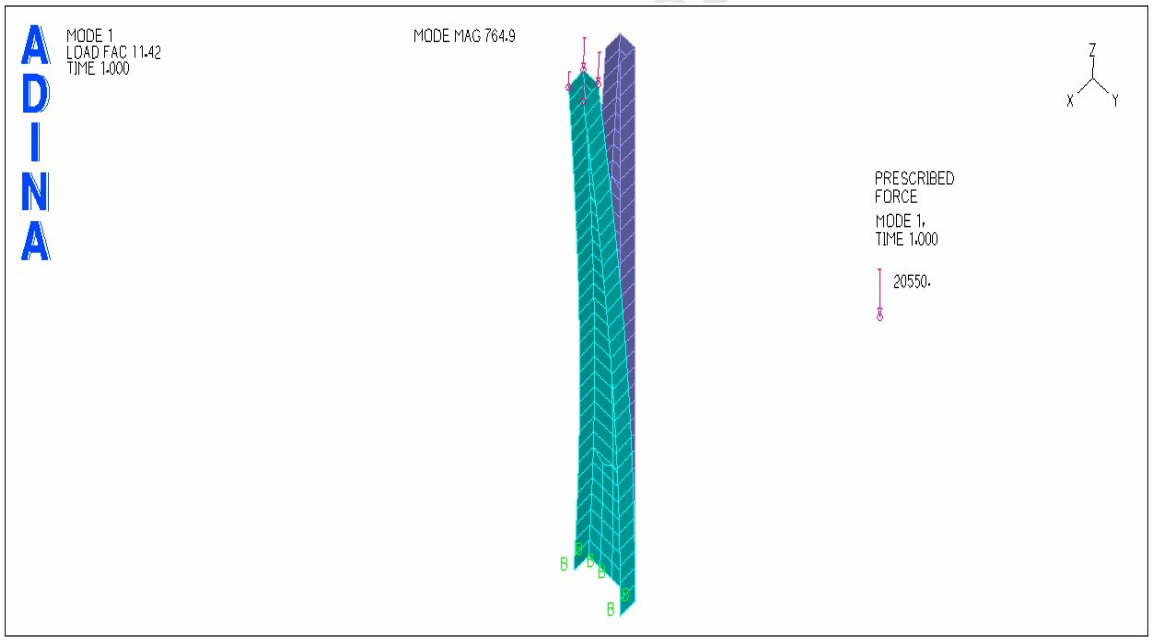

Figure 4.17. Web tapered channel section cantilever column member with larger section dimensions at the fixed support

Table 4.37. **Critical buckling load of a web tapered cantilever channel section column with larger dimensions at the fixed support**

Web depth at the fixed support, H_w (mm)	Web depth at the free end, h_w (mm)	Tapering ratio (h_w/H_w)	First critical buckling load, P_{cr} (N)	% increase in the critical buckling load
69.2	69.2	1.00	58748	0.0
73.2	65.2	0.89	59160	0.7
77.2	61.2	0.79	59552	1.4
81.2	57.2	0.70	59916	2.0
85.2	53.2	0.62	60252	2.6
89.2	49.2	0.55	60568	3.1
93.2	45.2	0.48	60864	3.6
97.2	41.2	0.42	61132	4.1
101.2	37.2	0.37	61384	4.5
105.2	33.2	0.32	61612	4.9
109.2	29.2	0.27	61824	5.2
113.2	25.2	0.22	62012	5.6
117.2	21.2	0.18	62184	5.8
121.2	17.2	0.14	62324	6.1
125.2	13.2	0.11	62452	6.3
129.2	9.2	0.07	62552	6.5

Table 4.37 shows a continuous increase in the load bearing capacity of the channel cantilever column as the tapering ratio (h_w/H_w), decreases. This behaviour can be attributed to the fact that there is an increase in the flexural rigidity at the support of the cantilever column as seen in Fig. 4.17**.** Therefore, this leads to an increase in the effective stiffness of the column.

b) Flange tapered cantilever C76 x 38 channel section columns

Following a similar procedure as for web tapered channel cantilever column, the channel section member with dimensions; C76 x 38, web thickness, t_w = 5.1mm, flange thickness, t_f = 6.8mm and a height of 1m were simulated for stability analysis. The flange width at the fixed end was increased by 2mm increment while that at the free end was reduced by the same amount simultaneously in order to keep the weight and volume constant as seen in Fig. 4.18. The resulting critical buckling load for every changing flange tapering ratio was recorded, thus Table 4.38.

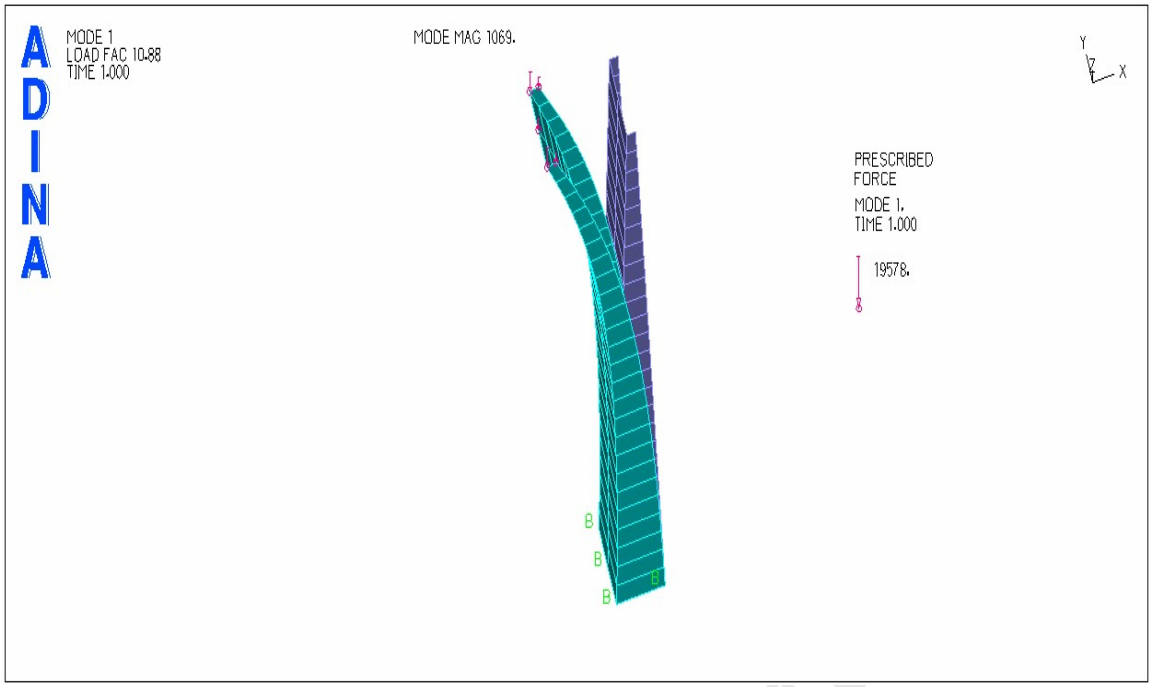

Figure 4.18. Flange tapered channel section cantilever column member with larger section dimensions at the fixed support

Table 4.38. **Critical buckling load of flange tapered cantilever channel section column with larger dimensions at the fixed support**

Flange width at the support, W_f (mm)	Flange width at the free end, w_f (mm)	Tapering ratio (w_f/W_f)	First critical buckling load, P_{cr} (N)	% increase in the critical buckling load
34.6	34.6	1.00	58748	0.0
38.6	30.6	0.79	65496	11.5
42.6	26.6	0.62	70868	20.6
46.6	22.6	0.48	67956	15.7
50.6	18.6	0.37	56240	-4.3
54.6	14.6	0.27	45976	-21.7
58.6	10.6	0.18	35588	-39.4

The first critical buckling load of flange tapered cantilever column increases initially with decreasing tapering ratio (w_f/W_f) up to 0.62, then it starts decreasing as the tapering ratio decreases, thus Table 4.38. The abrupt reduction in the buckling load could be as a result of change in the buckling mode, which is due to lost of load bearing capacity of smaller section as the flange width is reduced gradually (Fig.4.18). Therefore, the optimum tapering ratio for a flange tapered cantilever column is 0.62. Moreover, this shows the effect of positioning of taper on non-prismatic columns.

4.4.2 *Buckling analysis of pin-fix ended columns*

Structural members are termed pin-fix ended columns when one end is prevented from any possible movement while at the other end, only rotations are allowed. The boundary conditions affect the effective length of columns. This eventually affects the buckling configurations and the load bearing capacity of the columns.

4.4.2.1 Effect of web tapering ratio on 152 x 152 x 23 H-section fix-pin ended column members

The 152 x 152 x 23 H-section pin-fix ended columns with web thickness, t_w = 6.1mm and flange thickness, t_f = 6.8mm were simulated for the effect of tapering ratio on the stability of member. The H-section steel member can either be tapered in the web or flange.

a) Web tapered 152 x 152 x 23 H-section pin-fix ended columns

Firstly, the web depth at the pinned support was reduced at 10mm interval and that of the fixed support was increased by the same interval in order to keep the weight and volume constant as seen in Fig. 4.19a**.** The resulting critical buckling load for every changing web tapering ratio (h_w/H_w) was recorded in Table 4.39a.

Secondly, the web depth at the fixed end was reduced at 10mm interval and that for pinned supports was increased by the same interval in order to keep the weight and volume constant as seen in Fig. 4.19b. The resulting critical buckling load for every changing tapering ratio (h_w/H_w) was recorded in Table 4.38b. This analysis was done in order to compare the effect of different positioning of taper for the same column under the same fixities.

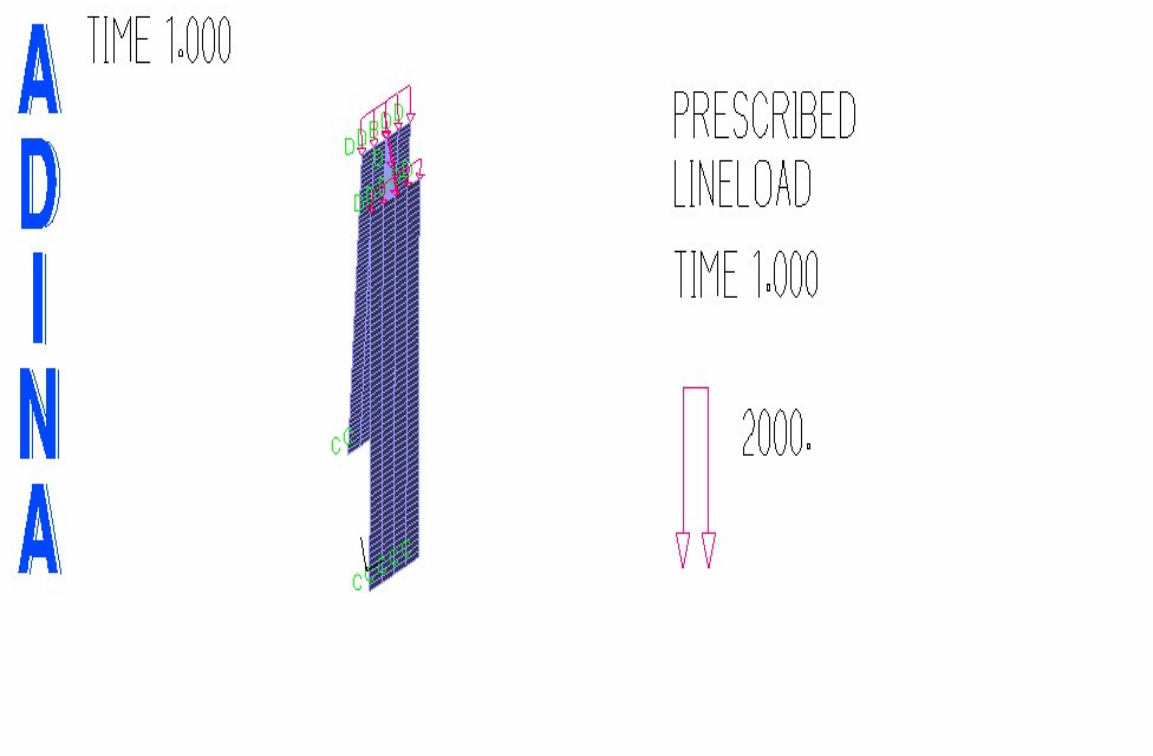

Figure 4.19a. Web tapered H-section pinned-fixed ends column members with larger dimensions at the fixed supports

Table 4.39a**. Global first critical buckling load of a web tapered 152 x 152 x 23 I-section pin-fix ended columns with larger dimensions at the fixed support**

Web depth at fixed end, H_w (mm)	Web depth at pinned end, h_w (mm)	Tapering ratio (h_w/H_w)	Critical buckling load, P_{cr} (kN)	% decrease in the critical buckling load
145.2	145.2	1.00	1362	0.0
155.2	135.2	0.87	1350	0.9
165.2	125.2	0.76	1301	4.5
175.2	115.2	0.66	1290	5.3
185.2	105.2	0.57	1279	6.1
195.2	95.2	0.49	1269	6.8
205.2	85.2	0.42	1258	7.6
215.2	75.2	0.35	1101	19.2
225.2	65.2	0.29	1100	19.2
235.2	55.2	0.23	1098	19.4
245.2	45.2	0.18	965	29.1
255.2	35.2	0.14	831	39.0

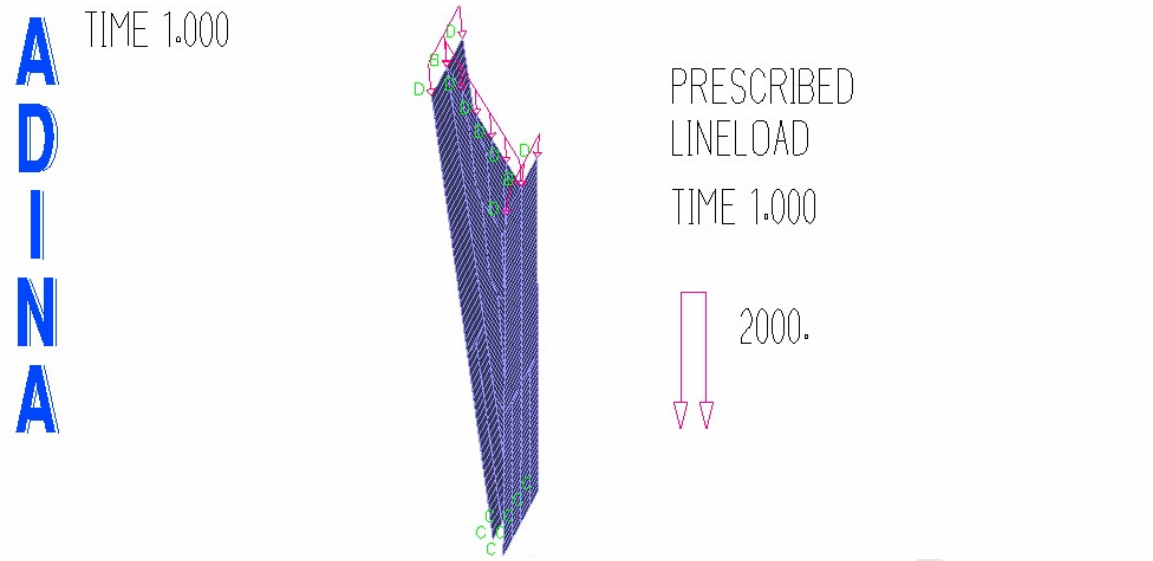

Figure 4.19b. Web tapered H-section pinned-fixed ends column members with larger dimensions at the pinned supports

Table 4.39b**. Global critical buckling load of a web tapered 152 x 152 x 23 I-section pin-fix ended columns with larger dimensions at the pinned support**

Web depth at fixed support, H_w (mm)	Web depth at pinned support, h_w (mm)	Tapering ratio (h_w/H_w)	Critical buckling load, P_{cr} (kN)	% increase in the critical buckling load
145.2	145.2	1.00	1201	0.0
135.2	155.2	1.15	1275	6.2
125.2	165.2	1.32	1288	7.2
115.2	175.2	1.52	1299	8.2
105.2	185.2	1.76	1313	9.3
95.2	195.2	2.05	1325	10.3
85.2	205.2	2.41	1340	11.6
75.2	215.2	2.86	1353	12.7
65.2	225.2	3.45	1365	13.7
55.2	235.2	4.26	1379	14.8
45.2	245.2	5.42	1393	16.0
35.2	255.2	7.25	1407	17.2

Tables 4.39a and 4.39b show different results for load bearing capacity of the same web tapered pin-fix ended columns. The column with larger dimensions at the fixed support shows a decrease in the load bearing capacity and vice versus. This behaviour can be attributed to the fact that pin-fix ended column experiences higher displacements near the pinned supports. Therefore, increase in flexural stiffness within that area will increase the bearing capacity of the column members.

Lastly, on the same column, the middle section of the column was made to have larger dimensions compared to the two extreme end supports, thus Fig. 4.20. Following the same procedures as for the previous cases, the critical buckling load was tabulated for every change in the tapering ratio.

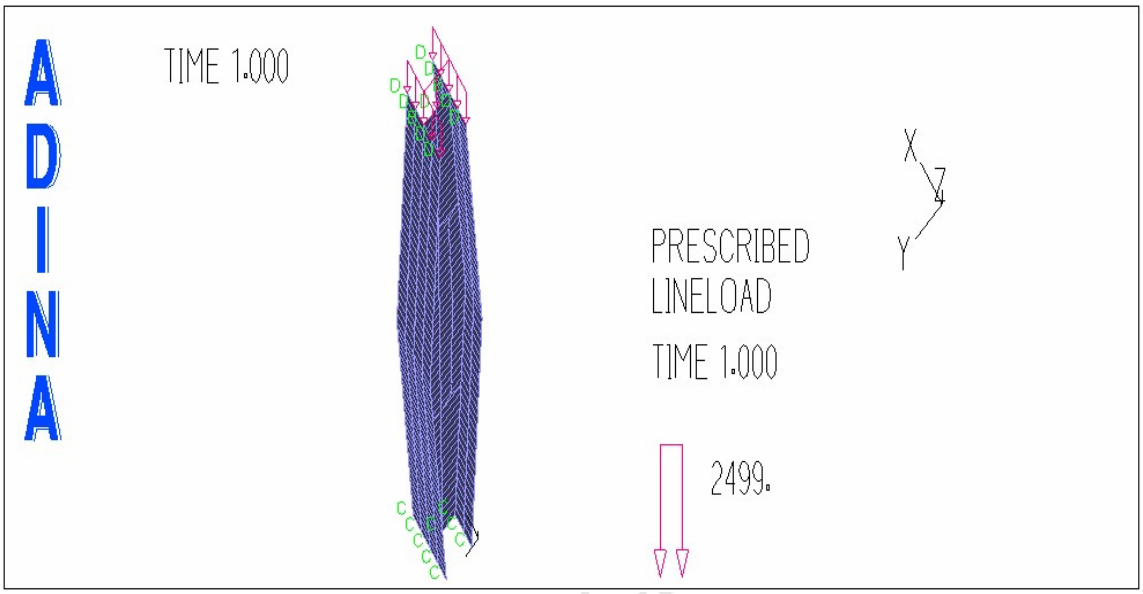

Figure 4.20. Web tapered pin-fix ended column with larger dimension in the middle

Table 4.40. **The first critical buckling load of 152 x 152 x 30 H-section web tapered column members with larger web depth in the middle**

Web depth at the supports, H_s (mm)	Web depth in the mid-height, h_m (mm)	Tapering ratio (h_m/H_s)	Critical buckling load, P_{cr} (kN)	%increase in the critical buckling load
145.2	145.2	1.00	1651	0.0
135.2	155.2	1.15	1650	0.1
125.2	165.2	1.32	1640	0.7
115.2	175.2	1.52	1620	1.9
105.2	185.2	1.76	1590	3.7
95.2	195.2	2.05	1560	5.5
85.2	205.2	2.41	1521	7.9
75.2	215.2	2.86	1483	10.2
65.2	225.2	3.45	1442	12.7
55.2	235.2	4.26	1401	15.1
45.2	245.2	5.42	1359	17.7
35.2	255.2	7.25	1317	20.4
25.2	265.2	10.52	1281	22.4

As the web tapering ratio (h_m/H_s) decreases, the critical buckling load decreases as seen in Table 4.40 hence a reduction in the load bearing capacity. This behaviour can be attributed to the buckling configuration of the member with this support condition. Therefore, any reduction in the moment of inertia near the pinned support will automatically reduce the stiffness and consequently the load bearing capacity of the whole column.

b) Flange tapered 152 x 152 x 23 H-section fix-pin ended column members

Following the same procedures as for web tapered pin-fix ended column's simulation, the flange width was tapered in order to compare the effect of tapering ratio on web tapered column with that of flange tapered columns under the same boundary conditions. The different geometrical arrangements of the flange tapered column together with the output results are shown in Fig. 4.21a, b and Table 4.41a, b**.**

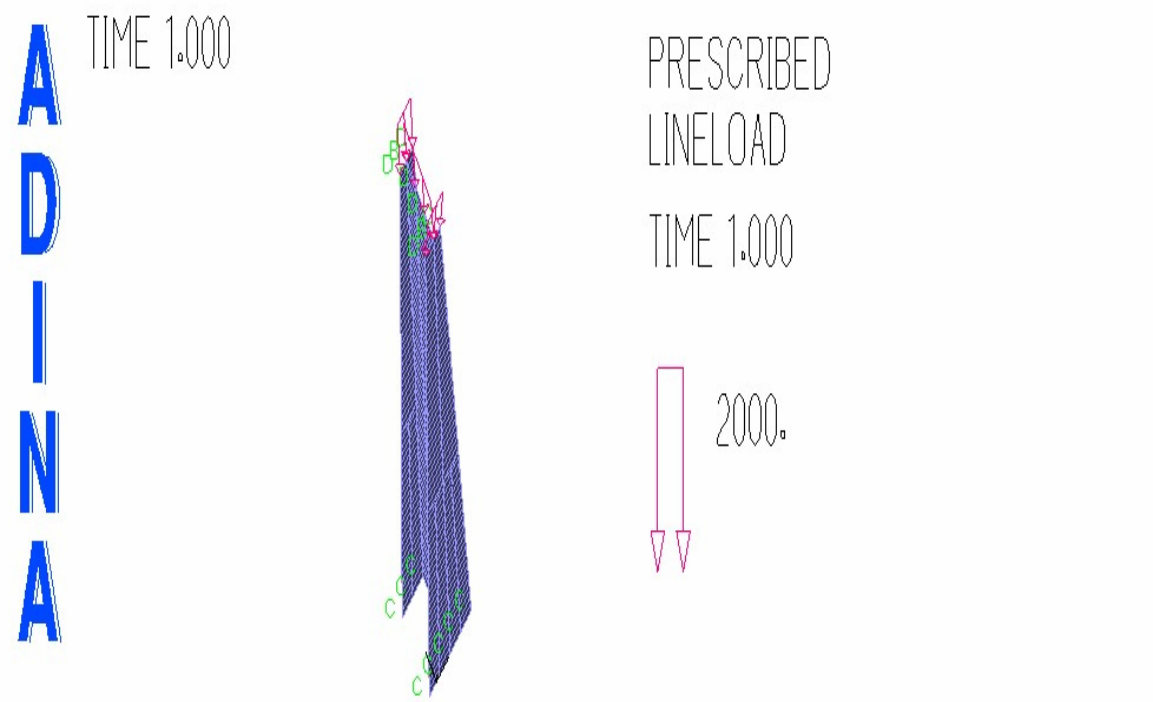

Figure 4.21a. Flange tapered H-section fix-pin ended column members with larger dimensions at the fixed end

Table 4.41a**. First critical buckling load of flange tapered 152 x 152 x 23 I-section fix-pin ended columns with larger dimensions at the fixed end**

Flange width at the fixed end, W_f (mm)	Flange width at the pinned end, w_f (mm)	Tapering ratio (w_f/W_f)	Critical buckling load, P_{cr} (kN)	%decrease in the critical buckling load
152	152	1.00	1359	0.0
162	142	0.88	1263	7.1
172	132	0.77	1170	13.9
182	122	0.67	1079	20.6
192	112	0.58	991	27.1
202	102	0.50	906	33.3
212	92	0.43	823	39.4
222	82	0.37	741	45.5
232	72	0.31	662	51.3
242	62	0.26	584	57.0
252	52	0.21	507	62.7
262	42	0.16	432	68.2

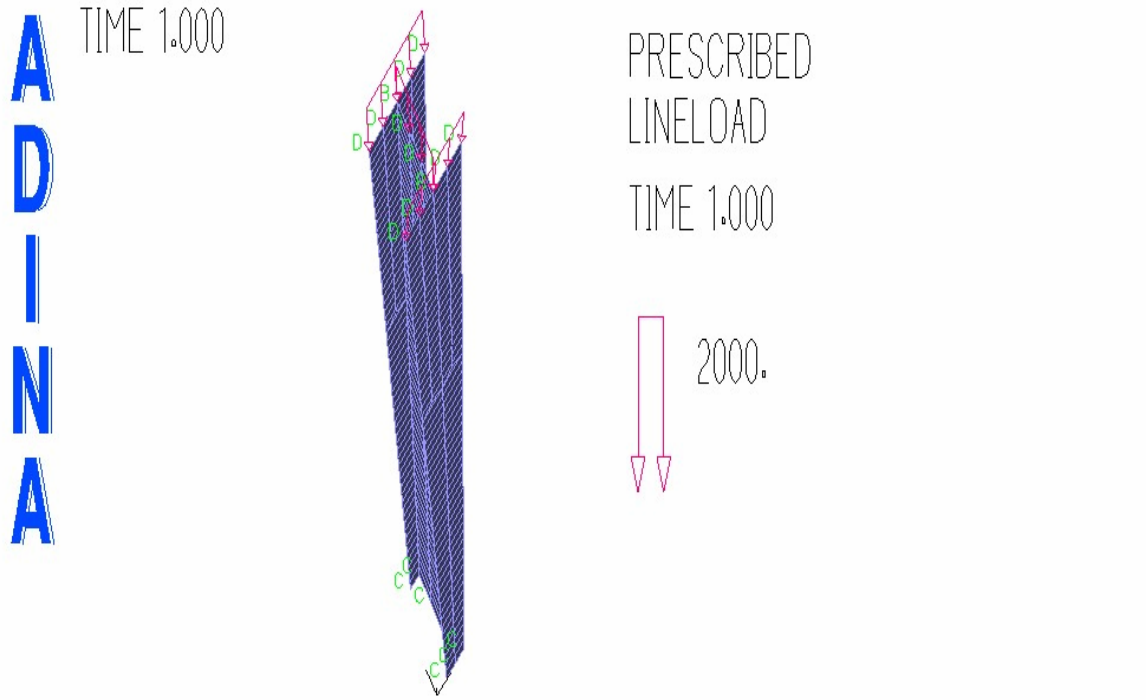

Figure 4.21b. Flange tapered H-section fix-pin ended column members with the larger dimensions at the pinned supports

Table 4.41b**. Global buckling load of a flange tapered 152 x 152 x 23 I-section fix-pin ended columns with larger dimensions at the pinned supports**

Flange width at the fixed end, W_f (mm)	Flange width at the pinned end, w_f (mm)	Tapering ratio (w_f/W_f)	Critical buckling load, P_{cr} (kN)	%increase in the critical buckling load
152	152	1.00	1359	0.0
142	162	1.14	1458	7.3
132	172	1.30	1561	14.9
122	182	1.49	1576	16.0
112	192	1.71	1517	11.6
102	202	1.98	1443	6.2
92	212	2.30	1354	-0.4
82	222	2.71	1249	-8.1
72	232	3.22	1130	-16.9
62	242	3.90	1000	-26.4

Both table 4.41a and 4.41b show general decrease in the buckling load of the column as the tapering ratio (w_f/W_f) increases except in table 4.41b where the buckling load initially increases as the tapering ratio increase up to 0.62, then the load bearing capacity of the members starts decreasing. This could be due to changes in the buckling modes.

4.4.2.2 Effect of tapering ratio on 25 x 25 x 5 angle section fix-pin ended column members

An angle 25 x 25 x 5 and 1m height was simulated under fixed-pinned conditions in order to investigate the effect of tapering ratio on different fixities. However, the geometrical arrangement was made to follow the bending moment envelope closely. Starting from tapering ratio of unity, the dimensions at the pinned support were reduced at 4mm interval while the ones at the fixed support were increased by the same interval as shown in Fig. 4.22. The resulting critical buckling loads for every changing tapering ratio were recorded in Table 4.42.

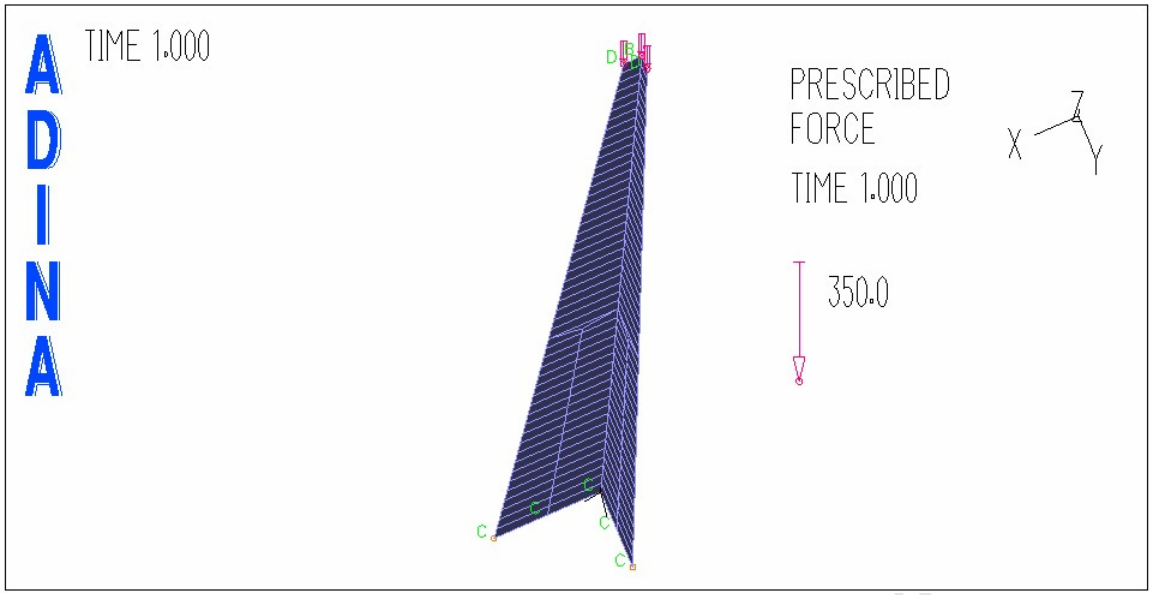

Figure 4.22 Tapered angle section pin-fix ended column members

Table 4.42**. The critical buckling load of 25 x 25 x 5 angle section non-prismatic pin-fix ended columns**

Dimensions at the fixed support, H (mm)	Dimensions at the pinned end, h (mm)	Tapering ratio (h/H)	Critical buckling load, P_{cr} (kN)	%decrease in the critical buckling load
25	25	1.00	20034.0	0.0
27	23	0.85	19833.0	1.0
29	21	0.72	19278.0	3.8
31	19	0.61	18378.0	8.3
33	17	0.52	17145.0	14.4
35	15	0.43	15603.0	22.1
37	13	0.35	15603.0	22.1
39	11	0.28	13791.0	31.2
41	9	0.22	11754.0	41.3
43	7	0.16	9558.0	52.3

As expected since buckling occurs near the pinned supports, a decrease in the cross-sectional dimensions in that area will reduce the flexural rigidity of the member hence a reduction in load bearing capacity. Therefore, a decrease in the tapering ratio (h/H), resulted into reduction in the critical buckling load of the members, thus Table 4.42. This behaviour is experienced by all member section types under fix-pin ended condition.

4.5 Behaviour of steel members under torsion

Steel members can be subjected to either pure or non-uniform torsion depending on the boundary conditions and the type of torque applied. Pure torsion occurs when both ends of the member are allowed to warp freely under constant applied torque. On the other hand, non-uniform torsion occurs when the ends of the member are prevented from warping freely or a variable torque is applied along the member.

Different steel sections can be used to resist both types of torsion. However, in this study, only I-section cantilever member was simulated for the effect of tapering ratio on maximum angle of twist for non-uniform torsion. The simulation was mainly performed on non-uniform torsion because this type of torsion has two variables, which are both functions of cross-sectional dimensions and therefore, they affect torsional behaviour of non-prismatic member. Equation (1.4) showed the application of the two variables; second moment of area (I) and torsional constant (J). The angle of twist for non-uniform torsion is a function of moment of inertia (I) and torsional constant (J), which are functions of cross-sectional dimensions. Therefore, any changes in the cross-section will affect these two parameters and consequently affect the maximum angle of twist for nonprismatic members.

4.5.1 Effect of web tapering ratio on the maximum angle of twist for a cantilever beam at the free end

A 203 x 133 x 30 I-section web tapered cantilever beam with web thickness, t_w = 6.4mm, flange thickness, t_f = 9.6mm and span length L = 4000mm was simulated for the effect of tapering ratio on non-uniform torsion. Beginning from prismatic beam members (h_e/H_s = 1), the web depth at the free end was reduced gradually by 10mm interval and at the same time, the web depth at the fixed support was increased by the same interval in order to keep the weight and volume constant, thus Fig.4.23. A constant torque of 500Nm was applied at the free end of the beam and the resulting maximum angle of twist at the free end of the beam was recorded for every change in the tapering ratio (h_e/H_s), thus Table 4.43.

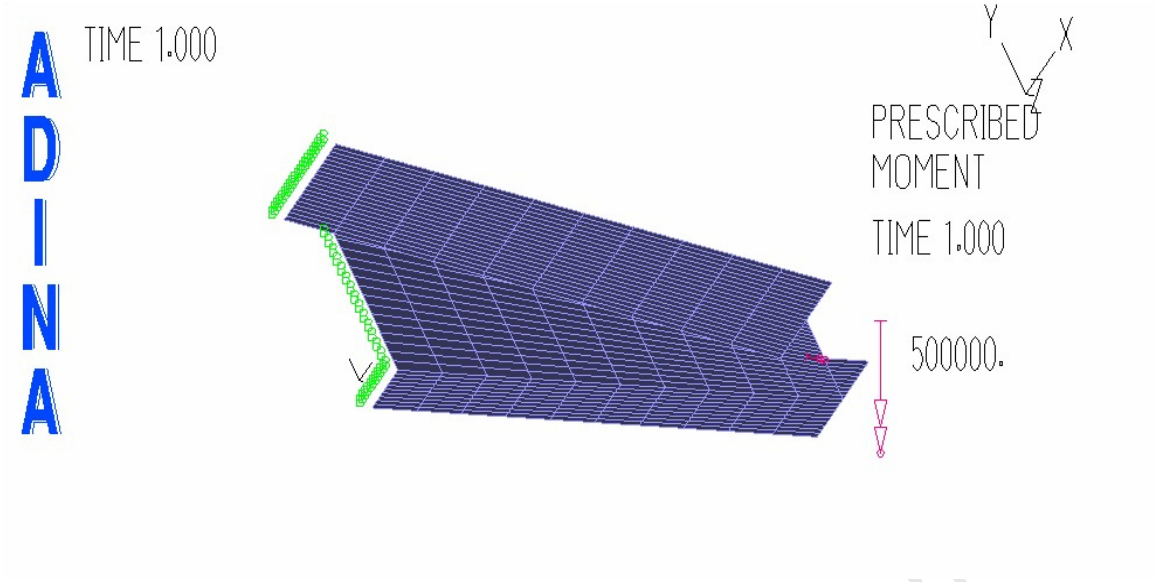

Figure 4.23. Web tapered cantilever beam with applied torque of 500Nm at the free end.

Table 4.43. **Maximum angle of twist for a web tapered cantilever 203 x 133 x 30 I-section beam with a 4m span under applied torque of 500Nm at the free end**

Web depth at the support, H_s (mm)	**Web depth at the free end, h_e (mm)**	**Tapering ratio (h_e/H_s)**	**Maximum angle of twist, ø$x10^{-1}$(radian)**	**% increase in the angle of twist**
195.2	195.2	1.00	4.17	0.0
205.2	185.2	0.90	4.20	0.7
215.2	175.2	0.81	4.22	1.2
225.2	165.2	0.73	4.23	1.4
235.2	155.2	0.66	4.24	1.7
245.2	145.2	0.59	4.24	1.7
255.2	135.2	0.53	4.23	1.4
265.2	125.2	0.47	4.21	1.0
275.2	115.2	0.42	4.17	0.0
285.2	105.2	0.37	4.12	-1.2
295.2	95.2	0.32	4.06	-2.6
305.2	85.2	0.28	3.97	-4.8
315.2	75.2	0.24	3.87	-7.2
325.2	65.2	0.20	3.74	-1.3
335.2	55.2	0.16	3.60	-13.7
345.2	45.2	0.13	3.42	-18.0
355.2	35.2	0.10	3.21	-23.0

The maximum angle of twist at the free end of the cantilever beam decreases as the web tapering ratio (h_e/H_s) decreases. This effect can be attributed to increase in both flexural rigidity at the support and torsional rigidity at the free end. Moreover, reduction in the web depth at the free end results into a decrease in the lever arm of the applied torque.

4.5.2 Effect of flange tapering ratio on the maximum angle of twist for a cantilever beam

In order to fully investigate the effect of tapering ratio on maximum angle of twist for a cantilever beam, both web and flange tapering ratios were simulated. Following a similar procedure as for web tapered cantilever beam, the flange width at the free end of a 203 x 133 x 30 I-section cantilever beam was gradually reduced at 10mm interval. At the same time, the flange width at the fixed end was increased by the same interval in order to keep the volume and weight constant as shown in Fig.4.24. The resulting maximum angle of twist at the free end of the beam was recorded for every changing tapering ratio as seen in Table 4.44.

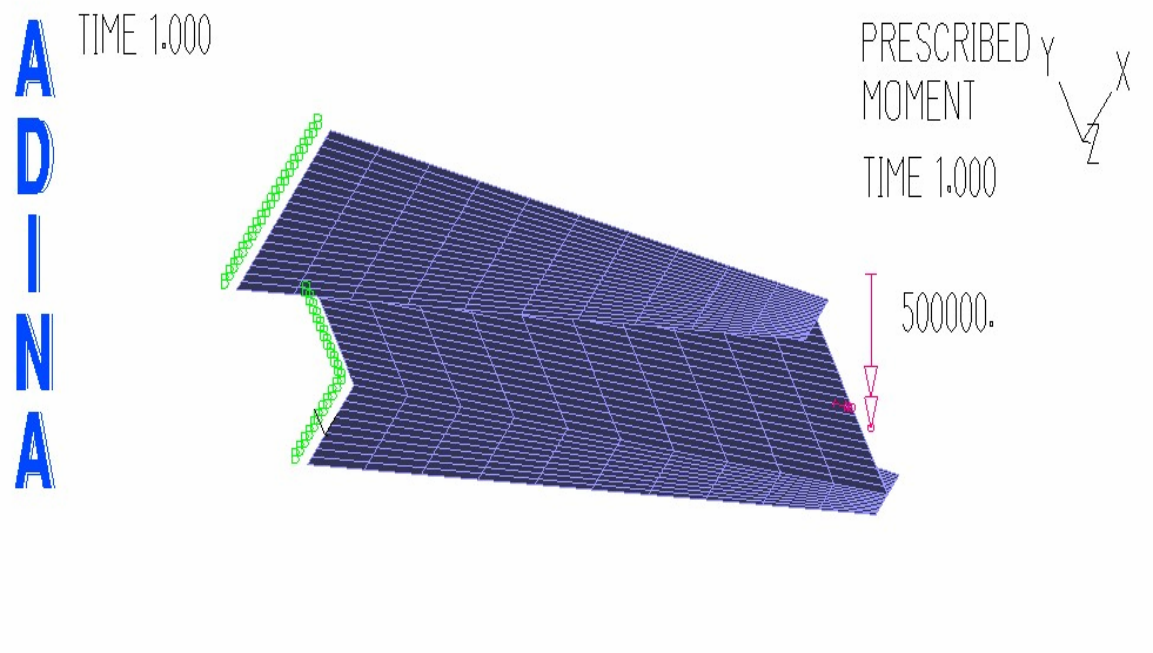

Figure 4.24. Flange tapered cantilever beam with applied moment of 500Nm at the free end

Table 4.44**. Maximum angle of twist for flange tapered cantilever 203 x 133 x 30 I-section beam of a 4m span under applied torque of 500Nm at the free end**

Flange width at the support, W_f (mm)	Flange width at the free end, w_f (mm)	Tapering ratio (w_f/W_f)	Maximum angle of twist, ø$x10^{-1}$ (radian)	% decrease in the angle of twist
133	133	1.00	3.82	0.0
143	123	0.86	3.76	1.6
153	113	0.74	3.68	3.7
163	103	0.63	3.62	5.2
173	93	0.54	3.58	6.3
183	83	0.45	3.56	6.8
193	73	0.38	3.55	7.1
203	63	0.31	3.56	6.8
213	53	0.25	3.59	6.0
223	43	0.19	3.65	4.5
233	33	0.14	3.73	2.4
243	23	0.09	3.87	-1.3

It can be observed from Table 4.43 and 4.44 that different positions of taper result into different behaviour of cantilever beam under torsion. This behaviour is attributed to the fact that web and flanges are under different actions. However, initially as the tapering ratio decreases, the maximum angle of twist decreases up to a tapering ratio of 0.38 then, it starts increasing due to rapid reduction in torsional rigidity of the flanges at the free end.

4.6 Frame systems

In most practical applications, Steel members are joined together to form portal frames, lattice frames, etc which make up steel structures. They are of various types e.g.; flat, pitched roof frames, etc. However, for this study, a single bay portal frames of either flat or pitch roof were simulated for critical buckling load.

4.6.1 Flat roof frames

A single bay frame of 5m width and 3m height was modelled with all the joints rigidly connected. The beams are made of I-sections with dimensions; 305 x 165 x 40, t_w = 6.1mm, and t_f = 10.2mm, L = 5000mm.

The columns are made of H-sections with dimensions; 203 x 203 x 46, t_w = 7.3mm and t_f = 11mm, L = 3000mm. The analysis of the frames was done for pinned supports under various tapering ratio with sway not prevented, thus Fig.4.25**.** For each change in the tapering ratio, the first critical buckling load was recorded in order to make direct comparison on the effect of tapering ratio and the load bearing capacity of the frame system.

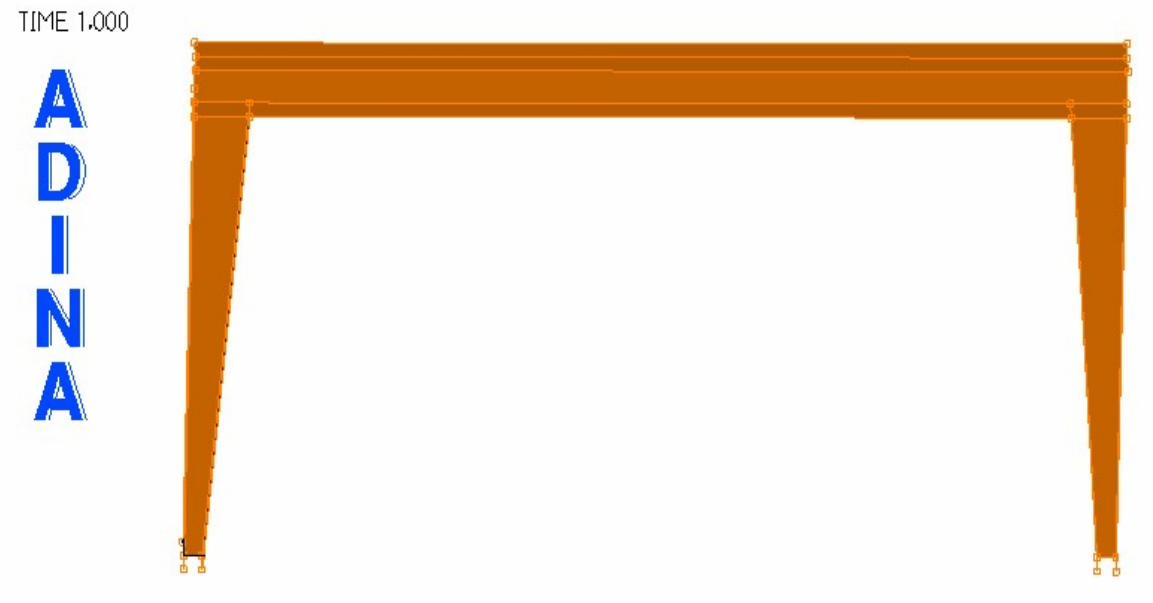

Figure 4.25. Flat roof steel frame with web tapered members

Table 4.45. **The first critical buckling load of flat roof frames made up of web tapered column members**

Web depth at the supports, H_s(mm)	**Web depth at the joints, h_j (mm)**	**Tapering ratio (h_j/H_s)**	**Critical buckling load, P_{cr} (N)**	**% increase in the buckling load**
203	203	1.00	18473	0.0
193	213	1.10	18692	1.2
183	223	1.22	18908	2.4
173	233	1.35	19119	3.5
163	243	1.49	19327	4.6
153	253	1.65	19530	5.7
143	263	1.84	19729	6.8
133	273	2.05	19925	7.9
123	283	2.30	20117	8.9
113	293	2.59	20306	9.9
103	303	2.94	20489	10.9
93	313	3.37	20670	11.9
83	323	3.89	20848	12.9
73	333	4.56	21023	13.8

Generally, the critical buckling load of the flat roof frame increases as the tapering ratio (h_j/H_s) of the column member increases, thus Table 4.45. The results obtained by ADINA/M 8.4.2 simulation are in close agreement with that presented in [50]. Arranging the frame system to resemble the bending moment envelope generated as seen in Fig 4.25, the load carrying capacity will be increased as shown in Table 4.45. This behaviour can be attributed to the fact that increasing the section dimension of the section with higher stress increases the load carrying capacity of the system. In addition, increasing the column web depth at the column-beam joint of the frames composed of tapered columns, leads to a decrease in the effective span of the beam as shown in Fig 4.25**.**

4.6.2 Pitched roof portal frame

The effect of both web and flange tapering ratios were simulated on a single bay frame of 5m width, 3m high up to the eaves and 3.5m high up to the ridge. For all the analyses, joints were rigidly connected. The beams are made of I-sections dimensions; 305 x 165 x 40, t_w = 6.1mm, and t_f = 10.2mm, L = 5000mm. While the columns are made of H-sections dimensions; 203 x 203 x 46, t_w = 7.3mm and t_f = 11mm, L = 3000mm.

The analysis of the frames was done for pinned supports with sway not prevented under various tapering ratio, thus Fig. 4.26**.** Uniformly distributed line load (UDL) applied along the beam span. The critical buckling load for every change in the tapering ratio was evaluated by multiplying the total applied load and the buckling load factor λ, to get the critical buckling load of the structure as seen in Table 4.46 and 4.47. However, there are number of other factors, which affect the stability of the frame system composed of non-prismatic members i.e. the restraint conditions, member classes of the beam and column, and the geometrical arrangements [50], are not considered in this study.

Figure 4.26. Pitched roof portal frame with web tapered members

Table 4.46**. The first critical buckling load of pitched roof frames with web tapered beam and column members**

Column web depth at supports, h_s (mm)	Column web depth at joints h_j (mm)	Column web tapering ratio (h_j/h_s)	Rafter web depth at eave, h_j (mm)	Rafter web depth at ridge, h_b (mm)	Rafter web tapering ratio (h_j/h_b)	Critical buckling load, P_{cr} (N)	% increase in the buckling load
203	203	1.00	305	305	1.00	4.284	0.0
193	213	1.10	315	295	1.07	4.416	3.1
183	223	1.22	325	285	1.14	4.560	6.4
173	233	1.35	335	275	1.22	4.708	9.9
163	243	1.49	345	265	1.30	4.868	13.6
153	253	1.65	355	255	1.39	5.036	17.6
143	263	1.84	365	245	1.49	5.220	21.8
133	273	2.05	375	235	1.60	5.412	26.3
123	283	2.30	385	225	1.71	5.616	31.1
113	293	2.59	395	215	1.84	5.836	36.2
103	303	2.94	405	205	1.98	6.072	41.7
93	313	3.37	415	195	2.13	6.324	47.6
83	323	3.89	425	185	2.30	6.592	53.9
73	333	4.56	435	175	2.49	6.868	60.3
63	343	5.44	445	165	2.70	7.112	66.0
53	353	6.66	455	155	2.94	7.440	73.7
43	363	8.44	465	145	3.21	7.792	81.9

The first critical buckling load of the frame structures increases as the web tapering ratio (h_j/h_s) increases, where h_j is the web depth at the joint between column and beam while h_s is the web depth at the supports as shown in Table 4.46**.** Increase in the cross-sectional dimensions of the frame with higher bending moment increases the flexural rigidity of the whole structures hence, increase in the stability of the structures.

Table 4.47**.The first critical buckling load of pitched roof frames with flange tapered members**

Column flange with at supports, w_s (mm)	Column flange width at joints, w_j (mm)	Column flange tapering ratio (w_j/w_s)	Rafter flange width at eave, w_j (mm)	Rafter flange width at ridge, w_b (mm)	Rafter flange tapering ratio (w_j/w_b)	Critical buckling load, P_{cr} (N)	% decrease in buckling load
203	203	1.00	203	203	1.00	4.284	0.0
193	213	1.10	213	193	1.10	4.282	0.0
183	223	1.22	223	183	1.22	4.278	0.1
173	233	1.35	233	173	1.35	4.272	0.3
163	243	1.49	243	163	1.49	4.264	0.5
153	253	1.65	253	153	1.65	4.248	0.8
143	263	1.84	263	143	1.84	4.224	1.4
133	273	2.05	273	133	2.05	4.192	2.1
123	283	2.30	283	123	2.30	4.152	3.1
113	293	2.59	293	113	2.59	4.104	4.2
103	303	2.94	303	103	2.94	4.040	5.7
93	313	3.37	313	93	3.37	3.960	7.6
83	323	3.89	323	83	3.89	3.848	10.2
73	333	4.56	333	73	4.56	3.708	13.4
63	343	5.44	343	63	5.44	3.513	18.0
53	353	6.66	353	53	6.66	3.231	24.6

Table 4.47 shows a different behaviour of frame structures with flange tapered members from the one with web tapered members. For frame with flange tapered members, as the tapering ratio (w_j/w_s) increases, the critical buckling load decreases which is in contrary to what was observed in Table 4.46. However, this unique behaviour could be attributed to the fact that web and flanges are under different action hence increase in flange width at the joints may result in decrease in the flexural rigidity which eventually leads to a reduction in the stiffness and/ or load bearing capacity of the structures.

4.7 Validation of ADINA/M 8.4.2 model results

Mesh density is a key factor in FEM analysis. Therefore, in order to check the validity of the results generated by ADINA/M 8.4.2, some closed form solutions were obtained for prismatic members using the available design guidelines. Since prismatic members were the starting point for every simulation in this research, it is realistic enough to test the models results from numerical analysis using those closed form solutions.

From Table 4.48**,** it is evident that there is negligible variation in the results obtained using ADINA/M 8.4.2 models and those from closed form solutions hence, the results from the numerical models using ADINA/M 8.4.2 can be used to draw conclusions on the behaviour of non-prismatic steel members under various tapering ratios, steel sections, steel structures, steel classes, boundary and loading conditions.

Table 4.48**. Comparison between ADINA and analytical calculated results**

Members	**Analysis types**	**Results from ADINA**	**Results from Calculations**	**% Variations**
Cantilever 203 x 133 x 30 I-section beam	Deflection	82.4mm	77.9mm	6
Cantilever 203 x 133 x 30 I-section beam	Stress	533.1MPa	526.8MPa	1.2
Cantilever 203 x 133 x 30 I-section beam	Buckling	89.3kNm	80.8kNm	10.5
Cantilever 152 x 152 x 30 H-section column	Buckling	207kN	215kN	3.7
Cantilever 25 x 25 x 5 angle section column	Buckling	2465.1N	2467.4N	0.1
Cantilever 76 x 38 channel section column	Buckling	58.7kN	52.8kN	11.2
Cantilever 356 x 171 x 45 I-section beam	Deflection	12.2mm	12.5mm	2.4
Cantilever 356 x 171 x 45 I-section beam	Stress	541.1Mpa	542Mpa	0.2

Chapter 5

Conclusions and Recommendations

5.1 Conclusions

5.1.1 Introduction

The effect of fixities, loading conditions, geometrical arrangements, section types and tapering ratio, on the behaviour of non-prismatic members, were investigated using FEM analysis with the help of ADINA/M 8.4.2 package. The results obtained were summarised under each factor considered to affect the general behaviour of non-prismatic members.

5.1.2 Effect of fixities on non-prismatic members

Maximum deflection, flexural stress and critical buckling load recorded depict the level under which different boundary conditions affect the behaviour of steel members. For instant, an I-section 203 x 133 x 30 web tapered beam shows a decrease in the maximum deflection of cantilever and fix ended beam members as the tapering ratio (h_w/H_w) decreases thus Table 4.1 and 4.21 by more than 35% for a tapering ratio of 0.2. However, for the same beam with pin supports, the maximum deflection and flexural stress, increases as the tapering ratio increases. For instance, Table 4.27 shows a 22% increase in maximum deflection for a tapering ratio of 3.6. Furthermore, the load bearing capacity of a cantilever 152 x 152 x 23 flange tapered column with the smaller dimensions at the free end increases as the tapering ratio (h_w/H_w) decreases, thus Table 4.33a shows a 2.5% increase for ($h_w/H_w = 0.14$). The same column member under fixed-pinned conditions and for the same tapering ratio of 0.14, shows 39% decrease in load bearing capacity as shown in Table 4.39a *section 4.4*. This behaviour can be attributed to different stress distribution for each boundary condition.

5.1.3 Effect of different Loading conditions

Different loading types do not have any significant effect on the behaviour of non-prismatic members under various tapering ratios. *Section 4.3* showed a decrease in the maximum deflection and flexural stress of a cantilever 203 x 133 x 30 I-section tapered beam as the tapering ratio (h_w/H_w) decreased, when a 50kN point load was applied, thus Table 4.1 and 4.3. The same behavioural trend was observed when a 17kN/m UDL was applied on the same cantilever beam, Table 4.6 and 4.7. This behaviour is expected from Bernoulli beam theory which shows that both deflection and flexural stress equations, are not functions of the load types applied but the geometrical properties.

5.1.4 The Influence of Geometrical arrangements on the effect of tapering ratios (h/H) on non-prismatic members

Non-prismatic steel members with geometry closely resemble the bending moment envelope, experience higher load bearing capacity and vice versus. Therefore, fix ended beam with larger dimensions at the supports, have higher critical bending moment compared to the same beam with smaller dimensions at the supports. For instance, Table 4.26 shows 13% increase in the critical buckling moment. Furthermore, the critical buckling load of a cantilever tapered column with larger dimensions at the support increases as the tapering ratio, (h/H) decreases as shown in Fig.4.14a and Table 4.34a. However, the same column with larger dimensions at the free end, experiences decrease in the critical buckling load as the tapering ratio, (h/H) increases, thus Fig.4.14b and Table 4.34b.

Positioning of geometrical non-uniformity is not only required for support conditions but also for sections under different actions. Considering I-section fix ended beam, when the web is made non-prismatic, the critical buckling moment decreases with decreasing degree of non-uniformity, (h_w/H_w), as seen in Table 4.23. However, the same beam whose flanges were made non-prismatic experienced increase in the critical buckling moment as the tapering ratio, (w_f/W_f) decreases, thus Table 4.26.

5.1.5 The influence of different steel sections on the effect of tapering ratio

The effect of different steel sections on the behaviour of non-prismatic members was demonstrated in *Section 4.3* where cantilever I, T and channel beams were simulated for stability analysis. For instance, I and channel section members under 0.74 and 0.67 tapering ratios, show 26.1% and 24.3% increase while T section member under 0.67 tapering ratio, shows 0.2% decrease in the critical buckling moment.

5.1.6 Effect of tapering ratio on different steel's classes

The results obtained from class 1 and 2 I-section beams members under various fixities, loading conditions and geometrical arrangements show negligible variations in maximum deflection, flexural stress and critical buckling moment. Table 4.9 shows 20.1% decrease in the maximum deflection for 0.14 tapering ratio under class one member while Table 4.12 shows 17.2% decrease for the same tapering ratio but under class two member.

5.1.7 Effect of tapering ratio on different steel's structures

Ranging from beams and columns to frames, the tapering ratio has the same effect on the steel structures. For instance, web tapered members experience increase in the load bearing capacity as long as their geometry closely resemble the bending moment envelope, thus Table 4.5 and 4.37. This is the same behaviour as for frames composed of web tapered members, thus Table 4.45 and 4.46.

5.1.8 General conclusion

Generally, the results obtained from the simulation using ADINA/M 8.4.2 package agreed with the hypothesis which stated that non-prismatic steel members provide more economical and safe design of structures than prismatic members. They provide effective usage of material and higher load bearing capacity. However, not all the non-prismatic steel members are more economical than the prismatic members. This is seen from the cantilever columns of any section types with larger dimensions at the free end having a reduction in its load bearing capacity as the tapering ratio increases.

Therefore, different geometrical arrangements of the same non-prismatic members play a major role in determining its stability.

The load bearing capacity of non-prismatic members does not increase indefinitely as the degree of non-uniformity increases. This is seen from the results obtained in Chapter 4 where the maximum deflection and flexural stress of non-prismatic beams start increasing at a certain point when the section of the members starts yielding.

Boundary conditions affect the load bearing capacity of non-prismatic members in the sense that they provide different point (tapering ratio) for which the buckling mode changes due to a reduction in the load bearing capacity of the structures.

5.2 Recommendations

The author recommends further study is carried out to investigate the general behaviour of non-prismatic members with stepped and parabolic geometrical arrangements under different degree of non-uniformity. For better accuracy, slower rate of change in the degree of non-uniformity is required.

There has always been questions concerning the validity of the numerical results, therefore, it is recommended that for realistic conclusions, experimental models must be performed to validate the numerical data.

A computer algorithm can be written to optimise the degree of geometrical non-uniformity for members of different sections, lengths, boundary conditions and geometrical arrangements in order to avoid the tedious procedures of determining the best degree of non-uniformity manually.

Further investigation is required for frame structures under fixed supports, pinned joints, different steel classes for both beams and columns, both sway and non-sway and point load. All these factors must be applied under various tapering ratios for both beam and column dimensions.

Bibliography

1. **ADINA R & D, Inc. (1996-2008).** *AUI Standard User's manuals*. Water Town, MA 02472 USA.

2. **AISC LRFD (1999).** American Institute of Steel Construction Load and resistance Factor Design

3. **Andrade, A. and Camotim, D. (2005).** Lateral-Torsional Buckling of Singly Symmetric Tapered Beams: Theory and Applications. *Journal of Engineering Mechanics*. 131(6).

4. **Apostol, V., Santos, J.L.T and Paiva, M. (2002).** Sensitivity Analysis and Optimization of Truss/Beam Components of Arbitrary cross-section. *Computer and Structures*, 80, 391-401.

5. **Baker, G.** (1996). Exact Deflections in Non-prismatic Members. *Computers and structures*. 61 (3) 515-528

6. **Baptista, A.M. and Muzeau, J.P. (1998).** Design of Tapered Compression Members According to Eurocode 3, *Journal of Constructional Steel Research*, 46(3)146-148.

7. **Bathe K. (1996).** *Finite Element Procedures*. Prentice-Hall, Inc. New Jersey. USA

8. **Bradford, M.A. and Cuk, P.E. (1988).** Elastic buckling of tapered monosymmetric I- beams. *Journal of Structural Engineering*. 114(5) 977-996.

9. **Brown, T.G. (1981).** Lateral torsional buckling of tapered I-beams. *Journal of Structural Division* 107(4) 689-697.

10. **Byoung, K. L., Li, G., Suk, K. K. and Dae, S. A. (2003**). Buckling Loads of linearly Tapered Columns Laterally Restrained by Multiple Elastic Springs. *Journal of Structural Engineering*. 7(3)305-311.

11. **Cary, W.C. (1997).** *Effective Lengths of Web-Tapered Columns in Rigid Metal Building*. Masters thesis, Dept. of Civil Engineering. Virginia polytechnic Institute and State University. Virginia, USA.

12. **Chambers, J.J., Almudhafar, S. and Stenger, F. (2003).** Effect of Reduced Beam Section frame elements on Stiffness of moment frames. *Journal of Structural Engineering*. 129 (3) 383-394.

13. **Chen, W.F and Toma, S. (1994).** *Advanced Analysis of Steel Frames*. Theory, Software, and Applications. CRC Press. Boca Raton, Florida.

14. **Chroscielewski, J., Lubowiecka, I., Szymczak, C. and Witkowski, W. (2006).** On some aspect of torsional buckling of thin-walled I-beam column. *Computers and structures*, 84, 1946-1957.

15. **Chu, K.H and Chow, H.L. (1969).** Effective Column Length in unsymmetrical frames. *International Association for Bridge and Structural engineering*. 29 (1).

16. **Corner, Q. (2003).** *Torsional Buckling and Instability of Steel Structural Members*. Masters thesis, Dept. of Civil Engineering. University of Cape Town. South Africa.

17. **Dude, G. P. and Dumir, P. C. (1996).**Tapered Think Open Section Beams on Elastic Foundation, Buckling Analysis. *Computers & Structures* 61(5) 845-857.

18. **Ermopoulos, J.C. (1997).** Equivalent Buckling Length of non-uniform Members. *Journal of Constructional Steel Research*, 42, 141-158.

19. **Federal Emergency Management Agency (FEMA) (2000).** *Recommended Seismic design criteria for new steel moment-frame building*. Washington D.C.

20. **Galambos, T.V. (1998).** *Guide to Stability Design Criteria for Metal Structures* 5th edn. John Wiley & Sons, New York.

21. **Galambos, T.V. (1988).** *Guide to Stability Design Criteria for Metal Structures.* 4th edn. John Wiley & Sons, New York.

22. **Gere, M.J and Timoshenko, S.P. (1997).** *Mechanics of materials*, 4thedn. Boston, 1878-1972.

23. **Grubbs, K.V. (1997).** *The effects of the dogbone connection on the elastic stiffness of steel moment frames*. Master's thesis, Dept. of Civil Engineering. The University of Texas at Austin.

24. **Guo-Qiang, L. Jin-Jun, L. (2002).** A Tapered Timoshenko-Euler Beam Element for Analysis of Steel Portal frames. *Journal of Constructional Steel Research,* 58, 1513-1544.

25. **Hiroyuki, S. and Muneaki. (1984).** Strength Formula for Tapered Beam-Columns. *Journal of structural Engineering*.110 (7)1630-1643.

26. **Horne, M.R., Shakir, K.H. and Akhtar, S. (1979).** Stability of tapered and haunched members. *Proceedings of Instability of Civil Engineering London UK*. 67(3) 677-699.

27. Http://www.bolokids.com/indexes/scitech.

28. Http:// www.coldsteels.com/images.html

29. Http://www.patentstorm.us/ useful_images/weldings/process.html.

30. Http://www.roymech.co.uk/useful_tables/Beams/Beam_theory.html.

31. Johnston, B.G. (1976). *Guide to Stability Design Criteria for Metal Structures 3rd edn*. John Wiley & Sons, New York.

32. Jong-Dar, Y. (2006). Stability of Tapered I-Beams under Torsional Moments. *Finite Elements in Analysis and Design*. 42(7) 914-927.

33. Just, D. J. (1977). Plane Frameworks of Tapering Box and I-section. *ASCE* 103ST1, 71-86.

34. Kee-Dong, K. and Michael, D.E. (2007). Non-prismatic beam elements for beams with RBS connections in Steel Moment Frames. *Journal of structural engineering*, 133 (2).

35. Kitipornchai, S. and Trahair, N.S. (1975). Elastic behaviour of tapered monosymmetric I-beams. *Journal of structural Division*. 101(8) 1661-1678.

36. Kitipornchai, S. and Trahair, N.S. (1972). Elastic Stability of tapered I-Beam. *Journal of the Structural Division*. 98(3)713-728.

37. Kitipornchai S. and Trahair N.S. (1972). Elastic Stability of tapered I-beams. *Journal of Structural Division*. 98(3) 713-722.

38. Lambert, T. (1974). *Structural Steel Design*. 2nd edn. New York.

39. Lee, G. C., Morels, M. L and Ketter, R. L (1972). Design of tapered members. *Welding Research Council,* New York, N. Y.

40. Li Q.S. (2000). Buckling of elastically restrained non-uniform columns. *Journal of Engineering Structures*. 22, 1231-1243.

41. **Mahachi, J. (2004).** *Design of structural steel work to SANS 10162*. CSIR building and construction technology, Pretoria South Africa.

42. **Muller, A., Werner, F., Osterrieder, P. (1999).** Optimum Design Of steel Frames with Non-uniform Members. *Institute of Steel Structures, Bauhaus-University Weimar, Germany, 6th Conference Proceedings.*

43. **Murray, W.N. (1986**). *Introduction to the Theory of Thin-Walled Structures*. Oxford Engineering Science series 13. Clarendon, Oxford. U.K.

44. **Nethercot, D.A. (2000).** Global performance of static and stability behaviour for frames structures. *Journal of constructional Steel Research*. 58, 109-124.

45. **Nethercot, D. A. (1973).** Lateral buckling of tapered beams. IABSE. 173-191.

46. **Nunez, E. and Fouad, H.F. (2000).** Estimation of Second-Order Effects for Pole-Type Structures. *Transportation Research Board of the National Academies*. 1740, 151-156.

47. **O'Rourke, M. (1977).** Buckling loads for non-uniform columns. *Computer and Structure*. 7(6) 717-720.

48. **Rajasekaran, S. (1994).** Instability of Tapered Thin-Walled beams of Generic Section. *Journal of Engineering Mechanics,* 120 (8) 0733-9399.

49. **Ramamurti, V. and Karthikeyan, R. (1997).** Stress Analysis of tapered locks. *Computer & structures*, 62, (4), 721-736.

50. **Saka, M.P. (1997).** Optimum design of steel frames with tapered members. *Computer & structures,* 63, (4), 797-811.

51. **SAP90 User's Manual, (1991).** *Computers and Structures*, Inc. Berkeley, California.

52. **Samir, Z.A. (2004).** Exact expression for stability functions of non-prismatic frames. *Journal of Constructional Steel Research*, 60, 1561-1584.

53. **SANS 10162-1 (2004).** South Africa National Standards.

54. **Sapalas, V., Samofalov, M., Saraskinas, V. (2005).** FEM Stability Analysis of Tapered Beam-Columns. *Journal of Civil Engineering and Management*, 11 (3) 211-216.

55. **Sapalas, V., Kvedaras, A.K. (2000).** Stability of axially loaded tapered columns. *Statyba (Civil Engineering)*. 6 (3) 158-161.

56. **Sapountzakis, E.J. and Mokos, V.G. (2004).** Non-uniform Torsion of Composite bars of Variable Thickness by BEM. *International Journal of Solids and Structures*. 41 (7) 1753-1771.

57. **Shiomi, H. and Kurata, M. (1984).** Strength formula for tapered beam-columns. *Journal of Structural Engineering*. 110 (7) 1630-1643.

58. **Siu, L.C. (1990).** Buckling Analysis of Structures Composed of Tapered Members. *Journal of Structural Engineering*. 116 (7) 24867.

59. **Southern African Steel Construction Handbook. (2005).** 5th edition. South Africa.

60. **Tena-Colunga A. (2001).** Behaviour and modelling of non-prismatic members having T-sections. *Journal of structural engineering*, 127 (8), 940-946.

61. Timoshenko, S. P. and Gere, J.M. (1961). *Theory of Elastic Stability,*2nd edn. McGraw- Hill, New York.

62. Timoshenko, S. (1936). *Theory of Elastic Stability*,1st edn. McGraw- Hill, New York.

63. Tochacek, M. (1995). Design of Struts with a variable cross-section. *Instability of steel Structures*. 1, 103-109.

64. Chen, W. and Kim, S. (1986). *LRFD (Steel Design Using Advanced Analysis).* Manual of Steel Construction. AISC, U.S.A

65. Xian-Xing, L. (2007). Flexural strength for General Lateral-Torsional Buckling, *Journal of Structural Engineering*, 133 (5) 0733-9445.

66. Yaozhi, L., Xu, X., Ji, W., Zhu, S., Zhang, B., Fu, X. and Gu, L. (2006). Arranging the Plastic hinges and improving the strength of Steel tubes with tapered ends: Analysis and tests. *Journal of Constructional Steel Research,* 62, 885-892.